METAL ION SEPARATION USING ELECTRICALLY SWITCHED ION EXCHANGE

METAL ION SEPARATION USING ELECTRICALLY SWITCHED ION EXCHANGE

By:
AHMED F. TAWFIC
B.A.Sc, M.A.Sc

A Thesis
Submitted to the School of Graduate Studies
In Partial Fulfillment of the Requirements
For the Degree of
Doctor of Philosophy

McMaster University

DOCTOR OF PHILOSOPHY (2014)
(Civil Engineering)

McMaster University
Hamilton, Ontario

TITLE	**Metal ion separation using electrically switched ion exchange**
AUTHOR	**Ahmed F. Tawfic** **B.A.Sc. (Military Technical College, Cairo, Egypt)** **M.A.Sc.(Military Technical College, Cairo, Egypt)**
SUPERVISORS	**Dr. Sarah Dickson** **Dr.Younggy Kim**
NUMBER OF PAGES	**xxiii, 140**

Abstract

Cs^{137} is generated from fission nuclear reactor operations. It has a half-life time of 30 years, and it is considered to be an excellent source of gamma radiation. Cs^{137} needs to be separated from nuclear waste before its disposal. Electrically switched ion exchange (ESIX) is one method which can be used for its separation from nuclear waste.

ESIX consists of an ion exchange film that is deposited onto a conductive electrode surface. Typically, for Cs^+ removal, this film is composed of nickel hexacyanoferrate, which is known for its selectivity for that ion. The ESIX method involves the sequential application of reduction and oxidation potentials to an ion exchange film to induce the respective loading and unloading of Cs^+. ESIX can be used to separate Cs^{137} from nuclear radioactive waste as well as Cs^+ from industrial wastewater.

The goal of this research was to enhance the capacity of the nickel hexacyanoferrate ion exchange film deposited on nickel electrodes by modulating the applied potential for the ESIX film preparation. This goal was achieved by preparing an ESIX film on a nickel substrate using a two-step process in which voltage is applied to a nickel electrode surface prepared prior to the film deposition using diamond sand paper 2500 grit. The results show the preparation of a film with capacity 63 times higher than that which is previously reported in the literature.

Another four ESIX films composed of nickel hexacyanoferrate were deposited on nickel substrates with varying potentials, again in a two-step process and with surface treatment using 800 grit diamond sand paper prior to the film deposition. The surface morphology of the films was studied using scanning electronic microscope (SEM) to note any differences which could have occurred from the changes in deposition procedures. Electrospray ionization-mass spectroscopy was used to quantify the Cs^+ loaded and unloaded onto the film. The results show that all of the four prepared ESIX film have a high capacity compared to those reported in the literature and that their performance regarding Cs^+ loading was affected by the applied potential used for the ESIX film preparation.

Another goal of this research was to enhance the capacity of the nickel hexacyanoferrate ESIX film by changing the substrate from nickel to graphite. This goal was achieved by adsorbing the film into the pores of graphite electrodes. X-ray tomography was used to visualize the nickel hexacyanoferrate film inside the graphite electrodes. Cyclic voltammetry was conducted to detect the response of the prepared film with Cs^+. Electrospray ionization-mass spectroscopy was used to quantify the amount of Cs^+ adsorbed and desorbed by the electrode. The x-ray tomography results show that the graphite electrode adsorbed nickel hexacyanoferrate material. The cyclic voltammetry figures confirm that the response of each electrode prepared with Cs^+ was related to the concentration of nickel hexacyanoferrate in the graphite electrode. Finally, the results obtained from electrospray ionization-mass spectroscopy about how much Cs^+ was

adsorbed and desorbed confirms that the two prepared electrodes have a higher capacity for Cs^+ adsorption based on their interaction with a prepared Cs^+ solution as a test solution.

Another goal was to observe the performance of a new ESIX film material, namely nickel hexacyanocobaltate. This film was also adsorbed by graphite electrodes. Cyclic voltammetry was conducted to measure the performance of the hexacyanocobaltate film with regard to Cs^+, and the results show a significant increase in the nickel hexacyanocobaltate material inside the graphite electrode and Cs^+ in the test solution. Electrospray ionization-mass spectroscopy was used to quantify the Cs^+ adsorbed and desorbed by the electrode. The Results show that nickel hexacyanocobaltate as an ESIX have high capacity for Cs^+ adsorption from test solution.

Acknowledgements

I would like to thank the many people who have helped me during my time at McMaster University. My supervisors, Dr. Sarah Dickson, Dr. Younggy Kim. They have all supported my research since the beginning, and I am thankful to have had their insight and advice concerning my research and experiments. I would also like to thank Dr. Carlos Filipe for his advice and support.

Peter Koudys is an excellent technician; his advice and work with the fabrication of my set-up were of great help to my research. I would also like to thank Connie Perry for her superb help in the use of the x-ray tomography. Furthermore, I would like to thank Carol Robinson who helped smooth the transition and helped me to keep track of all the administrative tasks that needed to be done.

I am very thankful to my colleagues Vickram Lakhian, Mohammed Mohktar, and Sean Cianflone for their great support and help during my research.

I would also like to thank the Egyptian Ministry of Defence for its financial support for my research, and I would like to thank NSERC and the McMaster University Department of Civil Engineering.

Special thanks to my family for their support, and my wife, Nesreen, for her care, patience, and her love.

Preface

This thesis has been prepared according to McMaster University regulations of theses consisting of previously published/prepared material. Chapter 3 consists of material previously accepted to be published as journal articles, and chapter 2, 4, 5 and 6 consist of material previously prepared for publication journal articles. As such, the material in chapters 2, 3, 4, 5 and 6 had multiple authors. The original contributions made by the thesis author to the material in each of these chapters are outlined below:

Chapter 2

Title: Electrically Switched Ion Exchange

Authors: Tawfic, A.F., Dickson, S.E., Kim, Y., and Mekky, W.

To be submitted in November 2014

The literature review was conducted by Tawfic, A.F. The text was written by Tawfic, A.F and edited by Dickson, S.E., Kim, Y., and Mekky, W.

Chapter 3

Title: Enhanced Capacity and Stability for the Separation of Caesium in Electrically Switched Ion Exchange

Authors: Tawfic, A.F., Dickson, S.E., Kim, Y., and Mekky, W.

Accepted for publication in the *Journal of American Nuclear Society*.

The experiments were designed and conducted by Tawfic, A.F. All aspects of testing electrode and film preparation and fabrication and characterization of the tested films was conducted by Tawfic, A.F. The analysis of the results was conducted by Tawfic, A.F. in consultation with Dickson, S.E., Kim, Y., and Mekky, W. The text was written by Tawfic, A.F and edited by Dickson, S.E., Kim, Y., and Mekky, W.

Chapter 4

Title: A Comparison between Four Prepared Films as Electrically Switched Ion Exchange

Authors: Tawfic, A.F., Dickson, S.E., Kim, Y., and Mekky, W.

To be submitted in November 2014.

The design of the experiment and its parameters were done by Tawfic, A.F. The preparation of the nickel electrodes, their respective films, and film characterization using cyclic voltammetry, as well as the SEM and the film capacity measurements by electrospray ionization-mass spectroscopy (ESI-MS) were conducted by Tawfic, A.F. The analysis of the results was conducted by Tawfic, A.F. in consultation with Dickson, S.E., Kim, Y., and Mekky, W. The text was written by Tawfic, A.F and edited by Dickson, S.E., Kim, Y., and Mekky, W.

Chapter 5

Title: Graphite Electrode as an Electrically Switched Ion Exchange

Authors: Tawfic, A.F., Dickson, S.E., Kim, Y., and Mekky, W.

To be submitted in November 2014.

The experiments were designed and conducted by Tawfic, A.F. The preparation of the two graphite electrodes, the film preparation by adsorption, the film characterization using cyclic voltammetry and X-Ray tomography, and the electrode capacity measurements by electrospray ionization-mass spectroscopy (ESI-MS) were conducted by Tawfic, A.F. The analysis of the results was conducted by Tawfic, A.F. in consultation with Dickson, S.E., Kim, Y., and Mekky, W. The text was written by Tawfic, A.F. and edited by Dickson, S.E., Kim, Y., and Mekky, W.

Chapter 6

Title: Nickel Hexacyanocobaltate as an Electrically Switched Ion Exchange

Authors: Tawficm A.F., Dickson, S.E., Kim, Y., and Mekky, W.

To be submitted in November 2014.

The experiments were designed and conducted by Tawfic, A.F. The graphite electrode surface preparation, the film preparation by adsorption, the film characterization using cyclic voltammetry, and the electrode capacity measurements by electrospray ionization-mass spectroscopy (ESI-MS) were conducted by Tawfic, A.F. The analysis of the results was conducted by Tawfic, A.F. in consultation with Dickson, S.E., Kim, Y., and Mekky,

W. The text was written by Tawfic, A.F and edited by Dickson, S.E., Kim, Y., and Mekky, W.

Permission has been granted to McMaster University by *Journal of American Nuclear Society* to reproduce material in Chapter 3 as part of this thesis. The material in chapter 2, 4, 5 and 6 has been prepared to be submitted in November 2014, and copyright has not been assigned.

Glossary

Bq	Becquerel
IAEA	International Atomic Energy Agency
HLW	High level waste
LLW	Low level waste
NRC	Nuclear Regulatory Commission
PUREX	Plutonium uranium extraction
TRUEX	Trans uranic extraction
TRAMEX	Transition metal extraction
IX	Ion exchange
ESIX	Electrically switched ion exchange
PPy	Polyprrole
PB	Prussian blue
E_{pf}	Potential of forward peak
E_{pr}	potential of return peak
E_{λ}	potential value at the inversion of the scan direction
i_{pf}	current of the forward peak with respect to its baseline
i_{pr}	current of the return peak with respect to its baseline
ΔE_p	peak to peak separation
$(i_{pr})0$	current of the return peak with respect to the zero current baseline
$(i_f)0$	current at the inversion potential with respect to the zero current baseline
EQCM	Electrochemical quartz crystal microbalance
PAR	Princeton Applied Research
SCE	Saturated Calomel Electrode
NiHCF	Nickel Hexacyanoferrate
PNNL	Pacific Northwest National Laboratory
BV	Bed volume
CNTs	Carbon Nanotubes
MWCNT	Multiwalled carbon nanotubes
EMD	Egyptian Ministry of Defence
NSERC	Natural Science and Engineering Research Council of Canada
PANI	Polyaniline
SHE	Standered Hydrogen Electrode

Table of Contents

List of Tables

List of Figures

Chapter 1

Introduction

1.1 Background

Radioactive Cs^{137} is of great importance as it has a reasonably long half life time (30.2 years), is highly radioactive, and is one of the primary fission products from the decay of U^{235}, which is used for power generation. It can also be used as an excellent source of gamma radiation for food preservation, sterilization of medical accessories, and in nuclear research facilities (Chen et al., 2013; Hao et al., 2008).

In March 2011, a massive tsunami hit Fukushima, Japan, and a local nuclear power plant was damaged. Thousands of tons of water were contaminated with Cs^{137}, causing grave human health concerns with the release of a vast quantity of highly radioactive material (Chen et al., 2013). Since Cs^+ is chemically similar to Na^+, it is just as easily dispersed in water and ingested by animal life. If it is ingested, it can travel throughout the body and accumulating in soft tissue, causing harm to the reproductive system as well as cellular functions (Chen et al., 2012; Shakir et al., 2007)

As Cs^{137} makes up a significant portion of radioactive waste, it is ideal to have it separated and removed from radioactive waste in order to increase the safety and management of high level radioactive waste deep underground (Li et al., 2012; Mohapatra et al., 2006).

Several techniques are used for the separation of Cs^{137} including precipitation, solvent extraction, sorption, and conventional ion exchange (IX) (Shakir et al., 2007). The focus of the work in this thesis is on the use of a specific method of ion exchange.

Conventional ion exchange (IX) is widely used for Cs^{137} separation before the final disposal of radioactive waste. The IX process produces a lot of secondary waste during the separation, however, and the elution process and the IX regeneration process are slow and expensive, as they consume large amounts of acids and alkali solutions. After numerous cycles of the ion exchange of Cs^+, the resins need to be replaced, and the old resins which are considered as a secondary radioactive waste need to be disposed of, as well as the radioactive waste itself (Borai et al., 2009). The notion and development of an electrically switched ion exchange (ESIX) technology for Cs^+ separation was put first by Lilga et al. as early as 1997.

In this technology, ion exchange and electrochemistry are combined to produce an effective process for the selective separation of Cs^+. This process produces a minimum amount of secondary waste: only that which is generated from the regeneration process of the IX and the associated rinse water, with the underlying substrate for the ion exchange being reused, are radioactive. The regeneration of this process occurs by electric current (Lilga et al., 1997; Lilga et al., 2001).

The main component of the ESIX process is metal hexacyanoferrate (MHCF) (Lilga et al., 1997; Lilga et al., 2001). This is an inorganic material from the Prussian blue family and known for its selectivity with regard to Cs^+. The MHCF is electrically deposited on the surface of a conductive substrate in order to be used as an ESIX film. Cs^+ loading and unloading from the surface of the film is controlled by changing the redox state of the deposited film on the substrate surface (Gomez et al., 2004).

This research will demonstrate the improvement of an existing ESIX film as discussed in the literature by preparing a nickel hexacyanoferrate film on nickel substrate using new preparation parameters, which results in an ESIX film of high ability and capacity for Cs^+ removal. Also demonstrated is the usage of graphite electrodes as the conductive substrate for nickel hexacyanoferrate electrodeposition to create a substantially larger capacity ESIX electrode.

Finally, the testing of a new ESIX material, nickel hexacyanocobaltate was deposited as an ESIX film within a graphite electrode, producing an ESIX electrode that was able to perform ESIX with Cs^+. This electrode shows good performance in Cs^+ separation. It suffered from a lower charge capacity than the other graphite ESIX electrode composed of nickel hexacyanoferrate, but it also shows a good durability for Cs^+ separation during running cycles.

1.2 Thesis Objectives

The goal of this research was to develop an ESIX process for Cs^+ separation by enhancing the film capacity and efficiency for previously prepared ESIX films and to introduce a new ESIX film material for Cs^+ separation. To achieve this goal research tasks were developed to address the following objectives:

1- Examine the ESIX process in Cs^+ separation. This was done by preparing an ESIX film according to a literature review (Chapter 3).

2- Enhance Cs^+ separation using ESIX film by increasing the capacity and efficiency of the prepared film. This objective was done by modifying the ESIX (Chapters 3, 4).

3- Prepare the nickel hexacyanoferrate ESIX films on a graphite substrate to enhance ESIX capacity and efficiency for Cs^+ separation. This was done by adsorbing the nickel hexacyanoferrate material throughout a porous graphite electrode (Chapter 5).

4- Introduce a new ESIX film material nickel hexacyanocobaltate for Cs^+ separation. This material was also adsorbed inside a graphite electrode. As a result, an ESIX electrode was prepared for CS^+ separation (Chapter 6).

5- Calculate the film's maximum charge capacity, the electrode surface/volume coverage of the ESIX material, as well as its ability to separate Cs^+ from test solution in order to monitor them as the performance metrics throughout these experiments. The electrode morphologies were also visualized using scanning electron microscopy and x-ray tomography (Chapters 4, 5, and 6).

1.3 Thesis Overview

The thesis has been prepared according to the McMaster university regulations for theses consisting of previously published/prepared materials. Thus, the following chapters 2-6 consist of papers accepted to be published in or prepared for academic journals. Each paper has its own introduction. As such, background material concerning electrically switched ion exchange (ESIX) is repeated in chapters 3-6. The chapters are presented as they will appear in the journal papers, but the text format and heading, figure, table, and equation numbering have been changed to be consistent with this thesis.

Chapter 2 describes a literature review on ESIX, the fundamentals of its operation and the current developments for this technology. Chapter 3 describes the experiments used to enhance the ESIX process for Cs^+ separation through the preparation of ESIX film made of nickel hexacyanoferrate on a nickel substrate. Chapter 4 describes the experiments used to prepare four different ESIX films made of nickel hexacyanoferrate on a nickel substrate and compares their performance using the metrics previously described. Chapter 5 describes the experiments used to prepare ESIX film made of nickel hexacyanoferrate on two graphite electrodes. The results shows variation in the values related to Cs^+ separation. Chapter 6 describes experiments used to prepare new ESIX film material nickel hexacyanocobaltate also using a graphite electrode as a substrate and details its characterization.

1.4 References

Borai, E., Harjulab, R., Leena, Malinenb, Paajanenb, Airi, 2009 “Efficient removal of cesium from low-level radioactive liquid waste using natural and impregnated zeolite minerals” *Journal of Hazardous Materials* 172, PP 416–422.

Chen, Rongzhi., Hisashi, Tanaka., Tohru, Kawamoto., Miyuki, Asai., Chikako, Fukushima., Masato, Kurihara., Masayuki, Watanabe., Makoto, Arisaka., Takuya, Nankawa., 2012 “Preparation of a film of copper hexacyanoferrate nanoparticles for electrochemical removal of cesium from radioactive wastewater” *Electrochemistry Communications* 25, PP 23–25.

Chen, Rongzhi., Hisashi, Tanaka., Tohru, Kawamoto., Miyuki, Asai., Chikako, Fukushima., Masato, Kurihara., Masayuki, Watanabe., Makoto, Arisaka., Takuya, Nankawa., 2013 “Thermodynamics and mechanism studies on electrochemical removal of cesium ions from aqueous solution using a nanoparticle film of copper hexacyanoferrate” *American Chemical Society Appl. Mater*. Interfaces 5, PP 12984−12990.

Chen, Rongzhi., Hisashi, Tanaka., Tohru, Kawamoto., Miyuki, Asai., Chikako, Fukushima., Masato, Kurihara., Masayuki, Watanabe., Makoto, Arisaka., Takuya, Nankawa., 2013 “Selective removal of cesium ions from wastewater using copper hexacyanoferrate nanofilms in an electrochemical system” *Electrochimica Acta* 87, PP 119–125.

Gomez J. Reyes., Antonio, J., Medina., , Kavita M., Jeerage, William, A., 2004 “High capacity SiO_2-graphite composite electrodes with chemically incorporated metal MHCFs for electrochemically switched alkaline cation exchange” *Journal of The Electrochemical Society* 151, PP D87-D92.

Hao, Xiaogang., Yongguo, Li., , Mark, Pritzkerb., 2008 “Pulsed electrodeposition of nickel hexacyanoferrate films for electrochemically switched ion exchange” *Separation and Purification Technology* 63, PP 407–414.

Li, Na., Zhongjie, Li., Junhua, Yuana., 2012 “Nickel hexacyanoferrate nanoparticles anchored to multiwalled carbon nanotubes with a grafted poly(4-vinylpyridine) linker for electrically switched ion exchange” *Electrochimica Acta* 72, PP 150–156.

Lilga M.A., Orth, R.J., Sukamto, J.P.H., Haight, S.M., Schwartz, D.T., 1997 “Metal ion separations using electrically switched ion exchange” *Separation and Purification Technology* 11, PP 147-158.

Lilga M.A., Orth, R.J., Sukamto, J.P.H., Rassat, S.D., 2001 “Cesium separation using electrically switched ion exchange” *Separation and Purification Technology* 24, PP 451–466.

Mohapatra, P.K, Ansari, S.A., Sarkar, A., Bhattacharyya, A., Manchanda, V.K., 2006 “Evaluation of calix-crown ionophores for selective separation of radio-cesium from acidic nuclear waste solution” *Analytica Chimica Acta* 571, PP 308–314.

Shakir K., Sohsah, M., Soliman, M., 2007 “Removal of cesium from aqueous solutions and radioactive waste simulants by coprecipitate flotation” *Separation and Purification Technology* 54, PP 373–381.

Chapter 2

Electrical Switched Ion Exchange

The contents of this chapter will be submitted to a journal in November 2014 as: Tawfic, A.F., Dickson, S.E., Kim, Y., and Mekky, W., 2014. Electrical Switched Ion Exchange

Abstract

Electrical switched ion exchange (ESIX) is an electrochemical method used in metal ion separation, which has typically been used for cesium (Cs^+) separation from nuclear waste. The ESIX method is based on a nickel hexacyanoferrate complex that is selective to group one elements in the periodic table, particularly Cs^+. This review paper discusses the development of the ESIX process and its evolution from a single-use nickel hexacyanoferrate rod through to the nickel hexacyanoferrate electrode, which can be regenerated but loses approximately 20% of its capacity every 2000 cycles. Recent developments in the ESIX process occurred with the formation of nanotubes from the nickel hexacyanoferrate complex, which led to increasing its capacity for Cs^+ removal due to the increased surface area. The primary drawback of the ESIX process as it stands now is that it is selective to group one element, as it has no ability to select elements from group two in the periodic table.

2.1 Introduction

Nuclear power plants supply approximately 14% of the global electricity and are a source of renewable energy (Chapman et al., 2012; Sellier et al., 2011). A serious drawback to nuclear energy, however, is the disposal of spent nuclear fuel due to the radioactive elements it contains. Nuclear waste is categorized according to its level of radioactivity measured in Becquerels (Bq).

Radioactive waste is classified into two categories: 1) high level waste (HLW) (4000 Bq/g or more); and 2) low level waste (LLW) (less than 4000 Bq/g) (IAEA, 1994; Baisden et al., 2004; Gustavo, A. et al., 2000).

HLW includes spent fuel resulting from reprocessed plutonium and uranium from solid irradiated fuel rods and the isolation of fissile radionuclides from irradiated materials associated with nuclear weapons production (Reynolds et al., 2012; Technical Training Center, 2004; Baisden et al., 2004; Runchal et al., 1985). LLW is further categorized into four classes: Class A, Class B, Class C, and Greater than Class C (IAEA, 1994; IAEA., 2004; Stuart et al., 1995; Baisden et al., 2004; Allard et al., 2012; Valsala et al., 2011; Katz et al., 2001).

Class A emits low levels of radiation and heat, requires no shielding, and should decay within 100 years. Class B emits higher radioactivity and requires greater isolation and shielding than Class A waste. Class C requires isolation from the biosphere for 500 years and must be buried at least 5m below Earth's surface. Greater than Class C contains transuranic material with a half-life greater than five years, an activity greater than 37 x 10^6 Bq /g, and must be buried a minimum of 200m below the surface.

LLW can be in the form of a solid, liquid, or gas (Solomon et al., 1982; Gonzallez et al., 2011) and is generated by the nuclear energy industry, research laboratories, and hospitals using radionuclides for diagnostic and therapeutic procedures. The LLW generated by the nuclear energy industry includes the reactor coolant (water), any materials coming into contact with the coolant, and byproducts from the Plutonium uranium extraction (PUREX) separation process. This waste typically does not exceed 100 Bq/g (Lacoste et al., 1997). Research laboratory and hospital LLW includes materials such as paper, rags, tools, protective clothing and filters that are contaminated due to exposure to radiation (IAEA., 2004; Baisden et al., 2004).

This type of waste does not require shielding; it is handled using the 'delay to decay' and 'dilute and disperse' principles. The waste generated by biomedical laboratories and nuclear medicine services typically has the most variable radiochemical composition due to the variety of radionuclides used (H^3, C^{14}, S^{35}, p^{32}, I^{125},Tc^{99}) (Choi et al., 2011; Shia et al., 2012; Higgy et al., 1977).

The total volume of nuclear waste at the Hanford site in the USA is 11,000,000m^3 of fluid and weighs 6900 metric tons (Reynolds et al., 2012; Niculae et al., 2009). The activity of this waste is estimated to be 1,6502 x 10^{13} Bq. Several technologies exist for pretreating or separating radioactive elements from HLW fission products to concentrate radioactive elements, and therefore produce smaller volumes of waste requiring highly specialized long term storage (Barc., 2003). These pretreatment processes are very specific to the waste, making detailed knowledge of the waste composition a requirement.

2.1.1 Separation Processes

The PUREX process employs a tri-butyl phosphate and kerosene solution to separate UO_2^{2+} and PU^{4+} from fission products, leading to separations of 70% of UO_2^{2+} and PU^{4+} or greater (Pusch et al., 2012; Nishad et al., 2012; Qafoku et al., 2010). The Transuranic extraction (TRUEX) process uses octyl (phenyl)-N,N-dibutyl carbamoyl-methlphosphine oxide in an alkane solvent to selectively extract transuranic elements from acidic solutions. The transition metal extraction (TRAMEX) process employs liquid cation exchangers such as tri-alkyl amines and tetra-alkyl ammonium salts dissolved an organic solvent to provide high selectivity in the separation of tri- and tetra-valent actinides from most fission products (Thakur et al., 2012; Ansari et al., 2009; Yuehelin et al., 2006).

A series of novel extraction chromatographic resins have been developed to selectively remove the nitrate complexes from actinides and uranium, which are ideal for process-scale nuclear waste treatment (Horwitzav et al., 1995; Cantlon et al., 1997; Poskas et al., 2012). The development of new extractants for the recovery of minor actinides (^{237}Np, ^{241}Am, ^{243}Am, ^{244}Cm, ^{246}Cm and Cr^{3+}) from HLW is an area of active research (Ansari et al., 2009; Watson et al., 2012; Rana et al., 2004). Hollow fiber-supported liquid membranes have also shown promise for separating of Am(III) and trivalent lanthanides and actinides from HLW, (Ambashta et al., 2012; Ansari et al., 2008; Raut et al., 2012; Alkhudhiri et al., 2012).

Radioactive cesium (^{137}Cs) is one of the most important fission products generated by nuclear power reactors and is frequently found in aqueous radioactive waste. One of the most practical methods of separating ^{137}Cs from nuclear waste is to incorporate it into hexacyanoferrate and, subsequently, to co-precipitate the metal ferrocyanide (Shakir et al., 2007; Valsala et al., 2009; Singh et al., 2009; Espinosa et al., 2012). This treatment process is typically achieved through ion exchange (IX). A drawback of this technology, however, is that a large volume of secondary waste is generated due to the numerous steps required by the process (sodium loading of the exchanger and acid elution). Further, the organic exchangers lose approximately 3% of their capacity per cycle and are therefore only useable for 20 to 30 cycles before they also become secondary waste (Lilga et al., 1997; Crooks et al., 1994; McDeavitt et al., 1998).

Electrically switched ion exchange (ESIX) was developed for separating ^{137}Cs from nuclear waste to address the secondary waste issue by reducing the number of process steps required (Rassat et al., 1999; Lilga et al., 1997; Lilga et al., 2001). ESIX combines the ion exchange process with electrochemistry to develop a reversible and selective separation technique. It is also highly energy efficient, requiring less than two volts for the uptake and elution of selected ions. The major drawback of the ESIX process is that it is currently limited to group one element with the selectivity order as follows: Cs^+ - Na^+ and K^+ - Na^+.

The ESIX process involves the electrochemical deposition of an electroactive IX film onto an electrode with a large surface area. The IX (ion uptake and elution) is controlled by modulating the potential of the film. The fact that Cs^+ can be eluted into the same solution many times without adding any chemicals enables this process to produce a relatively small volume of secondary waste. The ratio of the volume of secondary waste generated to the volume of waste processed is approximately 0.0006 % (Lilga et al., 1997; Lilga et al., 2001).

Ferrocyanide films are typically employed for Cs^+ separation. When a cathodic potential is applied to the film, however, Fe^{3+} is reduced to Fe^{2+} and a cation (i.e.. Cs^+) is intercalated into the film to maintain charge neutrality. Conversely, when an anodic potential is applied, Fe^{2+} is oxidized to Fe^{3+} and a cation (i.e Cs^+) is released from the film to maintain electroneutrality (Hao et al., 2008; Akieh et al., 2010; Inamuddin et al., 2010). Other compounds, such as conducting polymers, have also been employed in the ESIX process. Polyprrole (PPy), for example, has been used because of its electro-activity, which enables it to undergo reversible oxidation and reduction under electrochemical simulation similar to the Fe-based films. The PPy films load and unload cations onto the conductive polymer backbone under reduction and oxidation conditions respectively (Lin et al., 2006; Akieh et al., 2010; Rosa et al., 2010).

Ionic strength, pH, electric field, temperature, and photo irradiation all control the transport and separation of ions in composite membranes. The pH is adjusted to control the transport of the target ions through the solution while the electric field is altered to control the selectivity of the composite membrane to the target ion (Honda et al., 2011; Uruga et al., 2008; Katsounaros et al., 2009; Tan et al., 2010).

2.2 ESIX Film Analysis and Preparation

2.2.1 Analysis of ESIX film

Figure 2.1 shows a typical cyclic voltammetry curve, current versus potential, used to determine the potential at which the redox process will occur. This curve is also useful for determining the concentration of the active species, which are normally proportional to the size of the current generated by the relative faradic processes. Finally, the shape of the response as a function of the potential scan rate reveals any chemical complications accompanying the electron transfer process (Rieger., 1987; Pierozanello et al., 2012).

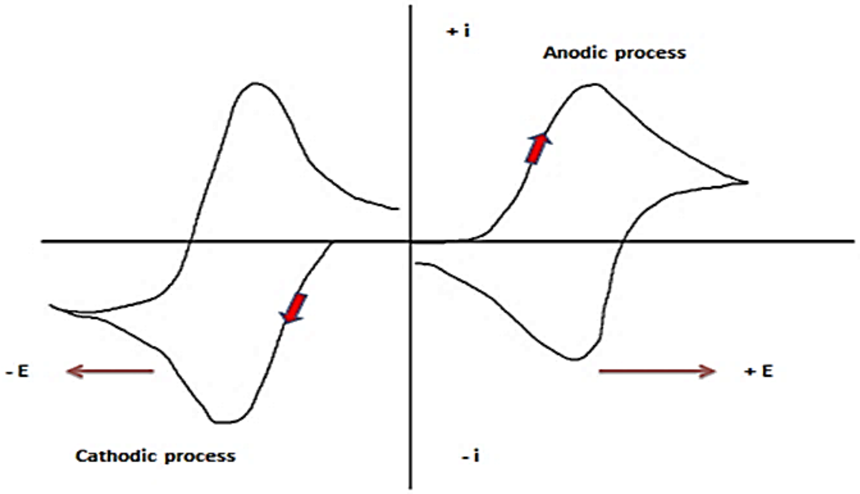

Figure 2.1: Conventional signs of currents and potential in cyclic voltammetry (source: Pierozanello et al., 2012).

Figure 2.2 shows the ratio of the currents of the reverse forward peaks, i_{pr}/i_{pf}, which enable the determination of the reversibility of the reaction. The electro-generated species are stable if the ratio is equal to one. The potential of the forward peak, $E_{pf,}$ is independent of the scan rate, which is the applied potential with respect to time. The peak to peak separation, ΔE_p, relates to the electrochemical reversibility of an electrode reaction (Rieger., 1987; Pierozanello et al., 2012).

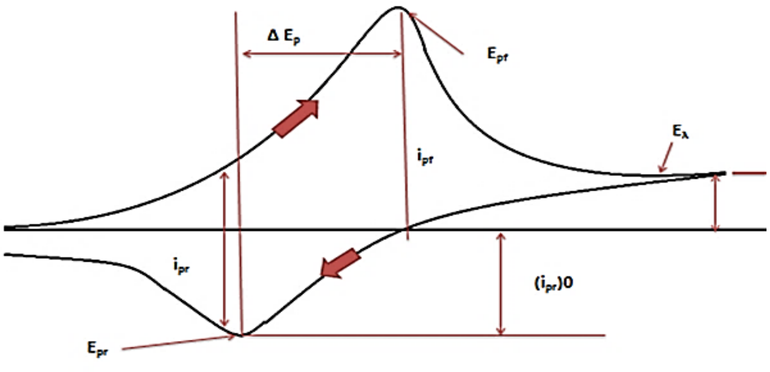

Figure 2.2: Basic parameters of a cyclic voltammogram (source: Rieger et al., 1987).

2.2.2 ESIX Film Preparation

Nickel hexacyanoferrate films are produced from ferric ferricyanide mixtures on a pre-cathodised platinum substrate or on non-cathodised gold (Pierozanello et al., 2012), covering more than 97% of the metal substrate. The derivatized nickel electrodes are fabricated by allowing a clean nickel wire to react with an acidic $K_3Fe(CN)_6$ solution, yielding an electrode surface consisting of a cyanide bridged nickel ferrocyanide polymer (Koryta et al., 1984; Sinha et al., 1984; Koryta et al., 1990). The reaction between nickel electrode surfaces and anionic metal cyanide complexes leads to the precipitation of aqueous Ni^{2+} onto Ni electrodes (Honda et al., 2011). Ni(II)hexacyanoferrate(III,II) films are produced by cycling the potential between 0 and 0.85 V at a rate of 50 $mV\cdot s^{-1}$ for five minutes in a freshly prepared colloidal mixture. The colloidal mixture is prepared by the consecutive mixing of 20 mL of 1 M KNO_3 (at pH 2) with 10 mL of 2 mM $K_3Fe(CN)_6$, 10 mL of 2 mM $AgNO_3$, and 10 mL of 2 mM $NiCl_2$. The ferricyanide is reduced to ferrocyanide in the presence of Ag^+ and Ni^{2+}, (Pawel et al., 1989; Jagadish et al., 1992). The deposited film demonstrates cation selectivity. The anionic metal cyanide complexes employed in these reactions include ($Ru(CN)_6^{-3}$ – $Fe(CN)_6^{-3}$ - ($Fe(CN)_6^{-x}$ $L_x)^{-n}$ – $Mn(CN)_6^{-3}$).

2.3 Nickel Hexacyanoferrate Electrodes

Sinha et al. (1986) precipitated a polycrystalline lattice composed of Ni^{2+} and $(metal)^{2+/3+}$ onto a one cm^2 nickel plate electrode using 0.63 mm diameter Ni wires. Surface corrosion of the electrode surface was inhibited by adding a small amount of the anion complex to the solution to be treated, which also enhanced the charge transfer reaction.

Bhcskai et al. (1995) prepared a polynuclear hexacyanoferrate film on a gold substrate by electrodeposition; the potential was cycled at 25 mV/ s between 0.85 and 0 V for approximately 15 min in a solution mixture of 0.002 M $K_3Fe(CN)_6$, 0.002 M $NiSO_4$, and 0.5 M K_2SO_4. In a second modification to the approach, the gold substrate was dipped at the electrolyte for a longer period of time (more than 30 min). The steady growth of the film is shown in figure 2.3, where the film's formation is related to potential cycling applied in the preparation solution mixture.

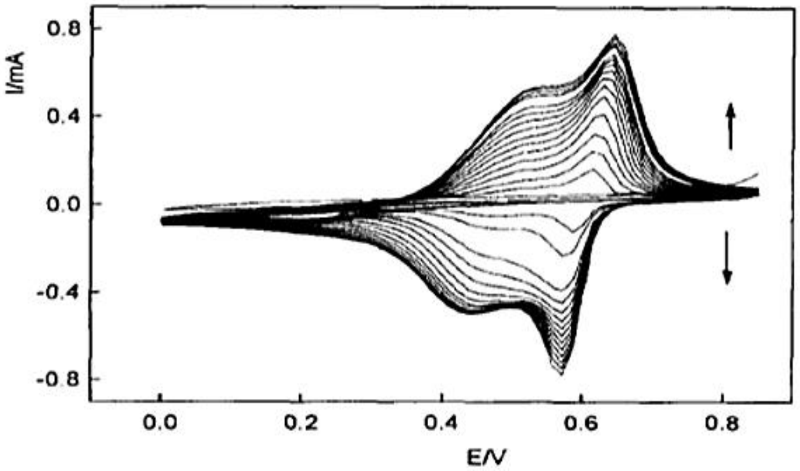

Figure 2.3: Film growth (source: Bhcskai et al., 1995)

Sinha et al. (1984) monitored the growth of a NiHCNFe film on a gold substrate during using an electrochemical quartz crystal microbalance (EQCM). Figure 2.4 shows the EQCM frequency versus time for the film, which is growing at a steady rate on the electrode surface. The coagulation approach is slower than electro-deposition rate resulting a loading nearly 1/6 of the electrodeposited film (Bhcskai et al., 1995).

The actual growth of the film occurred during the reductive potential scans, where the $Fe(CN)_6^{3-}$ component is reduced to $Fe(CN)_6^{4-}$ and instantaneously reacts with Ni^{2+} to yield sparingly soluble nickel(II) hexacyanoferrate(II), which is deposited onto the electrode surface. Since the precipitation proceeds in the presence of potassium ions, which can pair with ferrocyanide, it is unlikely that the precipitate is simply $Ni_2^{II}Fe^{II}(CN)_6$ (Bhcskai et al., 1995).

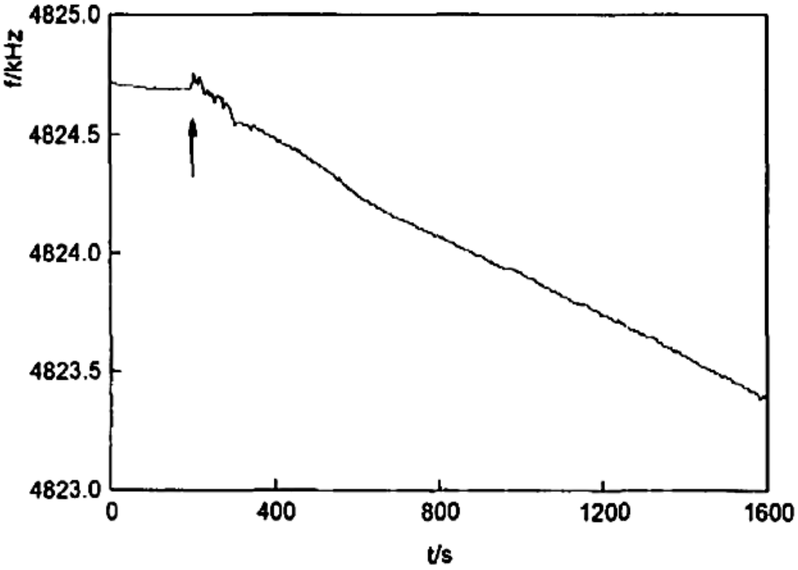

Figure 2.4 : EQCM frequency versus time (source: Bhcskai et al., 1995)

The primary drawback of the methods developed by Bhcskai et al. (1995) and Sinha et al. (1984) is that the columns cannot be regenerated, and thus the technology produces a large amount of secondary waste.

Lilga et al. (1997) developed ESIX to address the issue of secondary waste in electrochemical metal ion separation through enabling repeated loading and unloading of the film. Figure 2.5 is a schematic diagram of the ESIX process. It shows an ion exchange (IX) film electrochemically deposited on a high surface area electrode with ion uptake and elution controlled through modulating the potential of the film.

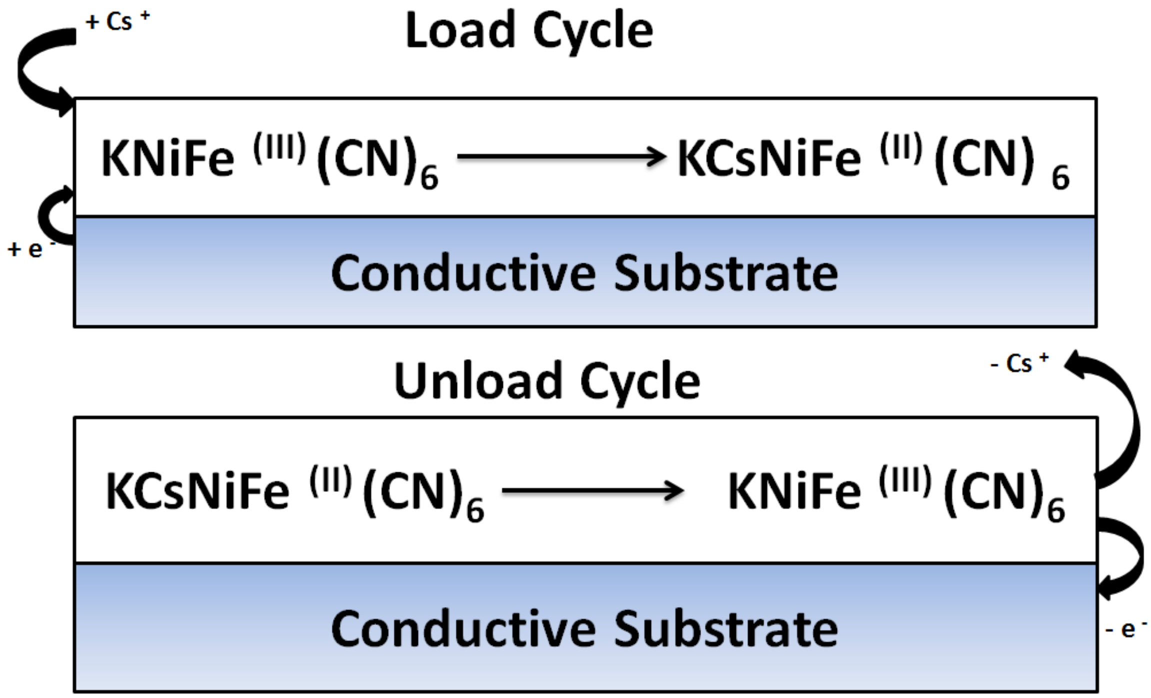

Fig 2.5: A schematic diagram of the ESIX process (source: Lilga et al., 1999)

Ligla et al. (1999) used a potentiostat / galvanostat to both deposit and characterize films on nickel electrodes. A 99.98% pure nickel substrate was exposed to a solution of 5 mM$K_3Fe(CN)_6$, and 0.1 M KNO_3. A 1.0 V (SCE) potential was applied to the nickel electrode for 300s. This method is referred as a “literature method.” A slightly modified method was also developed, requiring the application of 0.65 V for 10 min., followed by 1 V for 30 min., and was then used to prepare a film. Two additional modifications were made resulting in films referred to as PNNL-1 and PNNL-2. The preparation technique for these films was not disclosed in this work, however (Ligla et al., 1997; Ligla et al., 1999).

Equation 2.1 represents the oxidation of ferricyanide to ferrocyanide and how it loses an electron and thus helps in the unloading of the metal ion. Equation (2.2) represents the reduction of ferrocyanide to ferricyanide by gaining an electron, which leads to the loading of a metal ion (M^+) from the solution.

$$(M)_2NiFe^{II}(CN)_6 \longrightarrow (M)NiFe^{III}(CN)_6 + e^- + (M^+) \qquad (2.1)$$

$$(M)NiFe^{III}(CN)_6 + e^- + (M)^+ \longrightarrow (M)_2NiFe^{II}(CN)_6 \qquad (2.2)$$

Figure 2.6 shows a CV for the films prepared using the literature method, PNNL-1 and PNNL-2, and shows that the metal ion loading and unloading is controlled by modulating the electrode potential. It further demonstrates that the processes in equations 2.1 and 2.2 are chemically reversible.

The films in figure 2.6 are in the reduced state (i.e. they are loaded). The peak current in the unloading of sodium from the film was 400 mV; the current approached 0 at 800 mV as ferrocyanide was oxidized to ferricyanide. The peak current occurred at approximately 350 mV as ferrocyanide was reduced. These films are relatively simple to prepare and have a high selectivity to cesium in the presence of other transition elements. The films have both high capacity and good stability (Lilga et al., 1999).

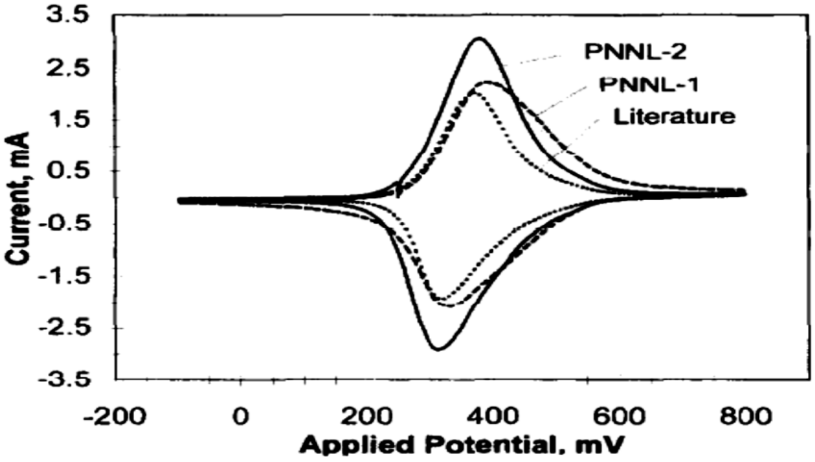

Figure 2.6 CV in 1 M $NaNO_3$ of hexacyanoferrate films prepared by three different methods (source: Lilga et al., 1999)

Figure 2.7 shows PNNL-1 after one, 1000, and 2000 loading and unloading cycles, and clearly demonstrates that repeated cycling results in a loss of capacity. By modifying the deposition procedure, however, the stability of the film is improved. The maximum charge passed for several film preparations as a function of cycle number was measured (Lilga et al, 1998).

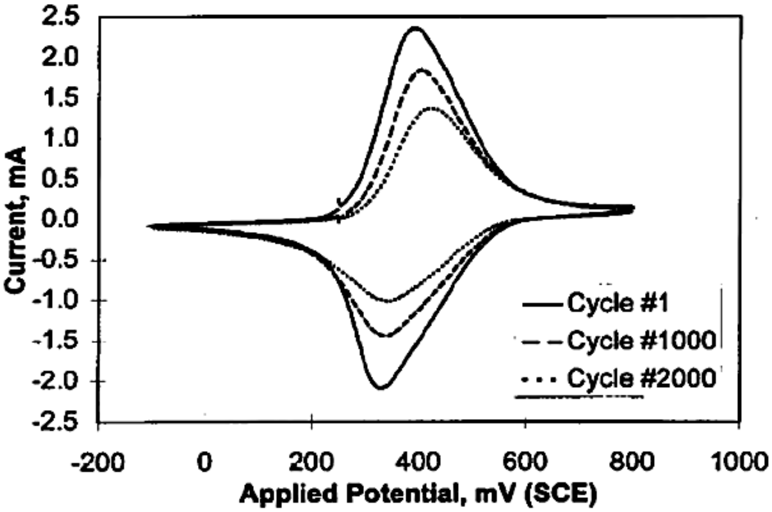

Figure 2.7: Repeated potential cycling of PNNL-1 (source: Lilga et al., 1998)

Rassat et al. (1999) developed an ESIX process for selective ion separation. The selectivity of nickel hexacyanoferrate (NiHCF) was determined using CV and a quartz crystal microbalance to quantify ion uptake in the film. Separation factors indicated a high selectivity for Cs^+ and a moderate selectivity for K^+ in high Na^+ content solutions. Figure 2.8 is a schematic diagram of the selective ESIX process. One electron is required per alkali cation exchanged into the electroactive material, which typically requires less than 2 V.

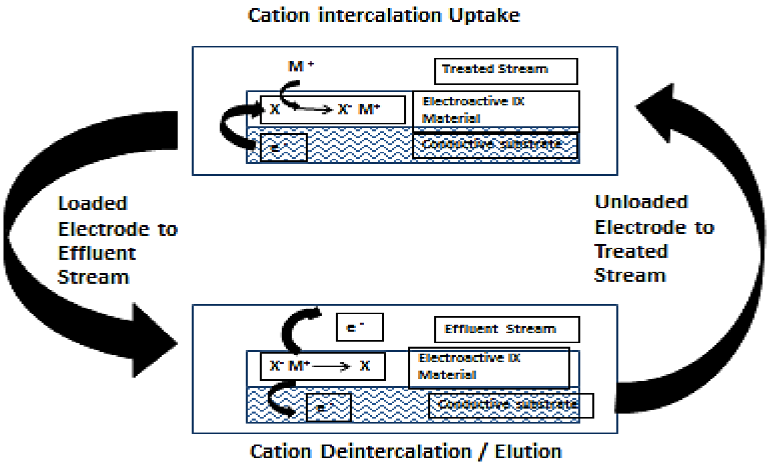

Figure 2.8: Schematic diagram of the selective ESIX process (source: Rassat et al., 1999)

Figure 2.9 shows the CV and after one, 1000, and 2000 loading and unloading cycles and demonstrates a clear decrease in cation loading capacity as a function of cycling. After 2,500 and 2000 cycles, the measured capacity is 3.1 x 10^{-8}, 2.7 x 10^{-8} and 1.7 x 10^{-8} mol·cm^{-2} respectively. The separation of the anodic and cathodic peak potentials in the 2000th cycle is greater (about 75 mV) than in the earlier cycles (from 25 to 40 mV), which shows that the film reaction starts to be quasi reversible.

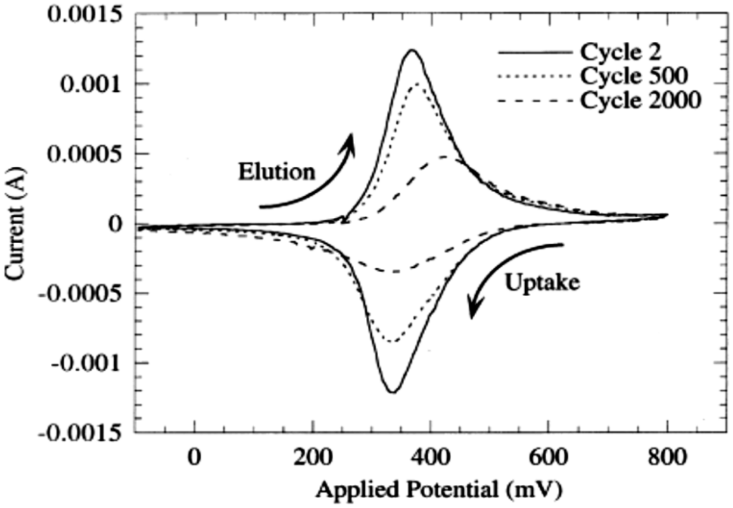

Figure 2.9: CVs showing the decreased capacity with increasing number of loading and unloading cycles (source: Rassat et al., 1999)

Figure 2.10 shows the CV for (a) the literature NiHCF film deposited on a nickel rod, and (b) the PNNL-3 film for one, two, 50, and 2000 cycles. The biggest change between the PNNL-3 and literature films occurs in the second cycle, where additional current peaks occur at 590 mV on the anodic sweep and at 475 mV on the cathodic sweep. These new CV features shift the potential and increase the magnitude as the number of cycles increases (Lilga et al., 1997).

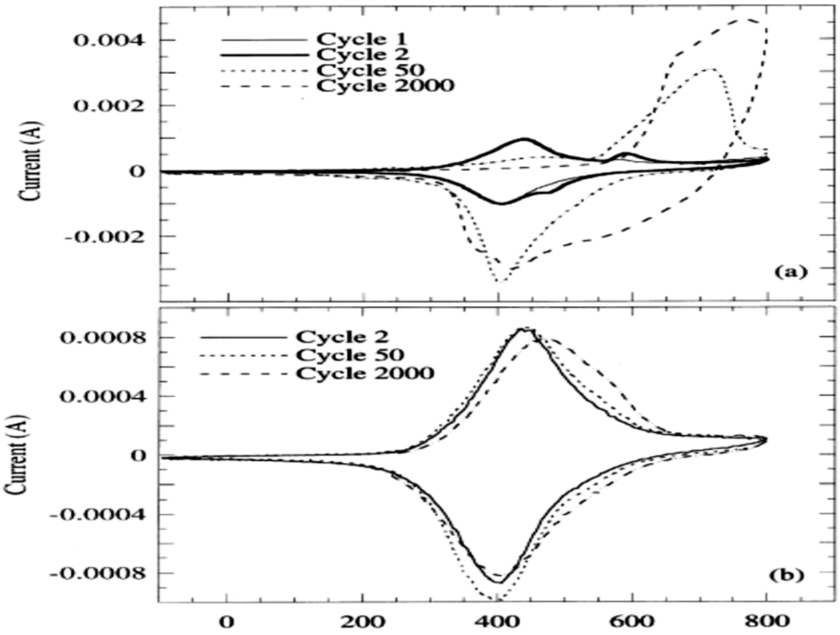

Figure 2.10 : CV in an electrostatic precipitator catch simulant solution: (a) a literature NiHCF film and (b) the PNNL-3 preparation (source: Lilga et al., 1997)

Lilga et al. (2001) employed nickel foam electrodes, with a surface area to volume ratio of 40 $cm^2 \cdot cm^{-3}$ (60 ppi), coated with nickel hexacyanoferrate. The nickel surface was exposed to a solution of 0.1 M KNO_3 and 5 mM $K_3Fe(CN)_6$ and a 1.0 V (SCE) potential was applied for 300 s. CV was conducted in 1 M $NaNO_3$ solution starting with an applied potential of 0.25 V, sweeping anodically to 0.8 V, then catholically to -0.1 V, and returning to 0.25 V at a scan rate of 50 mV/s. Chrono coulometry was conducted by stepping up to 0.25 V (SCE) and 0.5 V (SCE) to load and unload the film respectively.

The presence of Na^+ on the uptake of Cs^+ is shown in figure 2.11, which compares loading data for reduced films in contact with sodium-free cesium solutions and solutions containing Na/Cs molar ratios of 190 (0.01 M Na^+) and 17000 (1 M Na^+). The presence of Na^+ may slow the Cs^+ binding kinetics, since less Cs^+ was loaded after one hour.Overall capacity is not affected by Na^+, however, as very nearly the same loading was observed after 24 hours whether Na^+ was present or not.

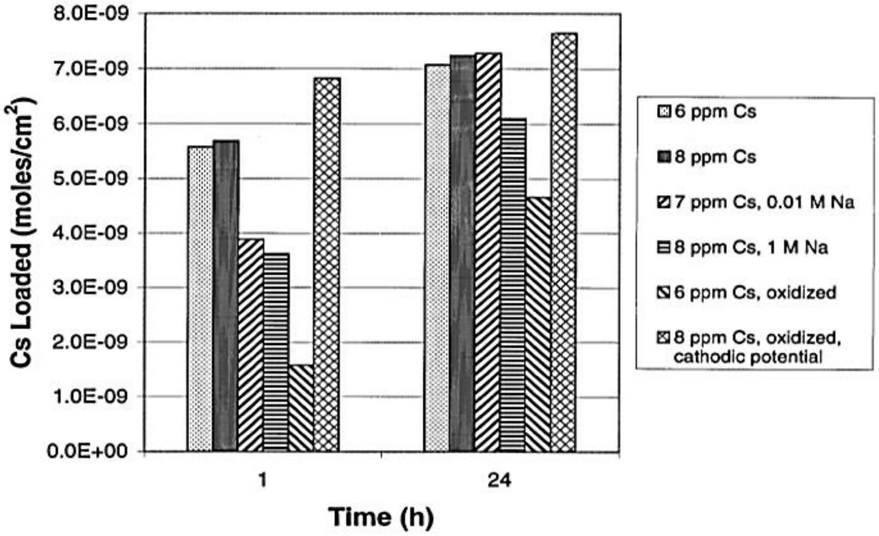

Figure 2.11: The effect of additional Na^+ and applied potential on Cs^+ uptake in batch experiments (source: Lilga et al., 2001)

Kertesz et al. (2002) formed a film from a solution containing potassium in excess. Figure 2.12 shows the CV obtained during preparation of a typical NiHCNFe modified electrode. The reversible peaks (peak 3 is the peak of $Fe^{III}(CN)_6^{-3}$- $Fe^{II}(CN)_6^{4-}$) were detected near +0.25 V during the first cycle. Two new reversible peak pairs (peak 1 and 2) appeared in the figure during cycles at +0.65 and +0.45 V. The growth of the film occurs in the reductive potential half-cycle where Ni (II) reacts with the reduced $Fe^{II}(CN)_6^{4-}$ on the electrode. Nickel hexacyanoferrate deposits on the surface of the electrode at the end of the cycle.

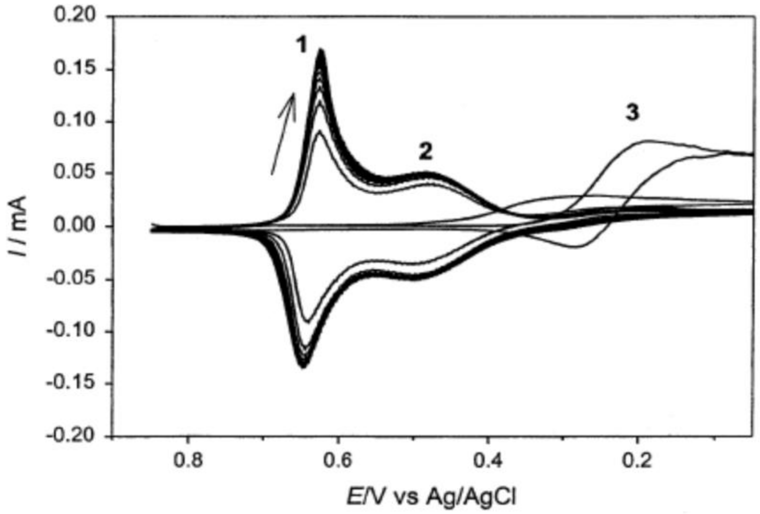

Figure 2.12: CV obtained during preparation of Ni-HCNFe from a solution with excess potassium (source: Kertesz et al., 2002)

Figure 2.13 shows (a) the Cs^+ signal as a function of time for 10 µmol /cm^3 Cs^+ solution with a non-modified working electrode, (b) the periodic uptake and release of Cs^+ by NiHCNFe modified electrode, and (c) the use of NiHCNFe modified electrode in a blank solution (0 µmol /cm^3 Cs^+). Figure (a) shows a steady signal indicating the presence of constant amounts of cesium in the solution. This data confirms that Cs^+ loading and unloading is reversible (Kertesz et al., 2002).

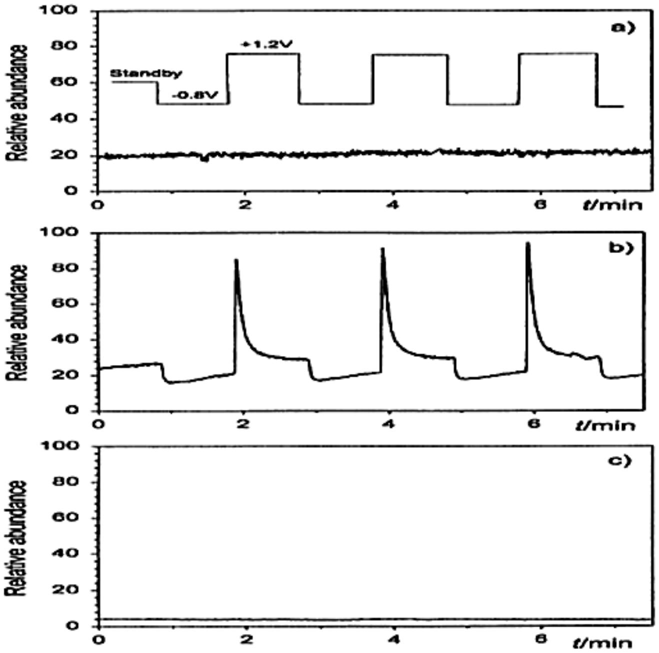

Figure 2.13: Cs^+ signal as a function of time (source: Kertesz et al., 2002)

Figure 2.14 presents the CVs for part films on platinum electrodes in 1 M KNO_3 solution. The positive currents correspond to the oxidation of NiHCF with K^+ intercalation from the matrix, and the negative currents denote the reduction with K^+ intercalation. This evidence shows that the different preparation procedures will lead to different CV shapes and different charge densities. Other CVs from Ni^{2+} show two comparable peaks and poor growth conditions 0.48 V and 0.6 V, separated by roughly 100 mV, (Hao et al., 2006).

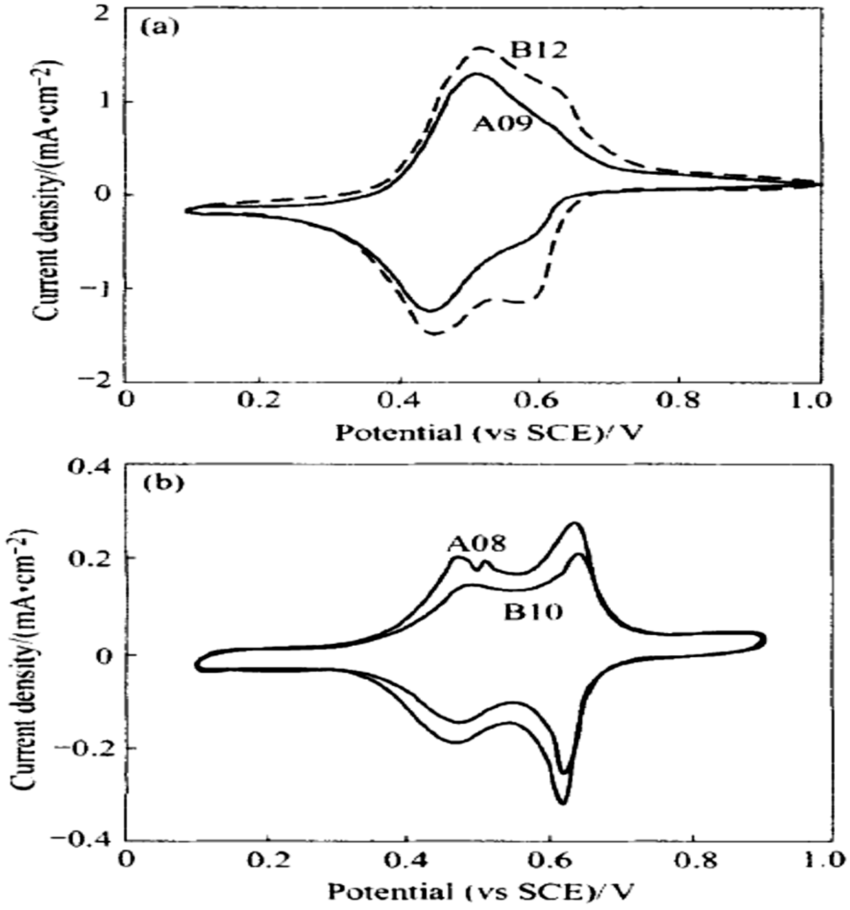

Figure 2.14: CVs for NiHCF thin films on Pt cycled in 1 M KNO_3, at 25 mV/s (source: Hao et al., 2006)

Honda et al. (2011) fabricated $Na_3Fe(CN)_5 \cdot H_2O$ electrolytes by dissolving $Na_3Fe(CN)_5NH_3$ in distilled water at pH 4. The $(Fe(CN)_5 \cdot H_2O)^{2-}$ solution was prepared by stirring a mixture of 50 mL of 0.2 M $Na_3Fe(CN)_5 \cdot H_2O$, 50 mL of 6% H_2O_2, and 2.3 grams of L-histidine in the dark for 45 minutes at approximately 5°C. MnO_2 was added as a catalyst at the end of the reaction to decompose the excess H_2O_2. The cyclic voltammetry curve for the film generated by Honda et al. (2011) is shown in figure 2.15.

The large peak width suggests intermolecular interactions of a repulsive nature. The Ni electrode surface shows good stability, but some deterioration in the amount of Ni surface attached to the film is noted after prolonged cycling (3000 cycles). The Ni/Fe(CN)$_6^{4-/3-}$ surface loses approximately 50% of its surface material after 3000 oxidation reduction cycles at 100 mV/s. This deterioration can be stopped by adding $(Fe(CN)_6)^{3-}$ to the electrolyte solution, however (Honda et al., 2011).

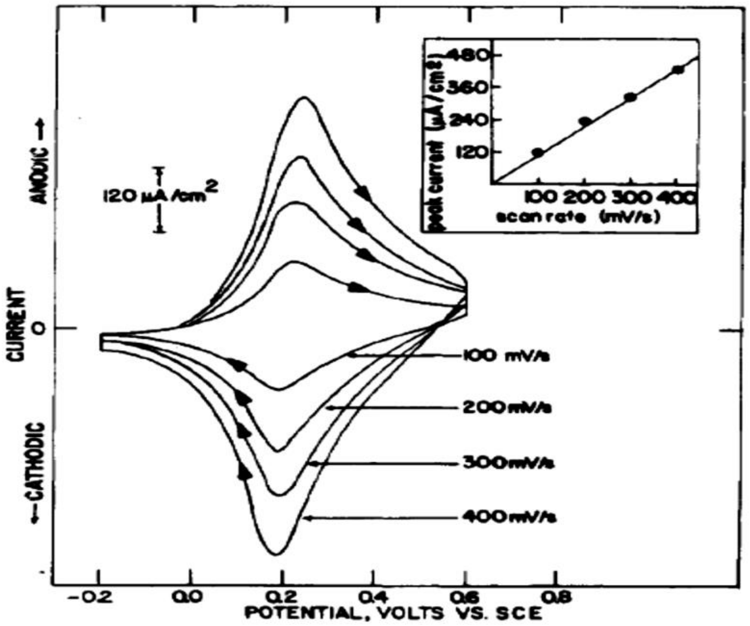

Figure 2.15: Cyclic voltammogram of nickel modified with $(Fe(CN)_5 \cdot H_2O)^{3-}$ (source: Honda et al., 2011)

Espinosa et al. (2012) developed a NiHCF film with improved redox cycling stability and with the ability to selectively separate K^+ over Na^+ and Cs^+ over Na^+. They oxidized nickel at anodic potential of 0.6 – 1.8 V for 30 min in a solution containing 10 mM (metal)$_3$Fe(CN)$_6$ and a supporting electrolyte (0.1 M (metal)NO$_3$), forming an insoluble and stable alkali (metal)$NiFe^{III}(CN)_6$ on the electrode surface. The resulting water-rinsed nickel hexacyanoferrate electrodes were characterized by CV in the range of 0.1 – 0.8 V in a solution of 0.1 M sodium nitrate ($NaNO_3$) or 0.5 M ($NaSO_4$) at a scan range 50 mV/s. The resulting film thickness was 45 nm and the coverage for all types of nickel electrodes used was in the order 3×10^{-8} $mol \cdot cm^{-2}$.

The main advantage of this process was that the prepared electrodes were able to regenerate, thus reducing the amount of secondary waste. About 20% of its capacity is lost after 2000 cycles, which gives it a long lifetime in Cs^+ separation performance.

2.4 Nickel Hexacyanoferrate Carbon Nanotubes

Lin et al. (2005) used nickel hexacyanoferrate for ESIX with a stable carbon nanotube-polyaniline-nickel hexacyanoferrate nano composite film, which was prepared using the electrodeposition method. Figure 2.16 illustrates the concept of ESIX based on the carbon nanotube–PANI–NiHCF nano composite. It was used in a porous polyaniline (PANI)-carbon nanotube (CNT) matrix, producing a hybrid material with a good capacity for ion exchange. The CNT–PANI–NiHCF nano composite films were synthesized using step-by-step electrodeposition on glassy carbon electrodes and characterized using CV.

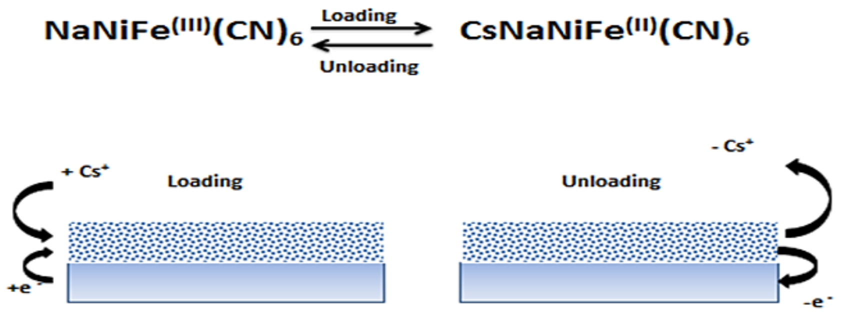

Figure 2.16: Schematic illustration of ESIX based on carbon nanotubes, polyanline and nickel hexacyanoferrate nanocomposite (source: Lin et al., 2005)

Using ultrasonic agitation, carbon nano tubes (CNTs) were dispersed in N,N-dimethyl formamide (DMF). The CNT-DMF solution was deposited onto the surface of a glassy carbon electrode (3 mm diameter). The solvent was then evaporated at room temperature and the glassy carbon electrode was polished carefully with alumina slurry, washed with water, ultrasonicated for five minutes in acetone and ultrapure water, and finally dried with air steam. Using the three-electrode cell and CV, PANI is electrochemically prepared using an aqueous solution of 0.1 M H_2SO_4 and 0.1 M aniline. The PANI film is obtained by cycling between 2200 mV and +700 mV (versus Ag/AgCl) at a sweep rate of 100 mV/s for 15 cycles and is then washed with ultra-pure water. NiHCF was electrodeposited from solutions containing 1 mM $Ni(NO)_3$, 1 mM $K_3Fe(CN)_6$, and 0.5 M $NaNO_3$. The procedure involved 13 full voltammetric cycles (26 segments) at 25 mV/s in the potential range of 850 mV to 0 mV. The deposition of NiHCF nanoparticles started at a potential where the reduction of $Fe(CN)_6^{3-}$ to $Fe(CN)_6^{4-}$ occurred. The Ni^{2+} reacted instantaneously with $Fe(CN)_6^{4-}$ to form NiHCF nanoparticles on the electrode surface. Finally the electrode was rinsed with pure water (Lin et al., 2005; Lin et al., 2006).

Figure 2.17 shows that the deposition of PANI results in several new peaks at around 0.6 V. This indicates that PANI was electrodeposited on the electrode surface (Lin et al., 2005; Lin et al., 2006)

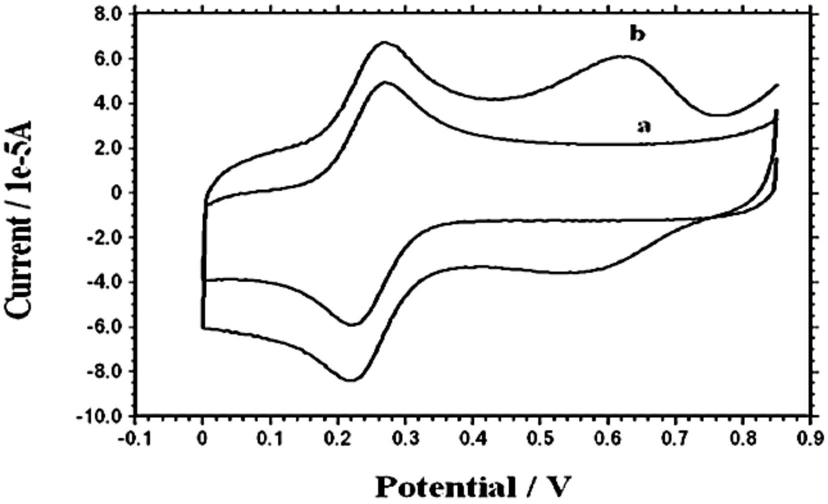

Figure 2.17: CVs of a glassy carbon electrode modified with CNTs (a) before and (b) after the electrodeposition of PANI in a solution of 2 mM $K_3Fe(CN)_6$ and 1 M $NaNO_3$ at 25 mV/s (source: Lin et al., 2006)

Figure 2.18 shows the CV obtained with NiHCF-CNT electrode for a solution of $CsNO_3$ and $NaNO_3$, demonstrating the sensitivity of the electrode to Cs^+. The CV becomes broader when the concentration of Cs^+ increases, indicating the relative selectivity for this species over Na^+ (Lin et al., 2005).

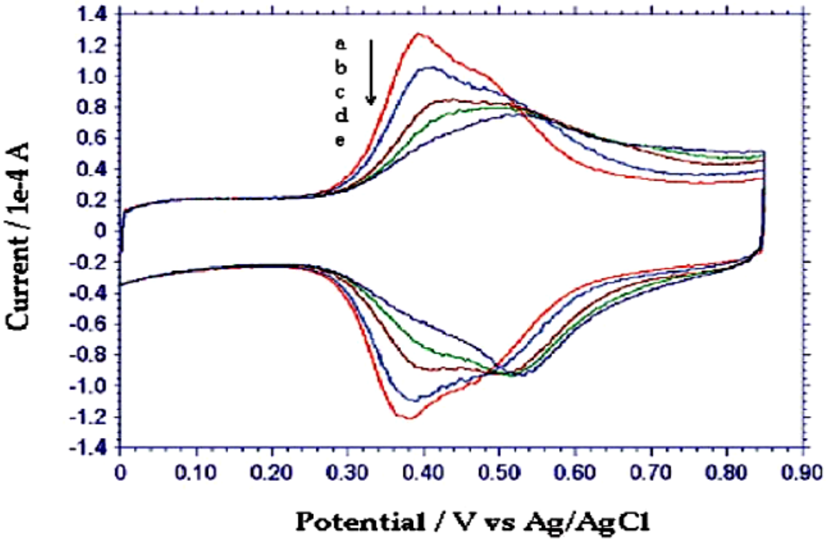

Figure 2.18: CV curve showing the sensitivity of NiHCF films, at the CNT surface, to Cs^+ in NaNO3 with different concentrations of $CsNO_3$ (source: Lin et al., 2005)

Figure 2.19 presents CV data showing the growth of NiHCF nanoparticles during potential cycling on (a) a bare glassy carbon electrode, (b) a glassy carbon electrode coated with CNTs, and (c) a glassy carbon electrode coated with CNTs–PANI. The reversible peaks of the $Fe(CN)_6^{3-}/Fe(CN)_6^{4-}$ system were recorded before the electrodeposition. The surface CV increased following each negative potential scan that involved the reduction of $Fe(CN)_6^{3-}$ to $Fe(CN)_6^{4-}$. Several new peaks appeared at approximately 0.38 V. At the same time, the reversible peaks of $Fe(CN)_6^{3-}$ and $Fe(CN)_6^{4-}$ disappeared. The growth of NiHCF occurs in the reductive potential half-cycle where the reduced $Fe(CN)_6^{4-}$ reacts with Ni^{2+} on the electrode and results in a sparingly soluble precipitate of Ni^{2+} hexacyanoferrate on the surface of the electrode (Lin et al., 2006).

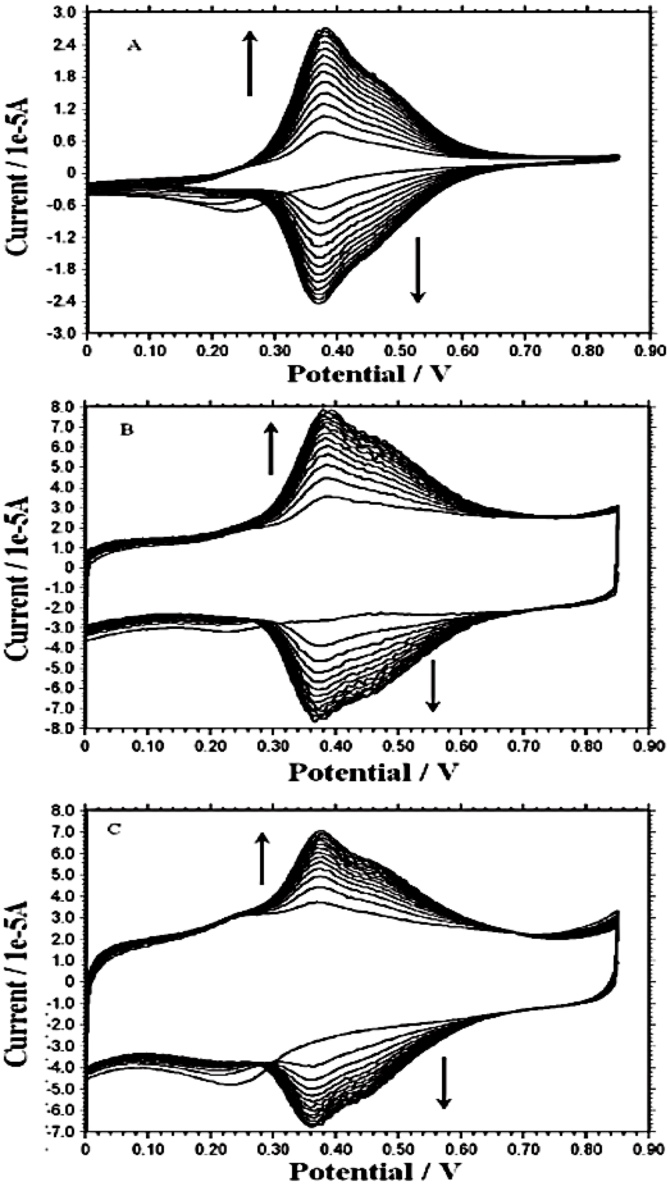

Figure 2.19: CV of NiHCF film on (a) a glassy carbon electrode, (b) a glassy carbon electrode modified with CNTs, and (c) a glassy carbon electrode modified with CNTs-PANI (source: Lin et al., 2006)

Figure 2.20a shows the stretching vibration of the CN group in the cyanometallatic lattice of $K_2Ni(Fe(CN)_6)$, and figure 2.20 b shows UV-vis spectroscopy of the NiHCF nanotubes. The UV spectrum peaks at 302 nm, which corresponds to the reduced form of NiHCF. These spectroscopic results demonstrate that the formation of NiHCF in the form of $K_2Ni^{II}(Fe^{II}(CN)_6)$ was achieved (Chen et al., 2007).

The chemical reaction can be formulated as follows

$$Ni^{2+}\ (aq) + Fe(CN)_6^{4-}\ (aq) + 2K^+ \longrightarrow K_2Ni(Fe(CN)_6) \qquad (2.3)$$

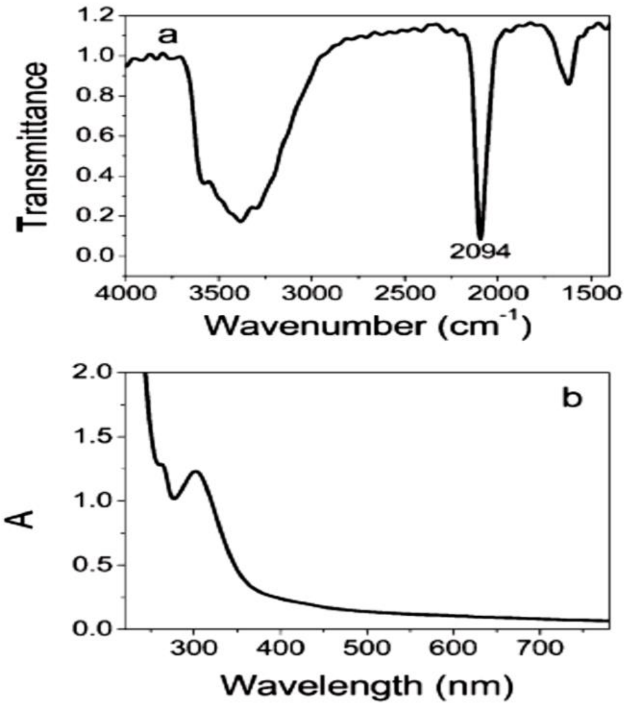

Figure 2.20: (a) IR spectrum, (b) UV spectrum of NiHCF (source: Chen et al., 2007)

Using the pulse electrodeposition method, new nickel hexacyanoferrate (NiHCF) thin films were prepared on graphite substrates. Graphite rods of 4 mm diameter were mechanically polished then rinsed with deionized water and dried by air. The effective area 4 cm^2 is exposed for deposition at room temperature. Preparing 0.002 M of $NiSO_4$ and 0.002 M $K_3Fe(CN)_6$ and 0.25 M Na_2SO_4 mixed solution.

Pulse electrodeposition involves the application of a periodic current density or potential waveform to the working electrode. The potential ranges from 0.2 V to 0.7 V followed by a zero current density during the off-time. The on time was fixed as 0.3s, while off-times of 0.1, 0.2, 0.3 and 0.4s were used, thereby yielding duty cycles of 75%, 60%, 50% and 43%, respectively. The number of deposition pulse cycles used to generate the films was varied from 1000 to 5000. NiHCF deposits on graphite electrodes were also produced by cycling the electrode potential between 0 and 1200mV at 25mV/s in freshly prepared 0.002 M $NiSO_4$, 0.002 M $K_3Fe(CN)_6$, and 0.25 M Na_2SO_4 mixed solution. Deposition was continued for 12 cycles to produce the film. The film was then thoroughly rinsed with water and dried (Hao et al., 2006).

Figure 2.21 shows the CVs of the electrode modified with NiHCF-MWCNTs composites in 0.5 M NaCl solution. A reversible couple of peaks response attributes to Na^+ intercalation / deintercalation takes place at 0.35 V. The positive currents correspond to the oxidation of NiHCF with the release of Na^+ from the matrix. The negative currents denote the reduction and concurrent uptake of Na^+. Thus, this cation uptake and release can be controlled by modulating the potential in the redox processes as follows:

$$NaNi^{II}(Fe^{III}(CN)_6) + Na^+ + e^- \longrightarrow Na_2Ni^{II}(Fe^{II}(CN)_6) \quad \text{(uptake)} \qquad (2.4)$$

$$Na_2\,Ni^{II}(Fe^{II}(CN)_6) \xrightarrow{\quad} NaNi^{II}\,(Fe^{III}(CN)_6) + Na^+ + e^- \qquad \text{(release)} \qquad (2.5)$$

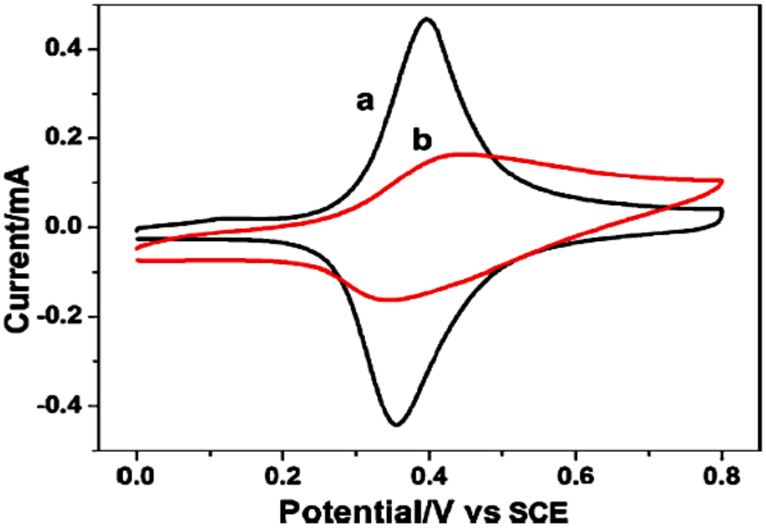

Figure 2.21: CVs of the electrode modified with (a) NiHCF -MWCNTs and (b) NiHCF/PV4P/MWCNTs composites in 1 M NaCl solution, scan rate: 50 mV/s.(source: Li et al., 2012)

The main advantage of this process was that the prepared electrodes have a large surface area comparable to the previously prepared electrodes, which provides a long lifetime in Cs^+ separation. The preparation, however, was expensive.

2.5 Conclusions

Nickel hexacyanoferrate is a complex that is very selective to Cs^+. It is used very successfully to remove radioactive Cs^+ from nuclear spent fuel. Many process developments have been achieved to modify this complex from a non-regenerable IX column to an ESIX electrode and, finally, to an ESIX nanotube electrode. These processes are used to recover Cs^+ from nuclear spent fuel and have occasionally been used to recover chromium and perchlorate from wastewater. The film has been deposited onto a range of substrates, and it has been shown to be more successful when it is deposited on graphite and nickel electrodes rather than on gold electrodes. The regenerable ESIX processes are further beneficial as they reduce the amount of secondary waste generated and are stable over a much longer period of time than traditional treatment methods.

2.6 Acknowledgements

The authors would like to thank the Egyptian Ministry of Defense (EMD) and the Natural Science and Engineering Research Council of Canada (NSERC) (Discovery Grants Program) for supporting this work.

2.7 References

Akieh, Marceline N., Stephen F. Ralph, Johan Bobacka, Ari Ivaska. 2010 “Transport of metal ions across an electrically switchable cation exchange membrane based on polypyrrole doped with a sulfonated calixarene” *Journal of Membrane Science* 354 162–170.

Allard Th., Balan E., Calas G., Fourdrin C., Morichon E., Sorieul S. 2012 “Radiation-induced defects in clay minerals: A review” *Nuclear Instruments and Methods in Physics Research* B 277 112–120.

Alkhudhiri, Naif Darwish, Nidal Hilal. 2012 “Membrane distillation: A comprehensive review” *Desalination* 287 pp 2–18.

Ambashta, Mika and E.T. Sillanp. 2012 “Membrane purification in radioactive waste management: a short review” *Journal of Environmental Radioactivity* 105 PP 76-84.

Ansari, S.A., Mohapatra, P.K., Raut, D.R., Kumar, M., Rajeswari B., Manchanda V.K., 2009“Fibre supported liquid membrane transport study using simulated highlevel nuclear waste” *Journal of Membrane Science* 337 PP 304–309.

Ansari, S.A., Mohapatra, P.K., Raut, D.R., Adya, V.C., Thulasidas, S.K., Manchanda, V.K., 2008 “Separation of Am(III) and trivalent lanthanides from simulated high-level wasteusing a hollow fiber-supported liquid membrane” *Separation and Purification Technology* 63, PP 239–242.

Baisden, A., Gregory, R., Choppin., 2004 “Nuclear waste management and the nuclear fuel cycle “radiochemistry and nuclear chemistry .

Barc., Waste management, 2003 “High level waste management “Nuclear fuel cycle, chapter 13.

Bhcskai, K., Martinusz, E., Inzelt., Kulesza, P.J., 1995 “Polynuclear nickel hexacyanoferrate: monitoring of film growth and hydrated counter-cation flux/storage during redox reactions” *Journal of Electro Analytical Chemistry* 385,PP 241 248.

Chapman, Neil, Hooper, Alan, 2012 “The disposal of radioactive wastes underground” *Proceedings of the Geologists’ Association* 123, PP 46–63.

Chen, Wei and Xing-Hua, Xia., 2007 “Highly Stable Nickel Hexacyanoferrate Nanotubes for Electrically Switched Ion Exchange” *Adv. Funct. Mater.* 17, PP 2943–2948.

Choi, Heui-Joo., Minsoo, Lee., Jong Youl, Lee., 2011 “Preliminary conceptual design of geological disposal system for high-level wastes from the pyro processing of PWR spent fuels” *Nuclear Engineering and Design* 241, PP 3348– 3356.

Crooks, C.A., Evans, S.F., Macchietto, S., 1994 “An application of automated operating procedure synthesis in the nuclear industry” *Computers Chem. Eng*, Vol. 18, Suppl., pp. S385-S389.

Espinosa, R.M Flores., Ortíz-Oliveros, H.B., Olguínb, M.T., Perusquia-Cueto, M.R., Gallardo-San-Vicente R. 2012 “Separation and treatment of ion-exchange resins used in cleaning systems of a research nuclear reactor” *Chemical Engineering Journal* 188, PP 71– 76.

Gustavo, A., Cragnolino, Sitakanta, Mohanty, Darrell, S., Dunn, Narasi, Sridhar., Tae M., 2000 “An approach to the assessment of high-level radioactive waste containment. I: Waste package degradation” *Nuclear Engineering and Design* 201, PP 289–306.

González-Romero E.M., 2011 “Impact of partitioning and transmutation on the high level waste management” *Nuclear Engineering and Design* 241, PP 3436-3444.

Hao, Xiao-gan., Guo, Jin-xia., 2006 “Electrochemically switched ion exchange performances of capillary deposited nickel hexacyanoferrate thin films” Trans. *Nonferrous Met. SOC. China* 16, PP 556-561.

Hao, Xiaogang., Yongguo, Li., Mark, Pritzker., 2008 “Pulsed electrodeposition of nickel hexacyanoferrate films for electrochemically switched ion exchange” *Separation and Purification Technology* 63, PP 407–414.

Higgy, H. R., 1977 “A dry storage pit for radioactive sources” *Annals of Nuclear Energy*, Vol 4, PP 201-204.

Honda, Kensuke, Masayoshi, Yoshimatsu, Koichi, Kuriyama, Ryosuke, Kuwabara, Hiroshi, Naragino, Kosuke, Yoshinaga, Takeshi, Kondo, 2011 “Electrically-switchable, perm selective membranes prepared from nano-structured N-doped DLC” *Diamond & Related Materials* 20, PP 1110–1120.

Horwitzav, Mark, L., Dietz, Renato, Chiarizia, 1995 “Separation and preconcentration of actinides by extraction chromatography using a supported liquid anion exchanger: application to the characterization of high-level nuclear waste solutions” *Analytica Chimica Acta* 310, PP 63-78.

Inamuddin, Yahya., Ismail A., 2010 “Synthesis and characterization of electrically conducting poly-o-methoxyaniline Zr(1V) molybdate Cd(II) selective composite cation-exchanger” *Desalination* 250, PP 523–529.

International Atomic Energy Agency. 2004 “Spent Fuel and High Level Waste: Chemical Durability and Performance under Simulated Repository Conditions”

International Atomic Energy Agency. Safety series, 1994 “classification of radioactive waste”, Vienna.

Jagadish, C., Panigrahi and Rama Krushna Panda., 1992 “Solid state electroactive materials: synthesis and solid state electro activity of some new materials derived from tris(2,2'-bipyridine- N, N'-dioxide)iron(HI)-(IV) and hexacyanoferrate(II)-(l/I)" *Materials Science and Engineering* B14, PP 5-9.

Katz, A., Brough, A.R., Kirk, R.J., 2001 "Cement solidification of simulated off-gas condensates from vitrification of low level nuclear waste solution" *Waste Management* 21, PP 543-553.

Katsounaros, I., Dortsiou, M., Kyriacou, G., 2009 "Electrochemical reduction of nitrate and nitrite in simulated liquid nuclear wastes" *Journal of Hazardous Materials* 171, PP 323–327.

Kazuyoshi, Uruga., Kayo, Sawada., Youichi, Enokida., Ichiro, Yamamoto., 2008 " Vitrification of high level radioactive waste considering the behavior of platinum group metals" *Progress in Nuclear Energy* 50, PP 514-517.

Kertesz, Vilmo., Nicole, M., Dunn, Gary, J., 2002 "Electrochemistry–electrospray-mass spectrometry study of cesium uptake in nickel hexacyanoferrate films" *Electrochimica Acta* 47, PP 1035–1042.

Koryta, Jiw, 1984 "Theory and applications of ion selective electrodes part 5a" *Analytical Chimical Acta* 159, PP 1-46.

Koryta, Jiw., 1990 "Theory and applications of ion-selective electrodes. Part 8 a" *Analytical Chimical Acta*, 233, PP l-30.

Lacoste, André-Claude, 1997 "The French approach to the safe management of very low level radioactive waste from nuclear installations" *Nuclear Engineering and Design* 176, PP 151–153.

Li, Na, Zhongjie, Li, Junhua, Yuan, Jianguo, Hu, Jigen, Miao, Qixian, Zhang, 2012 “Nickel hexacyanoferrate nanoparticles anchored to multi walled carbon nanotubes with a grafted poly(4-vinylpyridine) linker for electrically switched ion exchange” *Electrochimica Acta* 72, PP 150– 156.

Lilga M.A., Orth, R.J., Sukamto, J.P.H., Haight, S.M., Schwartz, D.T., 1997 “Metal ion separations using electrically switched ion exchange” *Separation and Purification Technology* 11, PP 147-158.

Lilga M.A., Orth, R.J., Sukamto, J.P.H., Rassat, S.D., 2001” Cesium separation using electrically switched ion exchange” *Separation and Purification Technology* 24, PP 451–466.

Lilga M.A., Orth, R.J., 1997 “Electrically Switched Cs^+ Exchange” University of Washington.

Lin, Yuehe and Xiaoli, Cui., 2005 “Novel hybrid materials with high stability for electrically switched ion exchange: carbon nanotube–polyaniline–nickel hexacyanoferrate nano composites” *Chem. Commun*, PP 2226–2228.

Lin, Yuehe and Xiaoli, Cui., 2006 “Electro synthesis, characterization, and application of novel Hybrid materials based on carbon nanotube–polyaniline–nickel hexacyanoferrate nano composites” *Journal of material chemicals.*, 16, PP 585–592.

McDeavitt S.M., Abraham, D.P., Park, J.Y., 1998 ” Evaluation of stainless steel-zirconium alloys as high-level nuclear waste forms” *Journal of Nuclear Materials* 257, PP 21-34.

Niculae, O., Andrei, V., Ionita, G., Duliu, O.G., 2009 ” Preliminary safety concept for disposal of the very low level radioactive waste in Romania” *Applied Radiation and Isotopes* 67, PP 935–938.

Nishad, Abdul, Anupkumar, Bhaskarapillai, Sankaralingam, Velmurugan, 2012” Cobalt (II) imprinted chitosan for selective removal of cobalt during nuclear reactor decontamination” *Carbohydrate Polymers* 87, PP 2690– 2696.

Pawel, J., Kuksza and Zbigniew, Galus, 1989 “Polynuclear transition metal hexacyanoferrate films In-situ electrochemical determination of their composition” *Journal of electroanalytical chemistry.*, 267, PP 117-127.

Pawel, J., Kuksza, Jedral, Teresa, 1989 “A new development in polynuclear inorganic films: silver (I)/ crosslinked nickel hexacyanoferrate microstructure” *Electrochemical Acta* vol 34 No 6 pp 851-853.

Pierozanello., 2003 “inorganic electro chemistry theory, practice and application”.

Pierozanello, Fabrizia., 2012 “Inorganic electro chemistry theory, practice and application” .

Poskas, P., Adomaitis, J.E., Ragaisis, V., Simonis, V., Smaizys, A., 2012 “Progress of radioactive waste management in Lithuania” *Progress in Nuclear Energy* 54, PP 11-21.

Pusch, Roland, Richard, Weston, 2012 “Superior techniques for disposal of highly radioactive waste (HLW)” *Progress in Nuclear Energy* 59, PP 75-85.

Qafoku. P., Evan, Dresel, Eugene, Ilton, James P., 2010 “Chromium transport in an acidic waste contaminated subsurfacemedium: The role of reduction” *Chemosphere* 81, PP 1492–1500.

Rana, P., Mohan, N., Rajagopal, C., 2004 “Electrochemical removal of chromium from wastewater Byusing carbon aerogel electrodes” *Water Research* 38, PP 2811–2820.

Rassat, S.D., Sukamto, J.H., Lilga, M.A., 1999 “Development of an electrically switched ion exchange process for selective ion separations” Journal of *Separation and electroanalytical. Chemistry.*, 210, PP 323-328.

Raut, D.R., Mohapatra, P.K., Manchand, V.K., 2012 “A highly efficient supported liquid membrane system for selective strontium separation leading to radioactive waste remediation” *Journal of Membrane Science* 390, PP 76– 83.

Reynolds, Gary A., Cooke, Daniel L., Herting, Wade, Warrant, 2012 “Evidence for dawsonite in Hanford high-level nuclear waste tanks” *Journal of Hazardous Materials* 209– 210, PP 186– 192.

Rieger, Philip H. 1987 “Electrochemistry”.

Rosa, Sureda, Xavier Martinez-Llado, MiquelRovira, Joan de Pablo, Ignasi Casas, Javier Gimenez, 2010 “Sorption of strontium on uranyl peroxide: Implications for a high-level nuclearwaste repository” *Journal of Hazardous Materials* 181, PP 881–885.

Runchal A. 1980 “The impact of a high level nuclear waste repository on the regional ground water flow” *Int. J. Rock Mech. Min. Sci. & Geomech. Abstr.* Vol. 17, pp. 253-64.

Sellier, A., Buffo-Lacarriere, L., El Gonnouni, M., 2011 “Behavior of HPC nuclear waste disposal structures in leaching environment” *Nuclear Engineering and Design* 241, PP 402–414.

Shia, Keliang, Xiaolin, Houa, Per Roosa, Wangsuo, W., 2012 “Determination of technetium-99 in environmental samples: A review” *Analytica Chimica Acta* 709, PP 1– 20.

Shakir K., Sohsah, M., Soliman, M., 2007 “Removal of cesium from aqueous solutions and Radioactive waste simulants by coprecipitate flotation” *Separation and Purification Technology* 54, PP 373–381.

Singh, Shraddha, Vidya, Thora., Kaushik, C.P., 2009 “Potential of Chromolaena odorata for phytoremediation of 137Cs from solution and low level nuclear waste” *Journal of Hazardous Materials* 162, PP 743–745.

Sinha, Sujit, and Bocarsly A.B., 1984 “Reaction of Nickel Electrode Surfaces with Anionic Metal-Cyanide Complexes: Formation of Precipitated Surfaces” *Inorganic Chemistry*, Vol. 23, No. 2. PP 203 - 212

Solomah, Ahmad Gabr and Lloyd R. Zumwalt, 1982 “High level radioactive solid waste form evaluation :model for predicting leaching behavior” *Nuclear and Chemical Waste Management* Vol 3 PP 111-116.

Solomon, Barry D., and Diane M., 1985 “Nuclear waste repository siting” Butterworth & Co (Publishers) Ltd.

Stuart R., Shipley, L., 1995 “Dynamic analysis of high level waste storage tanks” *Computers & Structures* Vol. 56, No. 2/3, pp. 415-424.

Watson K., Farré, M.J., Knight, N., 2012 “Strategies for the removal of halides from drinking water sources, and their applicability in disinfection by-product minimization: A critical review” *Journal of Environmental Management* 110, PP 276-298.

Tan, Sheng-Heng, Xue-Gang Chen, 2010 “Hydrothermal removal of Sr2+ in aqueous solution via formationofSr-substituted hydroxyapatite” *Journal of Hazardous Materials* 179, PP 559–563.

Technical Training Center, 2004 “Radioactive Waste Management”.

Thakur, P., Mulholland, G.P., 2012 “Determination of 237Np in environmental and nuclear samples: A review of the analytical method” *Applied Radiation and Isotopes* 70, PP 1747–1778.

Valsala, T.P., Sonavane, M.S., Kore, S.G., 2011 “Treatment of low level radioactive liquid waste containing appreciable concentration of TBP degraded products” *Journal of Hazardous Materials* 196, PP 22– 28.

Valsala, T.P., Roy S.A., 2009 “Removal of Radioactive cesium from low level radioactive waste (LLW) streamsusing cobalt ferrocyanide impregnated organic anion exchanger” *Journal of Hazardous Materials* 166, PP 1148–1153.

Yuehelin, Xiaolicui and Jagan bontha., 2006 “Electrically-Controlled Anion Exchange Based on Polypyrrole and Carbon Nanotubes Nanocomposite for Perchlorate Removal” *Enviro Sci. Technol.* 40, PP 4004-4009.

Chapter 3

Enhanced capacity and stability for the separation of cesium in electrically switched ion exchange

The contents of this chapter have accepted for publication as: Tawfic.A.F., Dickson.S.E., Kim.Y., Mekky.W., 2014. Enhanced capacity and stability for the separation of cesium in electrically switched ion exchange. American Nuclear society journal, In press.

Abstract

Electrically switched ion exchange (ESIX) can be used to separate ionic contaminants from industrial wastewater, including that generated by the nuclear industry. The ESIX method involves sequential application of reduction and oxidation potentials to an ion exchange film to induce the respective loading and unloading of cesium. This technology is superior to conventional methods (e.g electrodialysis reversal or reverse osmosis) as it requires very little energy for ionic separation. In previous studies, ESIX films have demonstrated relatively moderate ion exchange capacities and limited film stabilities over repeated potential applications. In this study, the methodology for the deposition of electroactive films (nickel hexacyanoferrate) on nickel electrodes was modified to improve the ion exchange capacity for cesium removal using ESIX. Cyclic voltammetry was used to investigate the ion exchange capacity and stability. Scanning electron microscopy (SEM) was used to characterize the modified film surfaces. Additionally, the films were examined for the separation of cesium ions. This modified film preparation

technique enhanced the ion exchange capacity and improves the film stability compared to previous methods for the deposition of ESIX films.

3.1 Introduction

Electrically switched ion exchange (ESIX) is a relatively new method for Cs^+ separation (Lilga et al., 1997; Rassat et al., 1999; Lilga et al., 2001). It combines the ion exchange process with electrode reactions for a reversible and selective separation of Cs^+, and has the added benefit of generating relatively small amounts of secondary wastes (Hao et al., 2008).

The ESIX process can be used to separate the first group elements and it is more selective to Cs^+ and K^+ than Na^+. Further, the ESIX process is highly energy efficient, with small voltages required (< 2 V) for the uptake and elution of ions (Rassat et al., 1999).

The ESIX system consists of an electroactive ion exchange film that is electrochemically deposited onto a nickel electrode figure (3.1). The deposition of the ion exchange film is regulated using an applied electric potential (Lilga et al., 1997; Hao et al., 2008; Akieh et al., 2010; Ismail et al., 2010).

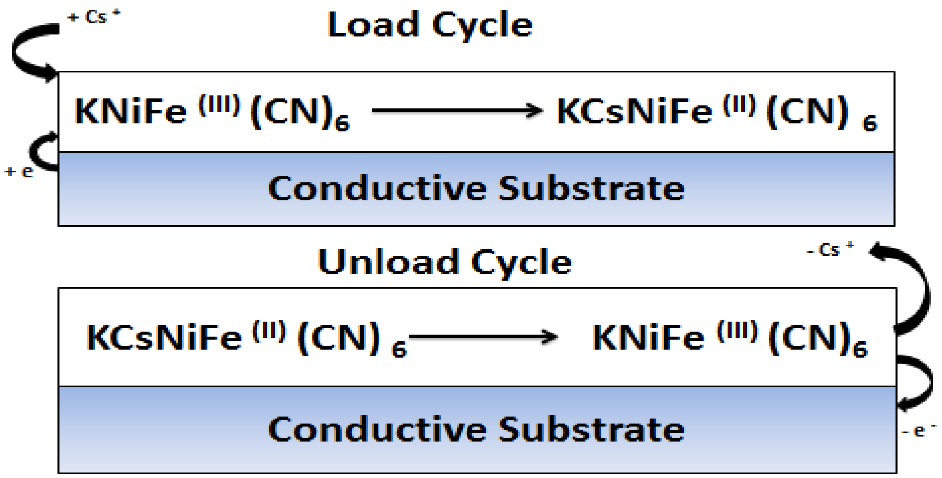

Figure 3.1: Conductive substrate covered with a nickel hexacyanoferrate film (source: Lilga et al., 1997)

When a cathodic potential is applied to a nickel hexacyanoferrate film, the Fe^{+3} in (ferrocyanide) is reduced to Fe^{+2} (forming ferricyanide) and a cation is inserted into the film to maintain charge neutrality. Conversely when an anodic potential is applied, a cation is released from the film and the ferricyanide is oxidized to ferrocyanide (Bheskai et al., 1995). Similarly, films formed from other compounds are reduced under cathodic potentials and oxidized under anodic potentials (Hao et al., 2006).

Lilga et al (Lilga et al., 1997) prepared ESIX films for Cs^{+} separation using a proprietary procedure, and achieved an ion exchange capacity of 3.5×10^{-3} $C.cm^{-2}$, which is equivalent to a surface coverage of 3.6×10^{-8} moles $.cm^{-2}$ (Lilga et al., 1997; Rassat et al., 1999; Lilga et al., 2001).

The main advantage of this process are that it does not require any additional chemicals, the power requirement is relatively low (< 2 V), and it produces a small amount of secondary waste (Lilga et al., 1997; Rassat et al., 1999; Lilga et al., 2001; Hao et al., 2008).

3.2 Experimental methods

3.2.1 General and electrochemical

A WaveDriver 10 Potentiostat / Galvanostat System (Pine Research Instrumentation) was used to deposit and characterize the electroactive films. A standard three electrode system was used in the preparation and characterization of the electroactive films. The saturated calomel (SCE) reference electrode was employed and all potentials presented in this work are with respect to this standard. (Aftermath 2.0) software was used to control all preparation and testing procedures.

A platinum counter electrode with a surface area of 5 cm^2 was employed in all experiments. The reference and counter electrodes were located less than 2 cm from the working electrode. Electrolyte solutions were 0.5 M KNO_3 with sufficiently high conductivities to render ohmic losses negligible. The nickel hexacyanoferrate film was deposited on a nickel working electrode. Described below in conjunction with the experimental system.

Reagent grade chemicals ($K_3Fe(CN)_6$, KNO_3, $CsNO_3$) with > 99% purity were used as purchased without further purification. Deionized water (18.2 MΩ cm^{-1}) was used in all salt solutions and for final rinsing of electrochemical cell components.

3.2.2 Surface preparation

Nickel disks (99.99%) were used as the working electrode. The nickel disk was embedded in a Teflon holder suspended in the test solution. The portion of the disk exposed to the test solution was 0.5 cm in diameter an area 0.196 cm^2. The nickel surface was abraded using diamond sand paper to a surface roughness of 2500 grit prior to film deposition.

3.2.3 Film preparation

The preparation of nickel hexacyanoferrate films was adapted from the method described by Bocarsly et al (Bocarsly et al., 1982; Bocarsly et al., 1982; Bocarsly et al., 1984).

In this method, metallic nickel was oxidized to Ni^{2+} at an anodic potential of 0.6 V– 1 V vs SCE (saturated calomel electrode) for about 30 min in a solution containing ferricyanide ion (10 mM $M_3Fe(CN)_6$ and a supporting electrolyte 0.1 M MNO_3). Ni^{2+} ions from the anode and $Fe(CN)_6^{3-}$ form an insoluble and stable alkali $MNiFe^{III}(CN)_6$ on the electrode surface (Bocarsly et al., 1982; Bocarsly et al., 1982; Bocarsly et al., 1984).

In this current work a solution with 10 mM $K_3Fe(CN)_6$ and 1 M KNO_3 was used for film preparation. Nitrogen gas was bubbled through the solution for 15 minutes before starting the deposition procedure to remove dissolved oxygen. An applied voltage at 0.2 V vs SCE for 30 min followed by 1.2 V vs SCE for another 30 min was used for the deposition of the ESIX film.

3.2.4 Film characterization

A scanning electron microscope (SEM) at Canadian Centre for Electron Microscopy (model JOEL 7000) was used for surface imaging of the prepared film.

The film was characterized using cyclic voltammetry, which was conducted in a 1 M $CsNO_3$ solution. The applied potential started at 0.2 V and was scanned anodically to 0.9

V then cathodically to -0.2 V at a scan rate of 50 mV. s^{-1}. During this process N_2 gas was bubbled to reduce dissolved oxygen.

3.3 Results and discussion

3.3.1 Film characterization

When a nickel substrate is subjected to an applied potential in a solution containing $K_3Fe(CN)_6$, the Ni^{+2} on the electrode surface reacts with the ferrocyanide anion in solution causing the formation and precipitation of insoluble nickel hexacyanoferrate on the electrode surface. This reaction is shown in equation (3.1).

$$Ni^{+2} + K_3Fe(CN)_6 \longrightarrow KNiFe(CN)_6 + 2\,K^{+} + 2\,e^{-} \tag{3.1}$$

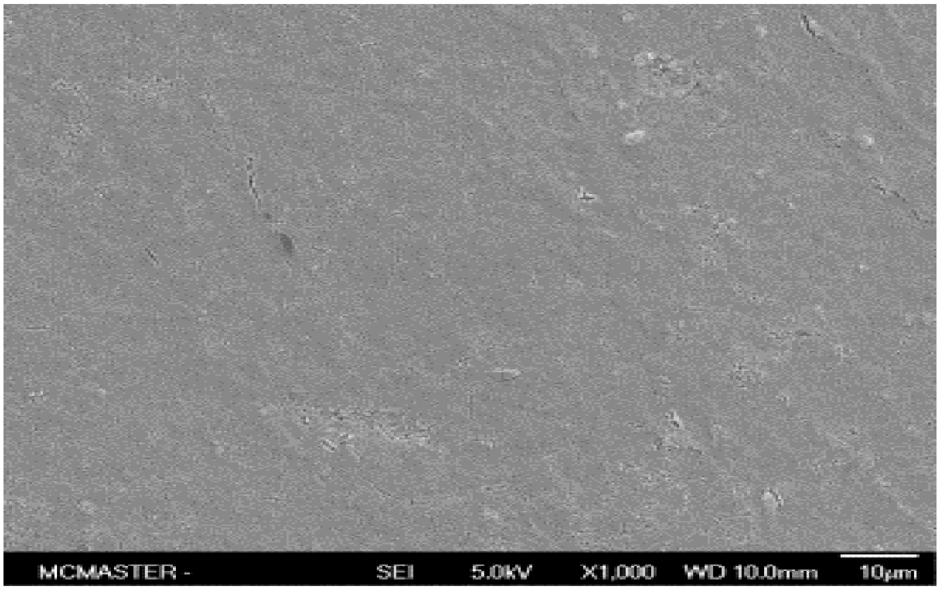

Figure 3.2: SEM for a nickel electrode coated with a hexacyanoferrate film at magnification1000 X

Figures (3.2) and (3.3) show SEM images of the surface of the nickel electrode coated with hexacyanoferrate at magnifications of 1000 x and 10000 x respectively.

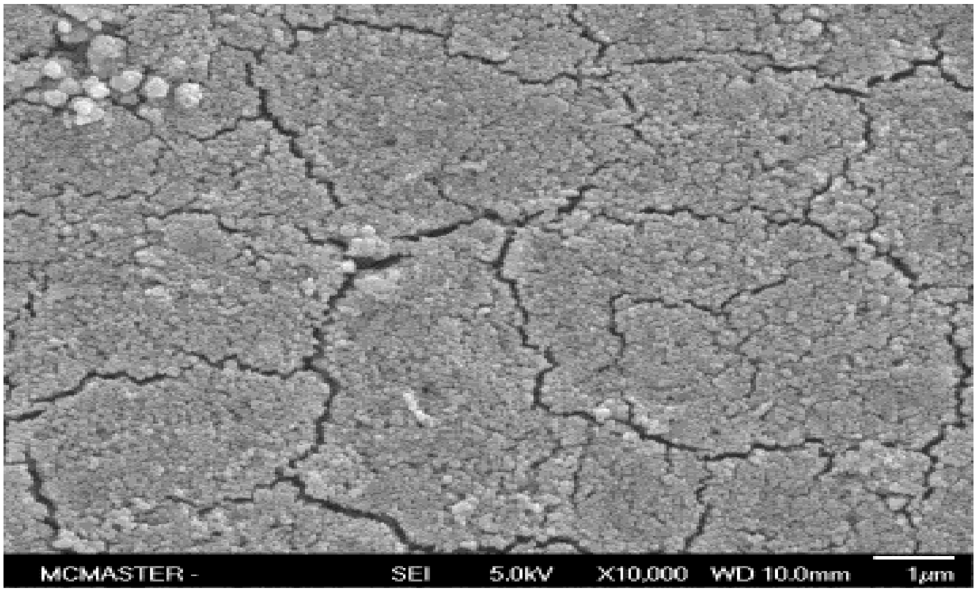

Figure 3.3: SEM for a nickel electrode coated with a hexacyanoferrate film at 10000 x magnification

The prepared film surface is relatively clean and flat in figure (3.2) while the magnified image shows cracks in figure (3.3).

Figure (3.4) shows the cyclic Voltammogram (CV) for a 1 M $CsNO_3$, and hence the redox behavior of the hexacyanoferrate films (i.e. the oxidation of the ferrocyanide film to the ferricyanide form equation (3.3), and the reduction of the ferricyanide film to the ferrocyanide form equation (3.2). The reduction of the ferricyanide film requires the uptake of Cs^+ while the oxidation requires the release of the same ion to maintain electro neutrality in the film.

$$KNiFe^{III}(CN)_6 + e^- + Cs^+ \longrightarrow CsKNiFe^{II}(CN)_6 \qquad (3.2)$$

$$CsKNiFe^{II}(CN)_6 \longrightarrow KNiFe^{III}(CN)_6 + e^- + Cs^+ \qquad (3.3)$$

The shape of the CV in Figure (3.4), confirms that the loading and unloading of Cs^+ occur during this process.

The peak current in the CV was approximately 600 mV and the current approached zero at 200 mV as the oxidation of ferrocyanide to ferricyanide neared completion. Ferricyanide was reduced at 500 mV, which is where the cesium ion was taken up.

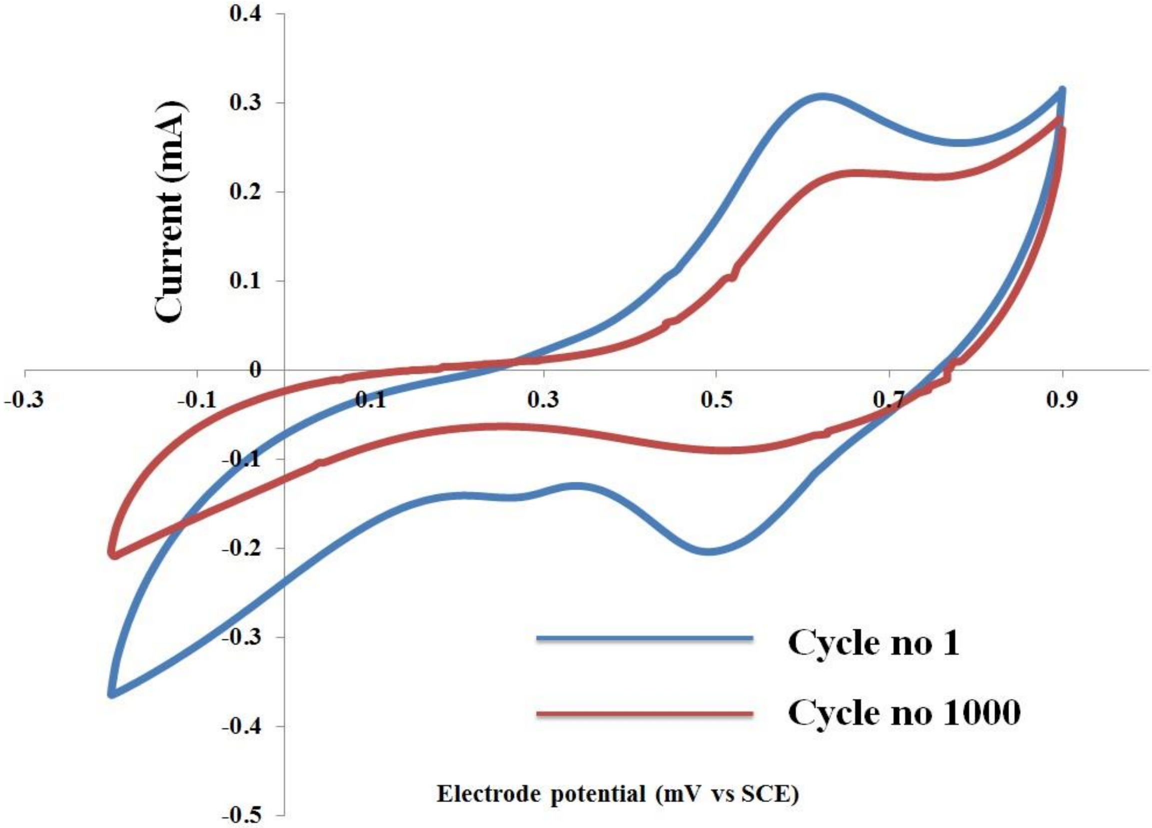

Figure 3.4: CV measured in a 1 M $CsNO_3$ solution

The robustness of the film is shown in figure (3.4) through a comparison of the two curves; the blue line represents the first CV result, while the red line represents the performance of the film after 1000 cycles of cesium loading and unloading. These results show a decrease in the capacity of the film by 30 % with repeated loading and unloading procedure.

The capacity of the film is shown in figure (3.5) and was obtained by integrating the current passes over the course of the entire CV sweep.

Figure (3.5) demonstrates that the film prepared using the modified deposition procedure developed in this work has 63 times greater capacity than the previous film prepared by Lilga et al for the same electrode area (Lilga et al., 1997; Rassat et al., 1999; M.A.Lolga et al., 2001). The maximum capacity achieved in this work is 15.1 x 10^{-3} C.cm^{-2} for electrode surface area of 0.196 cm^2 as compared to that of Lilga et al (Lilga et al., 1997; Rassat et al., 1999; Lilga et al., 2001) which was of 3.5 x 10^{-3} C.cm^{-2} for an electrode surface area of 2.84 cm^2.

This capacity corresponds to surface coverage of 1.56 x 10^{-7} mole.cm^{-2}, which is comparable to 3.6 x 10^{-8} mole.cm^{-2} achieved by Lilga et al (Lilga et al., 1997; Rassat et al., 1999; Lilga et al., 2001). A loss of capacity does occur upon repeated cycling.

The cumulative charge for each cycle normalized to the maximum charge is shown in figure (3.6) as a function of cycle number.

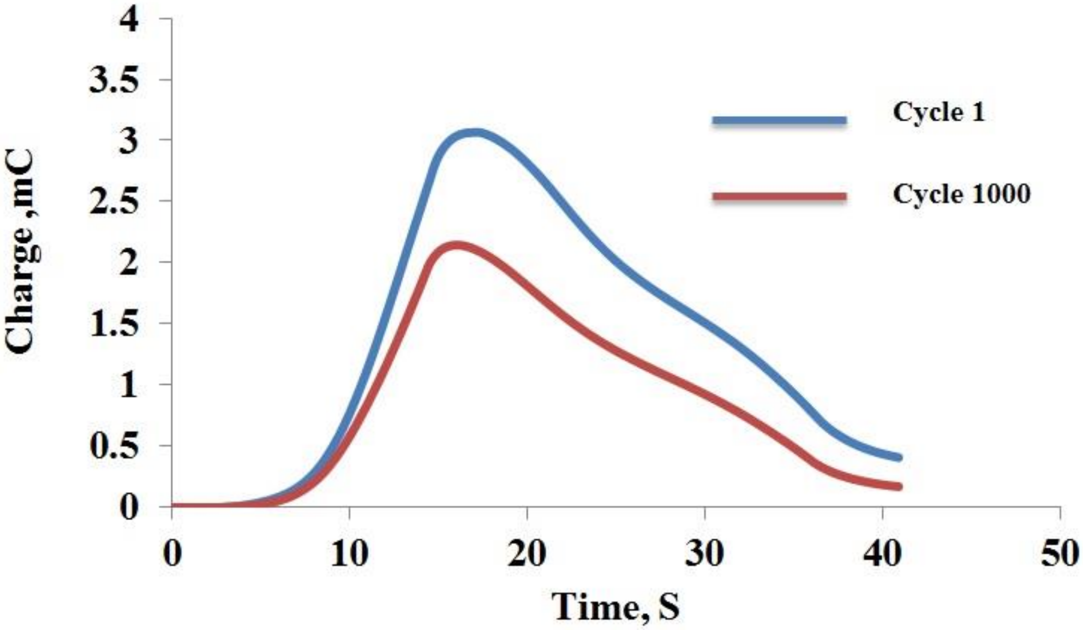

Figure 3.5: The integration of cycles (1 and 1000).

This film loses about 30% of its capacity after 1000 cycles while the film developed by Lilga (Lelga et al., 1997; Rassat et al., 1999; Lilga et al., 2001) loses only 20 % after 2000 cycles.

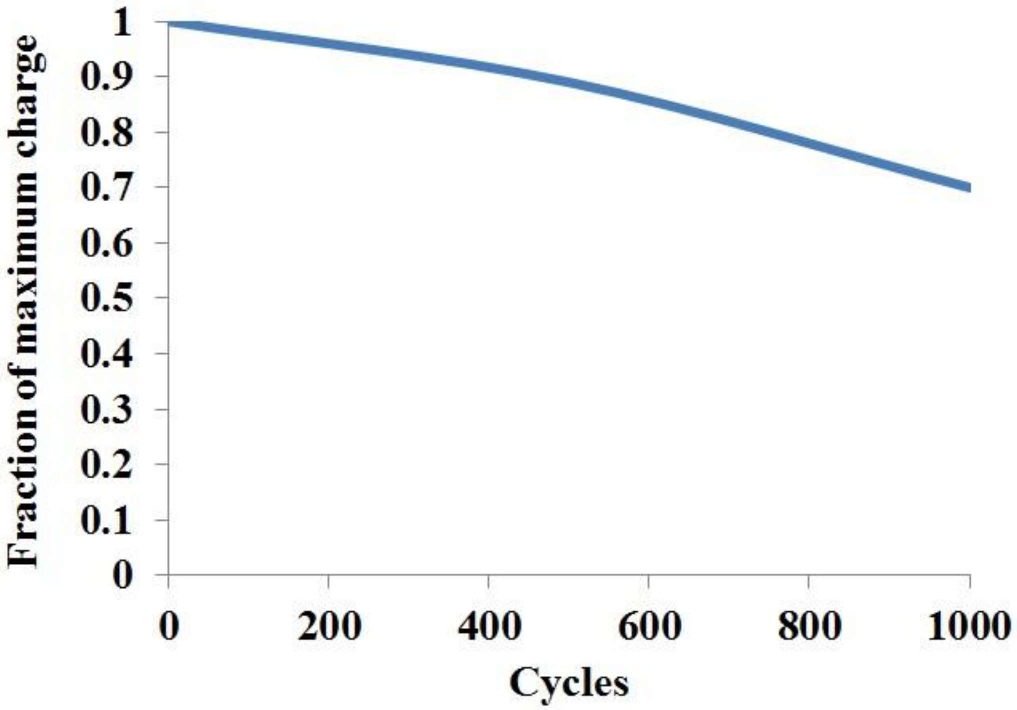

Figure 3.6: Normalized charge as a function of cycle number from cyclic voltammetry in 1 M $CsNO_3$ for a nickel electrode with surface area of 0.196 cm^2.

3.4 Conclusions

This work has demonstrated the ability of ESIX to separate Cs^+ from other group one elements, and has shown that the modified technique for film deposition results in a stable and insoluble film being deposited on a nickel electrode. This film has a capacity 63 times higher than films prepared in previous work. Also, the experiments show that it is easy to control the loading and unloading of the film by modulating the potential applied to the film. The new film shows a decrease in capacity after 1000 cycles of approximately 30 %.

3.5 References

Akieh Marceline N., Stephen F. Ralph., 2010 ” Transport of metal ions across an electrically switchable cation exchange membrane based on polypyrrole doped with a sulfonated calixarene” Journal of Membrane Science 354, PP 162–170.

Bhcskai J., Martinusz, K., Kulesza, p.j., Malik, M.A., 1995 “Polynuclear nickel hexacyanoferrates: monitoring of film growth and hydrated counter-cation flux /storage during redox reactions” Journal of Electroanalytical Chemistry 385, PP 241-248.

Bocarsly A. B., Sinha, A., 1982 Chemically derivatized nickel surfaces: synthesis of a new class of stable electrode interfaces, J. Electroanal. Chem. 137, PP 157.

Bocarsly A. B., Sinha, A., 1982 “Effects of surface structure on electrode charge transfer properties. Induction of ion selectivity at the chemically derivatize interface”, J. Electroanal. Chem. 140, PP 16.

Bocarsly A. B., Sinha, A., 1984 “Reactions of Nickelelectrodes surfaces with anionic Metal- cyanide complexes: Formation of precipitated surfaces” Inorganic Chemistry 23 , PP 203-212.

Hao, Xiao-gan., Guo, Jin-xia., 2006 “Electrochemically switched ion exchange performances of capillary deposited nickel hexacyanoferrate thin films” Trans. Nonferrous Met. SOC. China 16, PP 556-561.

Hao, Xiaogang., Yongguo, Li., Mark, Pritzker., 2008 “Pulsed electrodeposition of nickel hexacyanoferrate films for electrochemically switched ion exchange” Separation and Purification Technology 63, PP 407–414.

Ismail Yahya., 2010” Synthesis and characterization of electrically conducting poly-omethoxyanilineZr(1V) molybdate Cd(II) selective composite cation-exchanger” Desalination 250, PP 523–529.

Lilga M.A., Orth, R.J., Sukamto, J.P.H., Haight, S.M., Schwartz, D.T., 1997 “Metal ion separations using electrically switched ion exchange”Separation and Purification Technology 11, PP 147-158.

Lilga M.A., Orth, R.J., Sukamto, J.P.H., Rassat, S.D., 2001” Cesium separation using electrically switched ion exchange” Separation and Purification Technology 24, PP 451–466.

Rassat, S.D., Sukamto, J.H., Lilga, M.A., 1999“Development of an electrically switched ion exchange process for selective ion separations” Separation and ectroamai. Chem., 210, PP 323-328.

Chapter 4

A comparison between four prepared films as electrically switched ion exchange

The contents of this chapter will be submitted to a journal in November 2014 as: Tawfic, A.F., Dickson, S.E., Kim, Y., and Mekky, W., 2014. A comparison between four prepared films as electrically switched ion exchange

Abstract

The method of electrically switched ion exchange (ESIX) involves the sequential application of reduction and oxidation potentials to an ion exchange film to induce the respective loading and unloading of Cs^+. In this study, four films of nickel hexacyanoferrate were prepared on nickel electrodes with different preparation procedures. Each film shows a different performance with regard to Cs^+ separation. Scanning electron microscopy was used to characterize the modified film surfaces. Cyclic voltammetry was used to investigate the ion exchange capacity and stability. The four films show a better capacity for Cs^+ separation compared to previous methods for the deposition of ESIX films. An optimal nickel hexacyanoferrate film was generated when using an applied potential of 0.2 V relative to a saturated calomel electrode (SCE) to generate the nucleation sites, followed by a 1.3 V vs SCE potential during the growth stage of the film. This film demonstrated the highest film capacity for ion exchange initially (17.3×10^{-3} C cm^{-2}) and again after 1000 cycles (11.1×10^{-3} C cm^{-2}).

4.1 Introduction

A primary concern related to nuclear energy is the production of radioactive isotopes as fission products which require long-term specialized storage (Anthony et al., 1996). The major sources of radioactivity originating from the fission products is from the isotopes Cs^{137} and Sr^{90}, which have half-lives of 30.1 and 32 years, respectively. It is desirable to separate these elements from the rest of the waste in order to minimize the volume of radioactive waste requiring long-term specialized storage (Green et al., 1999). An additional cause for concern with Cs^{137} is its release into the environment; it could be ingested or absorbed by the body, as it is chemically similar to sodium and can affect blood pressure, cellular work, and bodily electrical activity (Mcdowell et al., 1992; Law et al., 2007; Romanovskiy et al., 2007).

An additional benefit of separating and recovering Cs^{137} from fission products is its application in gamma irradiation processes. Gamma irradiation is employed in several industrial processes such as food preservation, pollution control, oil pipeline leak investigations, and the sterilization of medical accessories (Mohapatra et al., 2009; Mohapatra et al., 2010). Typically, Co^{60} is the radioactive source used in gamma irradiation. However, Co^{60} only has a half-life of 5.2 years; replacing Co^{60} with Cs^{137} in some irradiation applications could significantly improve the process (Mohapatra et al., 2009).

Several separation techniques have been employed to remove Cs^+ from radioactive waste, including sorption, precipitation, and ion exchange. Natural zeolites have been used to sorb and, subsequently, precipitate Cs^+ from liquid radioactive waste. Zeolites are an ideal sorbent due to their selectivity, low cost, and stability (Borai et al., 2009; Sinha et al., 1995; Shakir et al., 2007). Inorganic ion exchange has been used due to its stability under the high temperature and radiation conditions of typical fission products (Someda et al., 2002). The resins employed include insoluble ferrocyanide and salts of polyacid ferrocyanide, which are both highly selective towards Cs^+. Only small amounts of Cs^+, however, are desorbed from their surfaces (Roy et al., 2002). The main drawback of this technology is that the extraction and sorption compounds are expensive (Liet al., 2012). Additionally, both of these methods have proven to be inefficient, as a relatively small mass of Cs^+ is recovered from the fission product waste (Rassat et al., 1999).

Electrically switched ion exchange (ESIX) combines electrochemistry and ion exchange and is an environmentally responsible method of separating ions by electrochemical modulation of the ion exchange material (Hao, 2006). Metal hexacyanoferrate (MHCF) is an inorganic compound capable of selectively exchanging alkali cations in an aqueous medium, which makes MHCFs selective for Cs^+ (Gomez et al., 2004; Hao et al., 2008). Nickel hexacyanoferrate is a polynuclear coordination compound in the Prussian blue family and is a candidate for separations involving alkali cations due to their high selectivity for these metals (Steen, A. et al, 2002; Tanihara., 1994).

In the ESIX process, ion adsorption and desorption, are controlled by regulating redox states of the ion exchange material. A thin film of the ion exchange material is deposited on an electrically conductive substrate to achieve Cs^+ separation and the regeneration of the ion exchange film as shown in figure 4.1. As the electrical potential is the main driving force for both the Cs^+ separation and the regeneration of the ion exchange film, the generated secondary waste from the process is kept to a minimum (Sun et al., 2012).

When a nickel electrode is subjected to an applied potential in a solution containing $K_3Fe(CN)_6$, the nickel on the surface is oxidized to Ni^{2+} on the electrode surface and reacts with the $Fe(CN)_6$ anion in solution, causing the formation and precipitation of insoluble nickel hexacyanoferrate on the exposed portion of the electrode. The reaction is shown in equation 4.1 (Lilga et al., 1999).

$$Ni^{+2} + K_3Fe(CN)_6 \longrightarrow KNiFe(CN)_6 + 2K^+ + 2e^- \quad (4.1)$$

Nickel hexacyanoferrate can be used as an ESIX film through the redox reactions which take place with ferricyanide upon the nickel surface.

The reduction of the ferricyanide film requires the uptake of Cs^+ from waste solution. While the oxidation requires a release of the same ion back into concentration solution in order to maintain electro neutrality of the film, the oxidation of ferrocyanide film to the ferricyanide form, equation 4.2, and the reduction of the ferricyanide film to the ferrocyanide form, equation 4.3, are the main driving forces behind the ion exchange (Lilga et al., 1997; Lilga et al., 2001).

$$CsKNiFe^{II}(CN)_6 \rightarrow KNiFe^{III}(CN)_6 + Cs^+ + e^- \quad (4.2)$$

$$KNiFe^{III}(CN)_6 + Cs^+ + e^- \rightarrow CsKNiFe^{II}(CN)_6 \qquad (4.3)$$

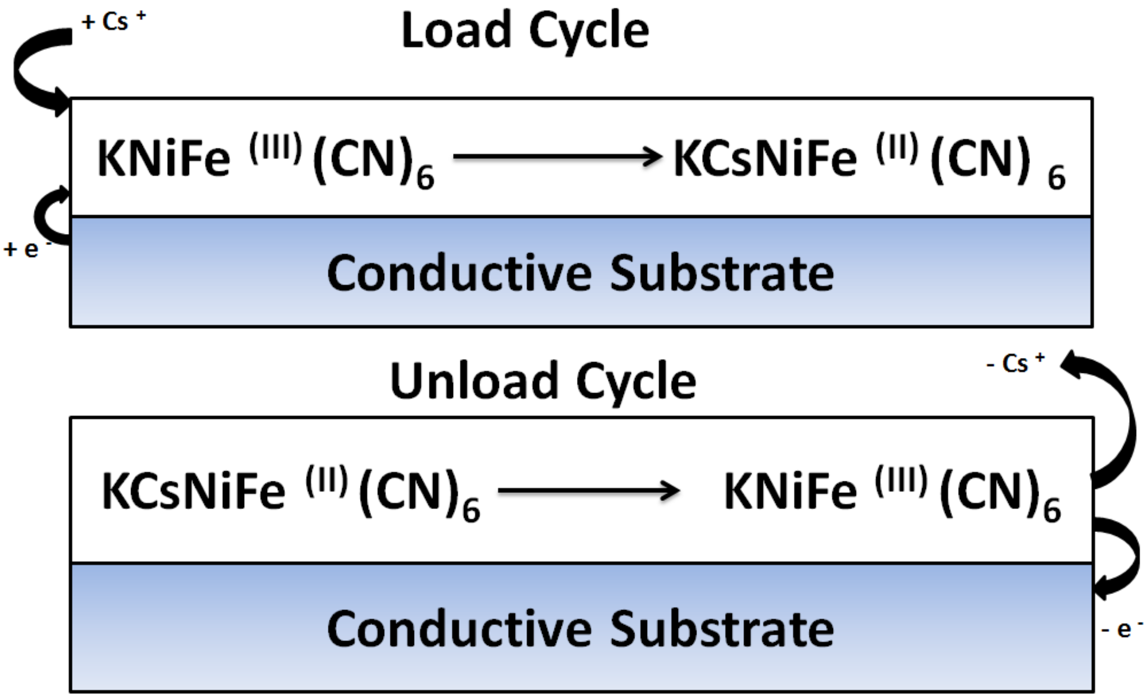

Figure 4.1: Conductive substrate coated with nickel hexacyanoferrate (source: Lilga et al., 1997)

This work represents the preparation of four different nickel hexacyanoferrate films on a nickel substrate by electrodeposition using different applied voltages to study the characteristics of the prepared films. The different applied voltages affect the rate at which the film is grown and, potentially, its performance for ESIX. The film morphologies were examined using scanning electron microscopy and they were individually tested for their film capacity and their repetitive loading and unloading capabilities using cyclic voltammetry.

4.2 Experimental methods

4.2.1 General and electrochemical

A Potentiostat (Wave Driver 10, Pine Research Instrumentation) was used to deposit and characterize films. The software that was used to control the Potentiostat (Aftermath 2.0) was provided by Pine Research. A standard three-electrode system was used in the preparation and characterization of electroactive films. A saturated calomel electrode (SCE) was used as a reference electrode for the potential measurements. A platinum counter electrode with a surface area of 5 cm^2 was employed in all experiments. It is important to note that all voltage measurements mentioned in this work are relative to the SCE. The reference and the counter electrode were located less than two cm from the working electrode. The working electrode was composed of nickel and its composition and preparation is further described in Section 4.2.2.

The chemicals which were used, $K_3Fe(CN)_6$, KNO_3, and $CsNO_3$, were all reagent-grade with greater than 99% purity and were used without further purification. Deionized water (18.2 $M\Omega\ cm^{-1}$) was used in all salt solution preparations and cleaning of electrochemical cell components.

4.2.2 Surface preparation

Nickel disks (99.99% pure) were used as the working electrodes. A nickel disk was embedded in a Teflon holder suspended in the test solution. The portion of the disk exposed to test solution has a diameter of 0.5 cm and an area 0.196 cm^2. The nickel surface was abraded using 800 grit diamond lapping film prior to film deposition.

4.2.3 Film preparation

The nickel hexacyanoferrate films preparation methodology was adapted from the method described by Bocarsly et al. (1982). In their work, nickel was first oxidized at an anodic potential of 0.6 V – 1 V relative to SCE for approximately 30 min. in a solution containing 10 mM $M_3Fe(CN)_6$ and a supporting electrolyte 0.1 M MNO_3, and an insoluble, stable alkali $MNiFe^{III}(CN)_6$ was formed on the electrode surface, where M was K, Na, or Cs.

In this work, a solution containing 20 mM $K_3Fe(CN)_6$ and 1 M KNO_3 was used for the film preparation. The solution had oxygen stripped from it by bubbling nitrogen gas through the solution before starting the deposition procedure. Table 4.1 represents the different parameters for film preparation.

Table 4.1: Four film preparation voltage

Film number	**1st step (30 min)**	**2nd step (30 min)**
A	0.2 V	1.2 V
B	0.2 V	1.25 V
C	0.2 V	1.3 V
D	0.3 V	1.3 V

Four ESIX films were prepared by submerging a nickel electrode in a solution of 20 mM $K_3Fe(CN)_6$ and 1 M KNO_3 and then applying the electrical potential for the initial phase of the film deposition. For three of the test films a potential of 0.2 V was applied for 30 minutes and then a potential of either 1.2 V, 1.25 V, or 1.3 V was applied for a further 30 minutes. A final film was prepared by applying 0.3 V for 30 minutes, followed by 1.3 V for an additional 30 minutes.

The purpose of using low voltage for the first step was to form a very thin mononuclear layer on the ESIX film to act as a nucleation sites for the other layers of the ESIX film, which were deposited under the higher voltage in the second step.

4.2.4 Film characterization

The film was characterized in multiple ways. First, the surface morphology for the prepared films was imaged using scanning electron microscopy conducted using a JOEL 7000 electron microscope to examine the film morphology.

The film capacity for Cs^+ sorption was measured by applying -0.2 V for 3 minutes to the electrode, which contained the prepared film in a solution of 2.25 $x10^{-3}$ M Cs^+ to load the Cs^+ from the solution. These capacities were compared to standard solutions in order to determine the quantity of Cs^+ removal. The Cs^+ concentrations were measured by electrospray ionization-mass spectroscopy (ESI-MS), with samples being diluted with HPLC-grade methanol in order to be within the measurement range of the equipment.

The film's capability for repeated cycling of ESIX was characterized using cyclic voltammetry, which was conducted in a 1 M $CsNO_3$ solution. The applied potential started at 0.2 V and was scanned anodically to 0.9 V then catholically to -0.2 V then back to 0.2 V at a scan rate of 50 mV s^{-1}. N_2 gas was bubbled throughout the solution during the experiments in order to reduce the dissolved oxygen.

4.3 Results and discussion

4.3.1 Film morphology by SEM

Figure 4.2 is the SEM image of the four films. The surface of the nickel electrode coated with hexacyanoferrate is displayed at a magnification of 30,000x. The most common feature between the four SEM images is the presence of some fissures on the surface. These fissures are believed to be caused by the drying pre-treatment required for SEM imaging. This drying involved the nickel electrode coated with the film to be heated at 50 ºC for 30 minutes before it was coated with a 5 nm layer of graphite for the SEM imaging. It is, therefore, unlikely that these fissures were present in any films which were not imaged.

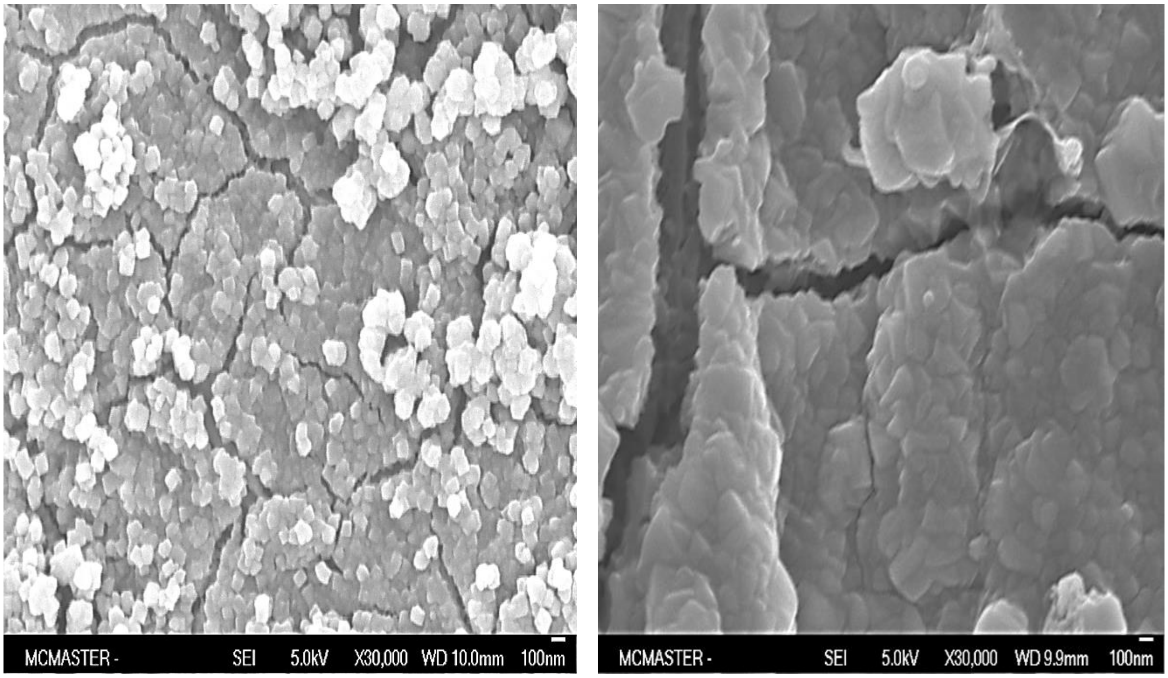

Film (A) Film (B)

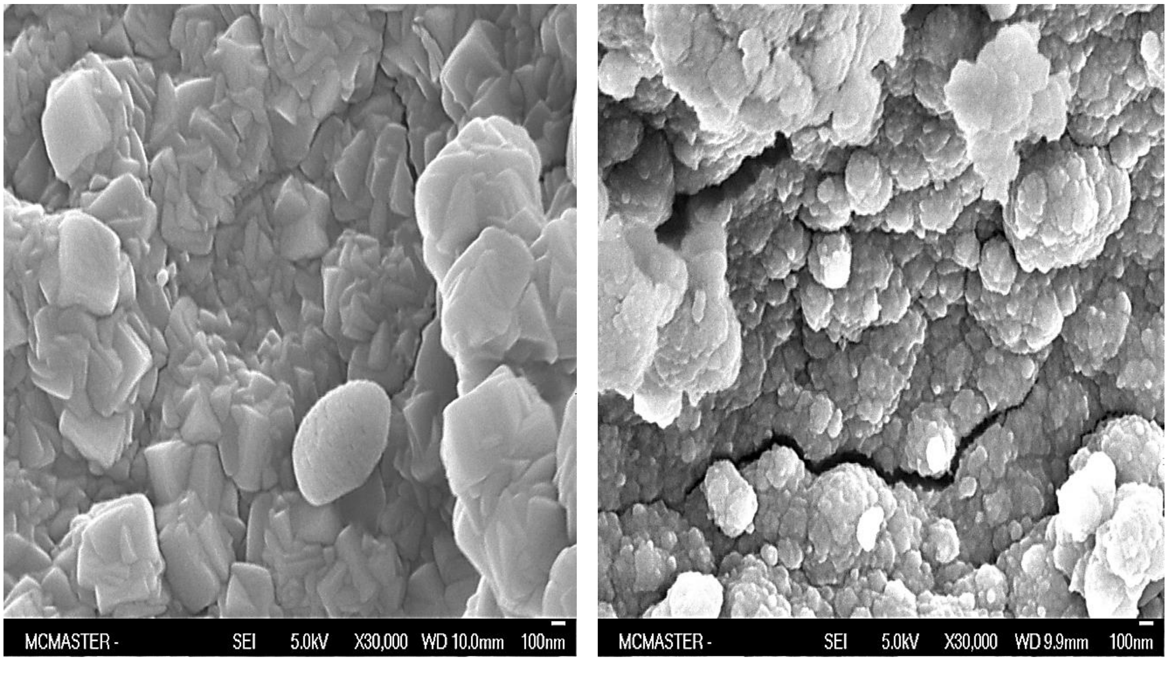

Film (C) Film (D)

Figure 4.2: SEM images of the four films

Film (A)'s image shows a uniform layer of the prepared film. However this film seems to be thinner than the other films. Their thinness suggests that the 2nd step in the film preparation (applying 1.2 V) was not sufficient to form multiple layers over the nucleation site layer formed when applying 0.2 V in the initial stage.

The image of Film (B) shows a more uniform and denser layer of the prepared film than Film (A). The higher voltage for the 2nd step in the film preparation (1.25 V) causes more layers of nickel hexacyanoferrate to be built up, forming this more densely layered film.

Film (C) shows a distribution of sizes of the deposited film upon the surface of the nickel electrode with minimal evidence of fissures. The higher level of robustness of this film is believed to be caused by the higher applied voltage (1.3 V) in the second stage of the creation of the film, making it a more resilient film.

Film (D) demonstrates a fused film, with non-uniform and larger spherical grains than those in the previous films, along with a lengthy fissure. It is believed that the non-uniformity and spherical morphology are due to the higher initial applied voltage (0.3 V) during the first stage of film growth. This approach created a non-uniform layer of mononuclear hexacyanoferrate film, creating larger nucleation sites, which then allowed for more growth on those nucleation sites during the second step of film preparation at (1.3 V).

4.3.2 Cs^+ quantification after uptake and release of a single cycle by ESI-MS

4.3.2.1 Cs^+ loading and unloading

Table 4.2 shows the Cs^+ loading results from test solution containing 2.25×10^{-3} M Cs^+ using the four ESIX films.

Table 4.2: Cs^+ loading and unloading results

	Film A	**Film B**	**Film C**	**Film D**	**Film E**
Initial Amount (M)	2.25×10^{-3}	2.25×10^{-3}	2.25×10^{-3}	2.25×10^{-3}	2.25×10^{-3}
Cs^+ in solution after loading (M)	6.3×10^{-4}	6.5×10^{-4}	4.5×10^{-4}	8.8×10^{-4}	2.25×10^{-3}
% loaded	72	71.1	80	60.8	0
Cs^+ in solution after unload (M)	1.38×10^{-3}	1.37×10^{-3}	1.6×10^{-3}	1.16×10^{-3}	2.25×10^{-3}
% unloaded	85.1	85.6	88.8	84.6	0

Table (4.2) shows the Cs^+ uptake and release by the four ESIX films, as well as a nickel electrode without the hexacyanoferrate ESIX film as a control (Film (E)). Electrode C was loaded with more Cs^+ than the other films, up to 80% of the original amount of Cs^+ (1.8×10^{-3} M out of 2.25×10^{-3} M). This agrees with the results from the cyclic voltammetry discussed in Section 4.3 for the same prepared ESIX films, demonstrating that Film C has superior performance in loading Cs^+ than the other three ESIX films. Films A and B showed comparable results for Cs^+ uptake and release, taking up roughly 72% of the available Cs^+ from solution. Film D performed significantly worse, with a 10% lower uptake. The control electrode shows no capability for ion exchange of any kind. For all films, less than 100% of the taken up Cs^+ was released, indicating that there is a loss of capacity of the film with cycling of Cs^+ from the ESIX electrode.

4.3.3 Film characterization (Cyclic Voltammogram)

The observed voltammetry waveforms demonstrate that all of the films are capable of the reactions for the uptake and release of Cs^+. Voltammogram curves are shown for each film which represents the electrical behavior of the films for cycles 1, 500, and 1000. From this measurement, it is possible to determine the maximum in peak current as a function of the applied potential in order to determine how the capacity diminishes during repetitive Cs^+ loading and unloading.

Also shown is the integration of the current signal obtained from the voltammogram. This was measured in order to calculate the maximum charge capacity of each film as well as its surface coverage. The maximum charge capacity is simply the total amount of charge that the film is able to retain per unit area, while the surface coverage is calculated by dividing the maximum charge capacity by Faraday's Constant to obtain the number of redox species that contribute to the current. These calculations give insight to the number of active site per unit area (Prodromidis et al., 2000).

4.3.3.1 Film A (0.2 V then 1.2 V)

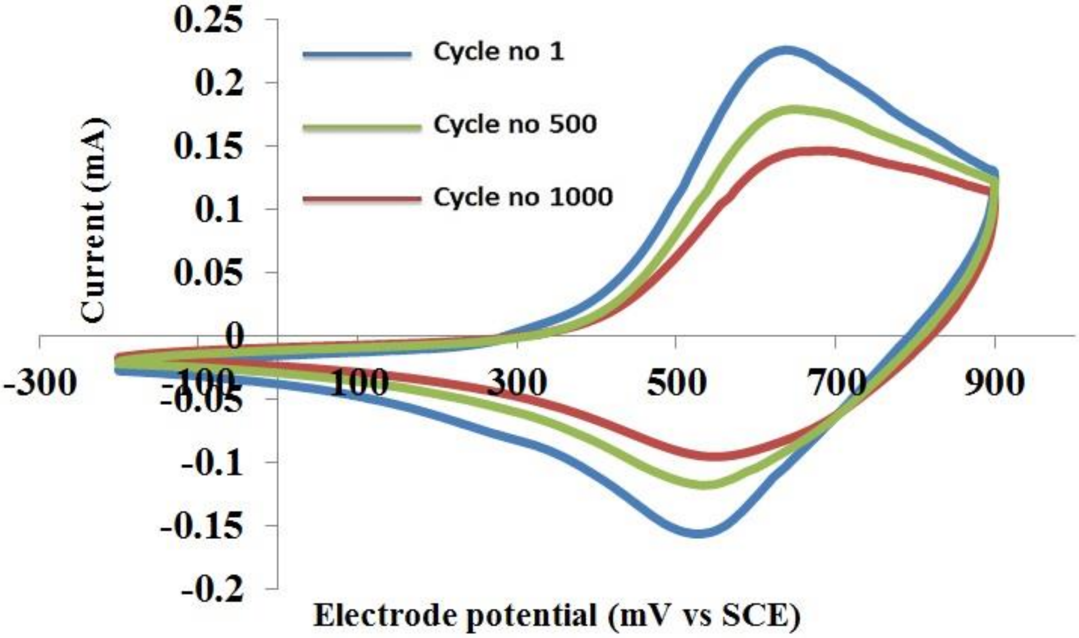

Figure 4.3: Cyclic voltammogram for Film A in 1 M $CsNO_3$

Figure (4.3) shows the cyclic voltammogram for Film A in a 1 M $CsNO_3$ solution. The shape of the cyclic voltammogram in the figure confirms that the loading and unloading of Cs^+ is occurring. The curves represent the voltammogram for cycles 1, 500, and 1000. The peak current during the reduction cycle occurred at an applied potential of approximately 550 mV, where Cs^+ was loaded and the current approached 0 mA at 300 mV as the reduction of ferricyanide to ferrocyanide neared completion and terminated the uptake of Cs^+. The oxidation of ferrocyanide to ferricyanide begins with the unloading of Cs^+ from the film, which occurred at 800 mV, and the peak current during the release of Cs^+ from the cyclic voltammogram occurred at 630 mV. The peak current was reduced in cycle 500 and even further in cycle 1000, which indicates that the film loses its capacity during the Cs$^+$ removal process. The film capacity was reduced by approximately 46% after 1000 cycles of loading and unloading Cs$^+$.

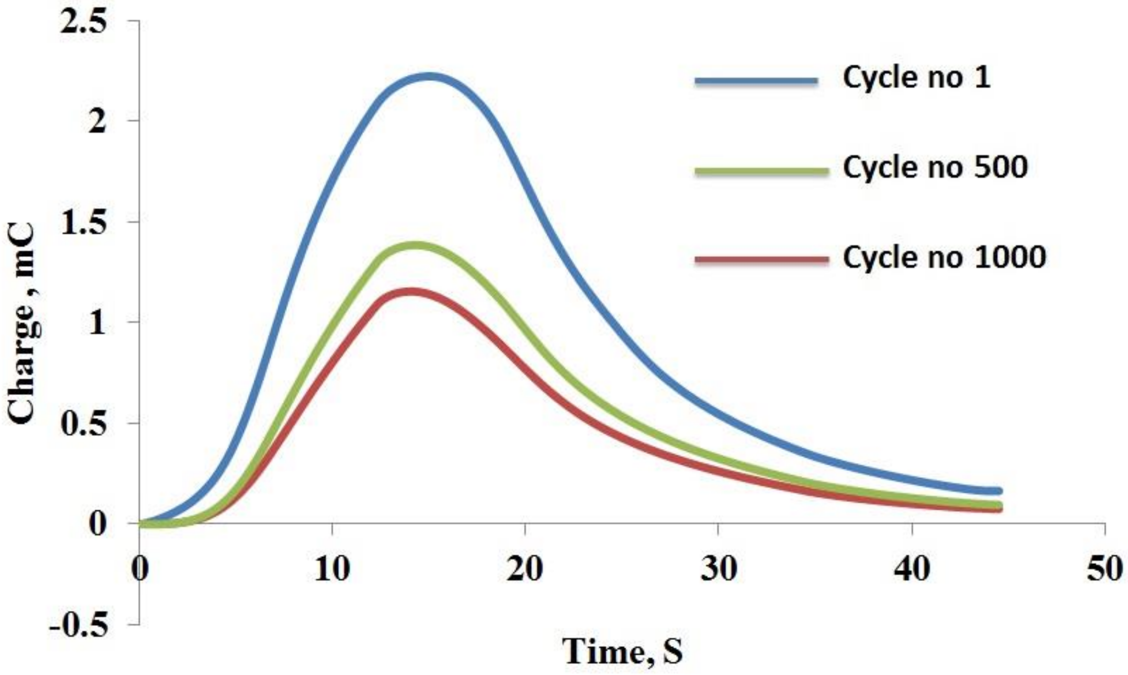

Figure 4.4: Integration of the current over the 1st, 500th and 1000th voltammetry sweeps for Film A

Figure 4.4 shows the capacity of Film A by integrating the current over the course of cycles 1, 500, and 1000 from the voltammetry sweeps with respect to time. It is noted that the charge did not return to zero after a complete cycle. This result indicates that there is not a complete exchange of all of the ions between the film and the solution after a complete cycle, which was also noted in Section 4.3.2. The maximum charge capacity of the film at cycles 1, 500, and 1000 is summarized in Table 4.3.

Table 4.3: Film A characterization after cycles 1, 500, and 1000

Cycles	Maximum charge capacity	Surface coverage
1	11.5×10^{-3} C cm^{-2}	1.18×10^{-7} mol cm^{-2}
500	7.14×10^{-3} C cm^{-2}	7.4×10^{-8} mol cm^{-2}
1000	6.12×10^{-3} C cm^{-2}	6.34×10^{-8} mol cm^{-2}

4.3.3.2 Film B (0.2 V then 1.25 V)

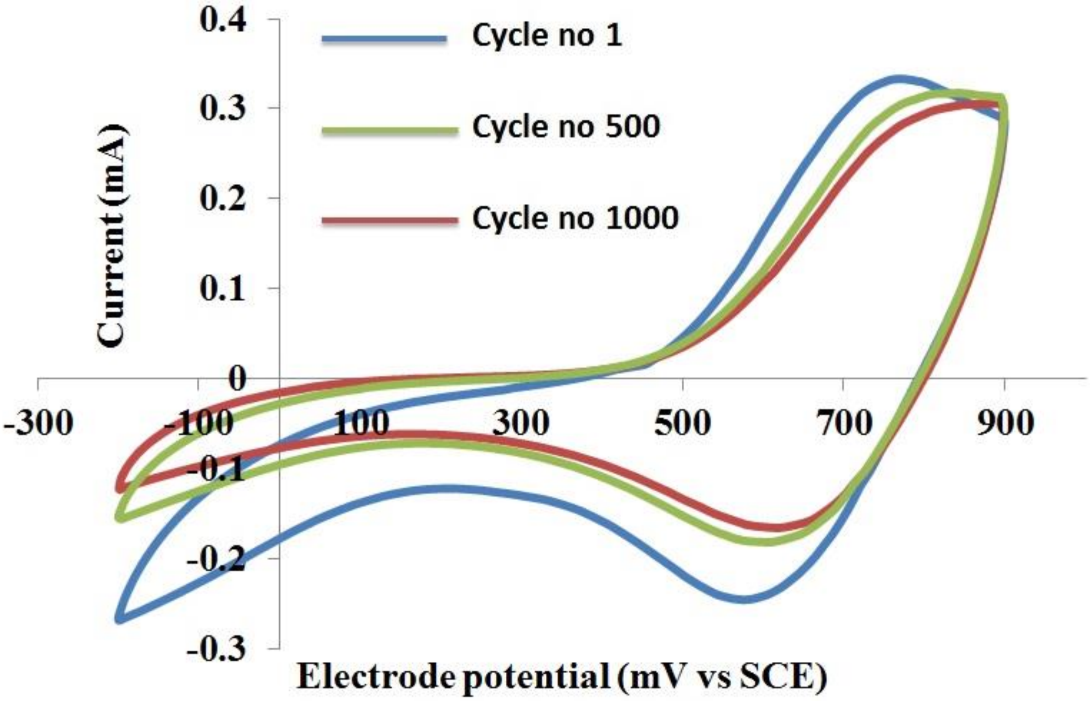

Figure 4.5: Cyclic voltammogram for Film B in 1 M $CsNO_3$

Figure 4.5 shows the behavior of Film B under cyclic voltammetry in a 1 M $CsNO_3$ solution. During Cs^+ loading, the peak current occurred at an applied potential of approximately 570 mV, and the current approached zero at 350 mV as the maximum amount of Cs^+ was removed from solution. The oxidation of ferrocyanide to ferricyanide occurs as Cs^+ is unloaded, and the peak current achieved was 700 mV. There was a 20% decrease in the peak current between cycle 1 and cycle 1000.

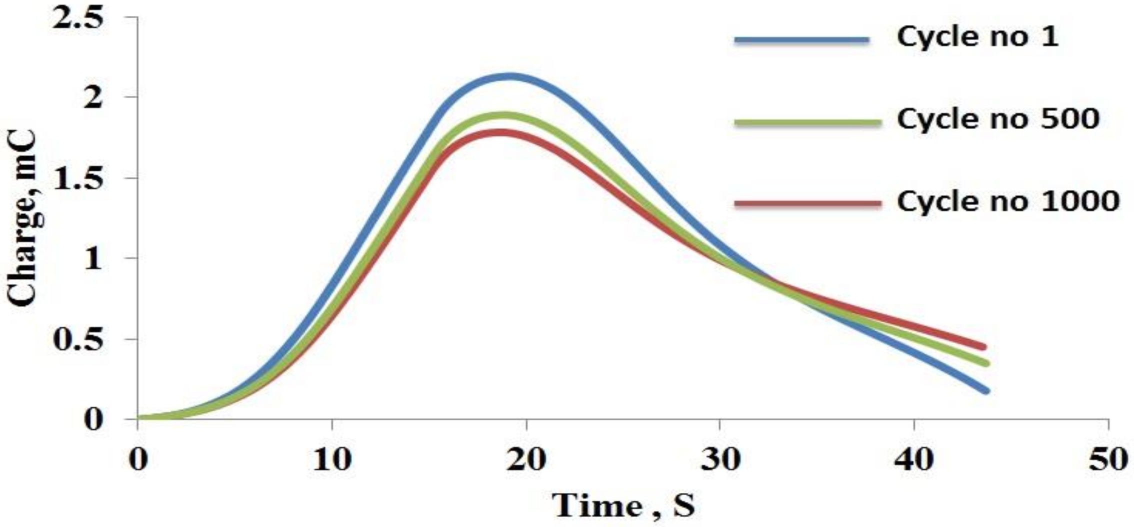

Figure 4.6: Integration of the current from cycles (1, 500 and 1000) of Film B.

Figure 4.6 shows the capacity of the film. It is again noted that the charge did not return to zero after a complete cycle for this film either.

The maximum charge capacity of the film at cycles 1, 500 and 1000 is summarized in table 4.4.

Table 4.4: Film B characterization after cycles 1, 500 and 1000.

Cycles	**Maximum charge capacity**	**Surface coverage**
1	11.2×10^{-3} C cm^{-2}	1.16×10^{-7} mol cm^{-2}
500	9.18×10^{-3} C cm^{-2}	9.5×10^{-8} mol cm^{-2}
1000	8.9×10^{-3} C cm^{-2}	9.2×10^{-8} mol cm^{-2}

4.3.3.3 Film C (0.2 V then 1.3 V)

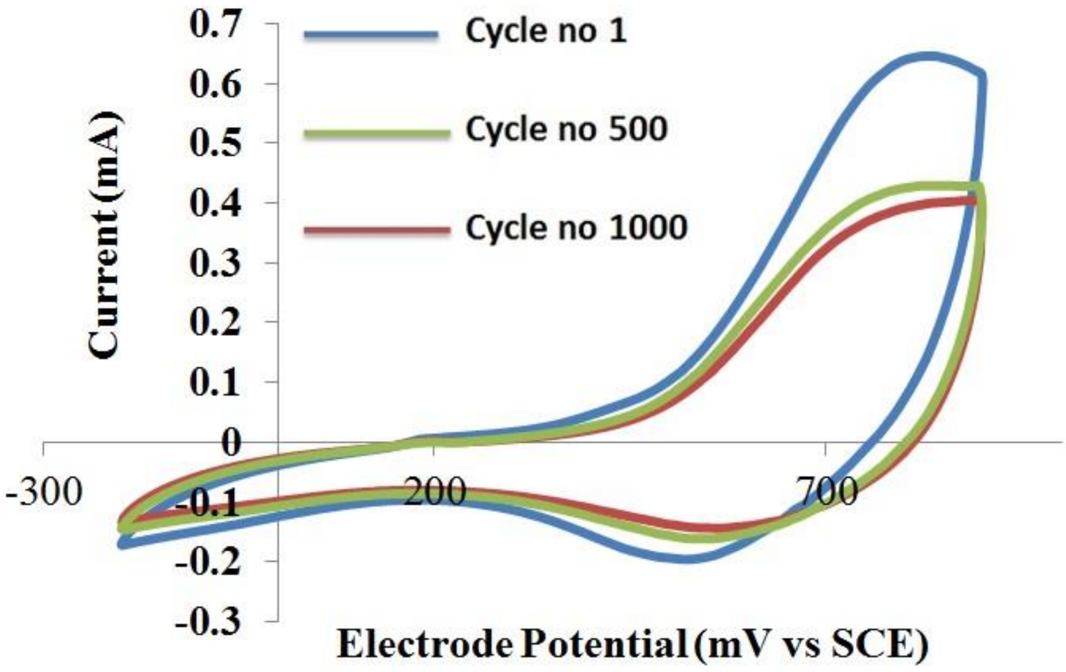

Figure 4.7: Cyclic voltammogram for Film C in 1 M $CsNO_3$

Figure 4.7 shows the cyclic voltammogram for Film C in a 1 M $CsNO_3$ solution. As Cs^+ is loaded, the peak current in the cyclic voltammogram was approximately 550 mV and the current approached zero at 200 mV. During Cs^+ unloading, the peak current occurred at 700 mV. There was a 36% reduction in peak current from cycle 1 to cycle 1000. The largest reduction occurred during between cycle 1 and cycle 500, however, at 34%.

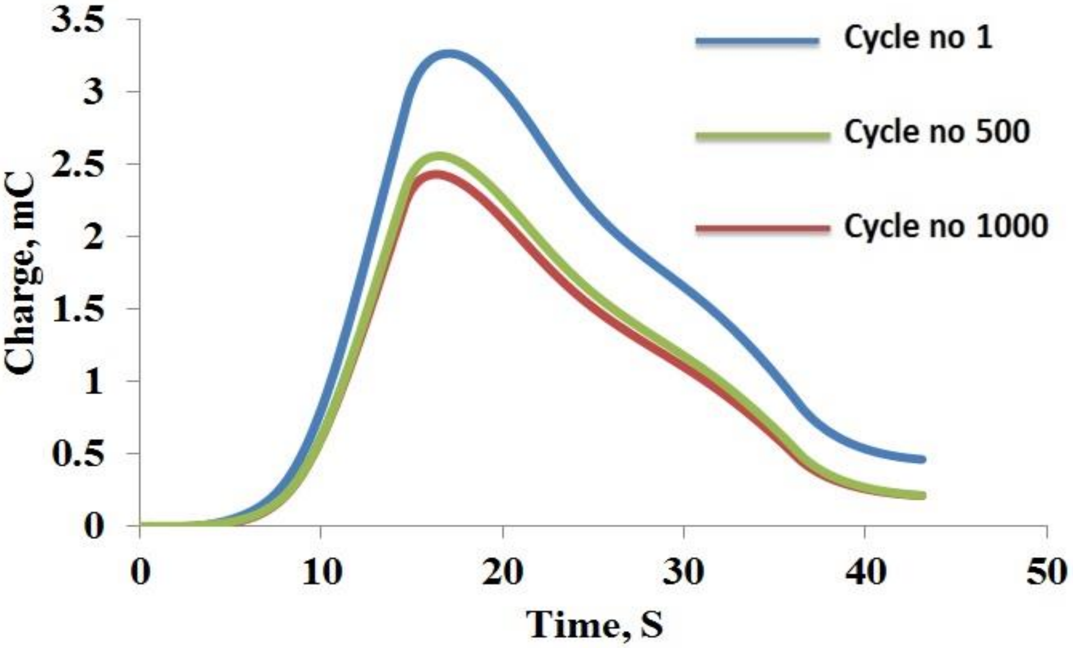

Figure 4.8: Integration of the current from cycles 1, 500, and 1000 for Film C

Figure 4.8 shows the integration the current passes over the course of the cycles (1, 500, and 1000) for film C. The fact that the current did not return to zero again shows that there was not the same number of charge carriers exchanged during the unloading phase as the loading phase, and, therefore, demonstrates the subsequent decrease in charge capacity. The maximum charge capacity of the film at cycles 1, 500, and 1000 is summarized in Table 4.5.

Table 4.5: Film C characterization after cycles 1, 500, and 1000.

Cycles	**Maximum charge capacity**	**Surface coverage**
1	17.3×10^{-3} C cm^{-2}	1.79×10^{-7} mol cm^{-2}
500	12.7×10^{-3} C cm^{-2}	1.31×10^{-7} mol cm^{-2}
1000	11.1×10^{-3} C cm^{-2}	1.15×10^{-7} mol cm^{-2}

4.3.3.4 Film D (0.3 v then 1.3 v)

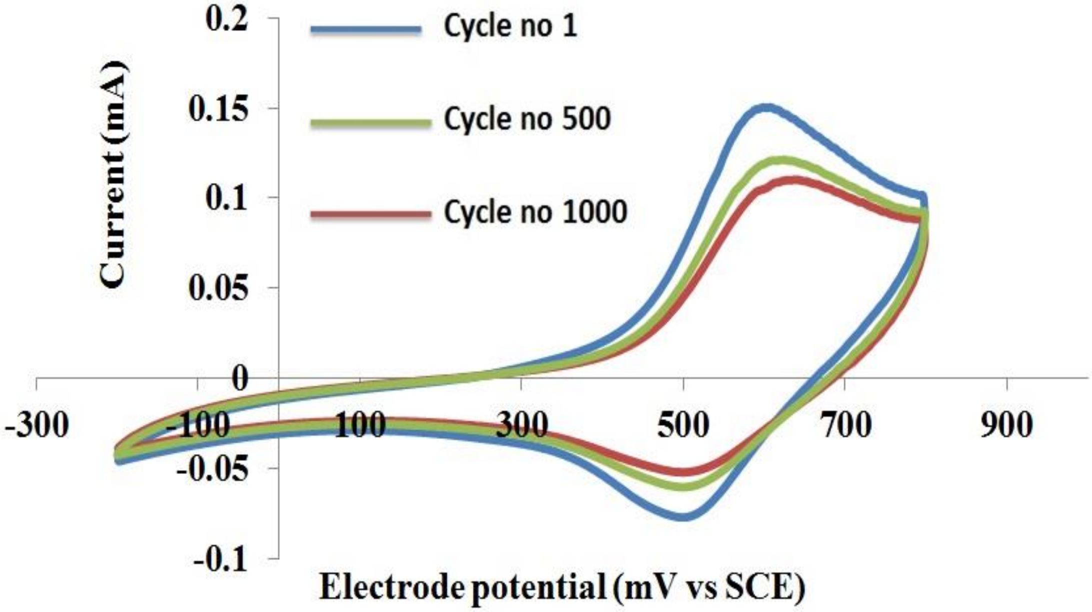

Figure 4.9: Cyclic voltammogram for Film D in 1 M $CsNO_3$

Figure 4.9 shows the cyclic voltammogram for Film D in a 1 M $CsNO_3$ solution. The peak current in the cyclic voltammogram during the loading of the film occurred at approximately 500 mV and the current approached zero at 200 mV as Cs^+ loading neared completion. Cs^+ unloading begins as oxidation of ferrocyanide to ferricyanide starts. The peak current during the release phase occurred at an applied potential of 580 mV, and the current went to 0 mA at 700 mV, signaling the end of unloading phase. The film’s peak height was reduced 36% after 1000 cycles.

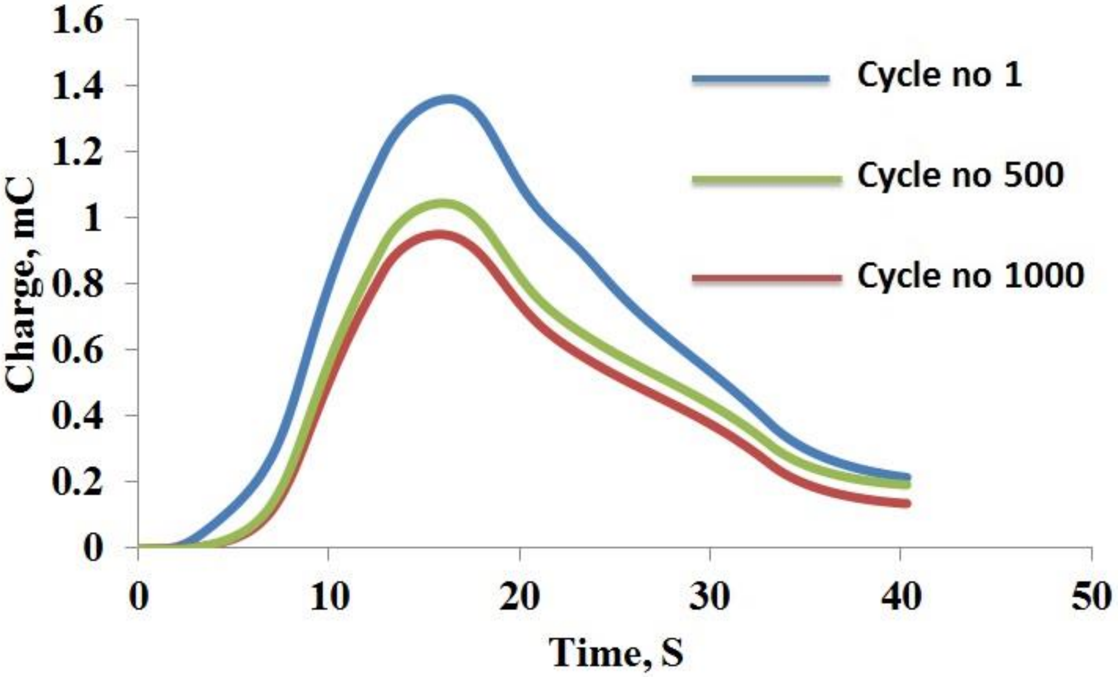

Figure 4.10: Integration of the current from cycles 1,500 and 1000 for Film D.

Figure 4.10 shows the capacity of the film by integrating the current over the course of cycles 1, 500, and 1000 of Film D. There is again a reduction in film capacity after a single cycle. The maximum charge capacity of the film at cycles (1, 500, and 1000) is summarized in Table 4.6.

Table 4.6: Film D characterization after cycles 1, 500 and 1000.

Cycles	Maximum charge capacity	Surface coverage
1	7.14×10^{-3} C cm^{-2}	7.4×10^{-8} mol cm^{-2}
500	5.35×10^{-3} C cm^{-2}	5.54×10^{-8} mol cm^{-2}
1000	4.84×10^{-3} C cm^{-2}	5.01×10^{-8} mol cm^{-2}

4.4 Summary of Results and Discussion

The results found in this study of the four films are shown by their characterization for ESIX in Table 4.7.

Table 4.7: Characterization of the four tested films.

	Film A	**Film B**	**Film C**	**Film D**
Max. capacity after first cycle (C cm^{-2}) mean value	11.5 x 10^{-3}	11.2 x 10^{-3}	17.3 x 10^{-3}	7.14 x 10^{-3}
Standard deviation	0.3	0.28	0.12	0.31
Surface coverage after the first cycle(mol cm^{-2}) mean value	1.18 x 10^{-7}	1.16 x 10^{-7}	1.79 x 10^{-7}	7.4 x10^{-8}
Standard deviation	0.29	0.26	0.14	0.27
Max. capacity after cycle 1000 (C cm^{-2}) mean value	6.2 x 10^{-3}	8.9 x 10^{-3}	11.1 x 10^{-3}	4.48 x 10^{-3}
Standard deviation	0.35	0.36	0.18	0.32
Surface coverage after1000 cycles (mol cm^{-2}) mean value	6.34 x10^{-8}	9.20 x10^{-8}	1.15 x 10^{-7}	5.01 x10^{-8}
Standard deviation	0.33	0.3	0.18	0.3

Table 4.8 and figure 4.11 show that although Film C had the highest initial charge capacity of, 17.3 x 10^{-3} C.cm^{-2}, it also suffered the largest decrease in capacity of 6.4 x10^{-8} mol cm^{-2} after 1000 cycles. even after this significant loss in capacity, 36% of the original, however, it still retained the same or a higher capacity than the initial value of all

other films tested. Films A and B had similar charge capacities of 11.5 x 10^{-3} C.cm^{-2} and 11.2 x 10^{-3} C.cm^{-2}, respectively. Film A, however suffered a much higher loss in capacity, losing 5.3 x 10^{-3} C cm^{-2}, or 46%, of its initial capacity, while Film B underwent a loss of only 2.3 x10^{-8} mol cm^{-2}, or 20%, of its initial capacity. These results suggest that the higher the applied potential in the initial stage, the greater the number of nucleation sites to develop, which, during the growth stage, generates a much higher-capacity film. The increased potential in the growth stage also allows for a more resilient film in terms of maintaining its charge capacity over repeated cycling. It seems, however, that too high an applied potential in the initial stage causes the film to have a much lower capacity and a much lower ability to maintain its charge capacity over repeated cycling.

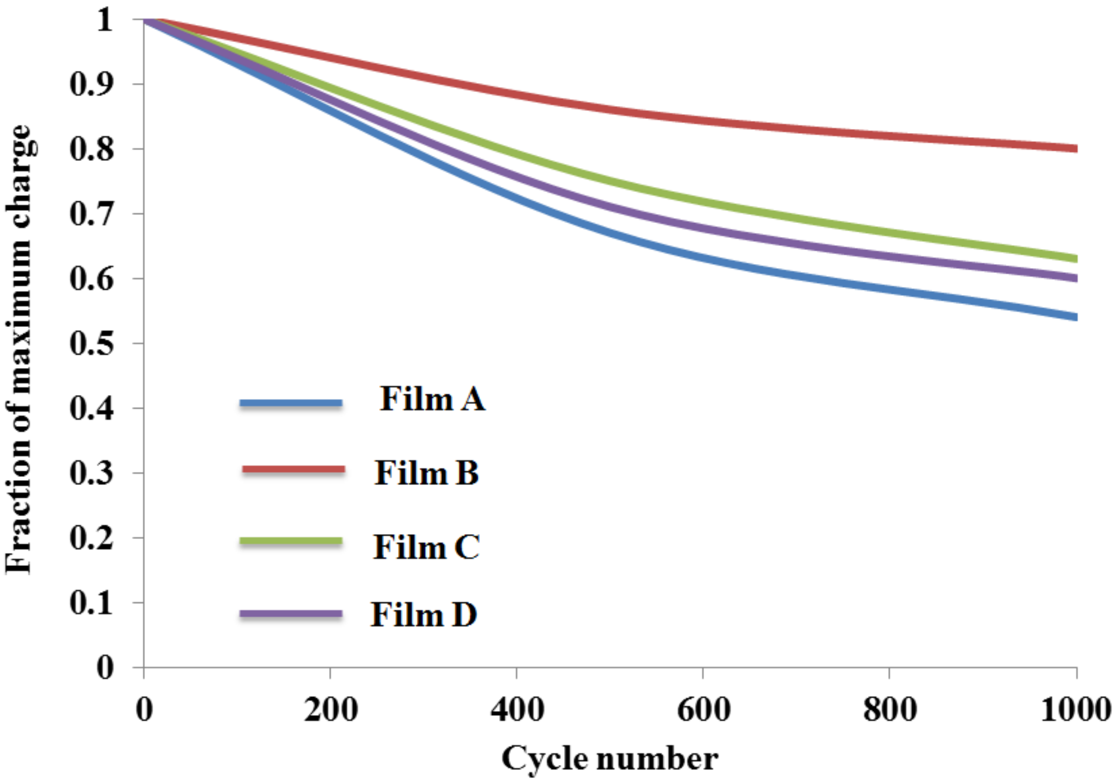

Figure 4.11: Evolution of film capacity with number of cycles

There are two potential causes for the reduction in film capacity: the first cause could be that some of the Cs^+ remains permanently attached to the active sites on the film and is unable to be unloaded. The second possibility may be that parts of the film detach from the electrode surface during the loading and unloading of Cs^+, causing a loss in the film itself. The solution was tested after concluding an experiment for the presence of either ferric or ferrous ions by ESI-MS, and there was no detectable amount of either of these ions. This absence indicates that the hexacyanoferrate ($(Fe(CN)_6)^{3-}$) film was stable. From these results, it is concluded that the loss in film capacity is caused by the depletion of active sites over the course of repeated cycling.

4.5 Conclusion

Four hexacyanoferrate films were prepared on nickel electrodes using different applied potentials in order to examine their capability for the electronically switched ion exchange of the Cs^+ ion from an aqueous solution. These four films were compared by examining the surface morphology using SEM, measurements of the film capacity, and studying their performance through cyclic voltammetry. The results show that there is a significant difference in the performance of the four films with regard to Cs^+ removal, and that its removal depends on the applied potentials used during the preparation of the film. In this instance, a film which was prepared by depositing nickel hexacyanoferrate using an initial voltage of 0.2 V relative to a SCE for 30 minutes in the initiation stage, followed by a voltage of 1.3 V relative to SCE for 30 minutes for film growth, demonstrates the best performance, as it had the highest capacity for Cs^+ removal from a contaminated solution. Furthermore, this film demonstrated the lowest reduction in capacity with repeated cycling; its reduced capacity was similar to that of the initial capacities of the two next best performing electrodes after 1000 cycles, which gives evidence that it would be a good candidate for electrically switched ion exchange film for the removal of Cs^+ from solution.

4.6 Acknowledgements

The authors would like to thank the Egyptian Ministry of Defense (EMD) and the Natural Science and Engineering Research Council of Canada (NSERC) (Discovery Grants Program) for supporting this work.

4.7 References

Anthony, R. G., Dosch, R. G., Gu, S. D., and Philip, C.V. (1994) "Use of silicotitanates for removing cesium and strontium from defense waste" *Ind. Eng. Chem. Res* 33, PP 2702-2705.

Bocarsly A. B., Sinha, A., (1982) "Chemically derivatized nickel surfaces: synthesis of a new class of stable electrode interfaces." *J. Electroanal. Chem.* 137, PP 157–162.

Bocarsly A. B., Sinha, A., (1982) "Effects of surface structure on electrode charge transfer properties, Induction of ion selectivity at the chemically derivatize interface," *J. Electroanal. Chem.* 140, PP 167–172.

Borai, E. H., Harjula, R., Malinen, L., and Paajanen, A. (2009). “Efficient removal of ceasium from low-level radioactive liquid waste using natural and impregnated zeolite minerals.” *Journal of Hazardous Materials*, 172(1), 416–22.

Green-Pedersen, H., and Korshin, G. V. (1999). “Separation of Ceasium from High Ionic Strength Solutions Using a Cobalt Hexacyanoferrate-Modified Graphite Electrode.” *Environmental Science & Technology*, 33, PP 2633–37.

Gomez Reyes- J., Medina, J. A., Jeerage, K. M., Steen, W. A., and Schwartz, D. T. (2004). “High Capacity SiO_2-Graphite Composite Electrodes with Chemically Incorporated Metal MHCFs for Electrochemically Switched Alkaline Cation Exchange.” *Journal of the Electrochemical Society*, 151, PP D87-D92.

Hao, Xiaogang, Yongguo, Li, and Mark, Pritzker, 2008 “Pulsed electrodeposition of nickel hexacyanoferrate films for electrochemically switched ion exchange” *Separation and Purification Technology* 63, PP 407–414.

Hao, Xiao-gan, and Guo, Jin-xia., (2006) “Electrochemically switched ion exchange performances of capillary deposited nickel hexacyanoferrate thin films” Trans. *Nonferrous Met. SOC.* China 16, PP 556-561.

Law, J. D., Herbst, R. S., Todd, T. A., Romanovskiy, V. N., Babain, V. A., Esimantovskiy, V. M., and Zaitsev, B. N. (2007) “The Universal Solvent Extraction (Unex) Process. Flowsheet Development and Demonstration of the Unex Process for the Separation of Cesium, Strontium, and Actinides from Actual Acidic Radioactive Waste” *Solvent Extraction and Ion Exchange*, 19, PP 23–36.

Li, Na., Zhongjie, Li., Junhua, Yuan., Jianguo, Hu, Jigen, Mia., and Qixian, Zhang (2012) "Nickel hexacyanoferrate nanoparticles anchored to multiwalled carbon nanotubes with a grafted poly(4-vinylpyridine) linker for electrically switched ion exchange" *Electrochimica Acta* 72, PP 150-156.

Lilga, M.A., Orth, R.J., Sukamto, J.P.H., Haight, S.M., and Schwartz, D.T., (1997) "Metal ion separations using electrically switched ion exchange" *Separation and Purification Technology* 11, PP 147-158.

Lilga, M.A., Orth, R.J., Sukamto, J.P.H., and Rassat, S.D. (2001) "Cesium separation using electrically switched ion exchange" *Separation and Purification Technology* 24, PP 451–466.

McDowell, W. J., Case, G. N., Mcdonough, J. A., and Bartsch, R. A. (1992) "Selective Extraction of cesium from Acidic Nitrate Solutions with Didodecyl naphthalene sulfonic Acid Synergized with Bis (tertbutylbenzo)",Analytical Chemistry, PP 3013–3017.

Mohapatra, P. K., Bhattacharyya, A., and Manchanda, V. K. (2010) "Selective separation of radio-cesium from acidic solutions using supported liquid membrane containing chlorinated cobalt dicarbollide (CCD) in phenyl trifluoromethyl sulphone (PTMS)." *Journal of Hazardous Materials*, 181, PP 679–85.

Mohapatra, P. K., Lakshmi, D. S., Bhattacharyya, A., and Manchanda, V. K. (2009) "Evaluation of polymer inclusion membranes containing crown ethers for selective cesium separation from nuclear waste solution." *Journal of Hazardous Materials*, 169, PP 472– 490.

Prodromidis, M. I., Florou, A. B., Tzouwara-Karayanni, S. M., and Karayannis, M. I.(2000) “The Importance of Surface Coverage in the Electrochemical Study of Chemically Modified Electrodes” Electroanalysis PP 1498–1501.

Rassat, S.D., Sukamto, J.H., and Lilga, M.A. (1999) “Development of an electrically switched ion exchange process for selective ion separations” Separation and Purification Technology, 210, PP 207-222.

Romanovskiy, V. N., Smirnov, I. V., Babain, V. A., Todd, T. A., Herbst, R. S., Law, J. D., and Brewer, K. N. (2007) “The Universal Solvent Extraction (Unex) Process. I. Development of the Unex Process Solvent for the Separation of cesium, Strontium, and the Actinides From Acidic Radioactive Waste” *Solvent Extraction and Ion Exchange*, 19, PP 1–21.

Roy, K., Pal, D., Basu, S., Nayak, D., and Lahiri, S. (2002) “Synthesis of a new ion exchanger, zirconium vanadate, and its application to the separation of barium and cesium radionuclides at tracer levels” *Applied Radiation and Isotopes*, 57, PP 471–474.

Shakir K., Sohsah, M., and Soliman, M. (2007) “Removal of cesium from aqueous solutions and Radioactive waste simulants by coprecipitate flotation” *Separation and Purification Technology* 54, PP 373–81.

Sinha, P. K., Panicker, and R. V. Amalraj (1995) “Original Contribution Treatment of Radioactive Liquid Waste Containing Cesium by Indigenously Available Synthetic Zeolites: A Comparative Study” Waste managment 15, PP 149-157.

Someda, H. ., El-Zahhar, A. ., Shehata, M., and El-Naggar, H. (2002) “Supporting of some ferrocyanides on polyacrylonitrile (PAN) binding polymer and their application for cesium treatment” *Separation and Purification Technology*, 29, PP 53–61.

Steen, W., Han, S.-W., Yu, Q., Gordon, R., Cross, J. O., Stern, E, and Schwartz, D. T. (2002) “Structure of Cathodically Deposited Nickel Hexacyanoferrate Thin Films Using XRD and EXAFS. Langmuir” *American chemical society* 18, PP , 7714-21.

Sun, B., Hao, X., Wang, Z., Zhang, Z., Liu, S., and Guan, G. (2012) “Continuous Separation of Cesium Based on NiHCF/PTCF Electrode by Electrochemically Switched Ion Exchange” *Chinese Journal of Chemical Engineering*, 20, PP 837–842.

Tanihara, K. (1994) “A new process using redox type of ion exchange for cesium separation” *Radio Analytical and Nuclear Chemistry*, Vol. 185, PP 57-67.

Chapter 5

Graphite electrode as an electrically switched ion exchange

The contents of this chapter will be submitted to a journal in November 2014 as: Tawfic, A.F., Dickson, S.E., Kim, Y., Mekky, W., 2014. Graphite electrode as an electrically switched ion exchange

Abstract

Electrically switched ion exchange (ESIX) can be used for the separation of Cs^+ from nuclear wastewater. In ESIX, an ion exchange film is deposited onto an electrode surface. Cs^+ is separated from the wastewater and held in the ESIX film during the electrical reduction step. The ions are then unloaded from the film by applying oxidizing potentials to the electrode. In this study, a graphite electrode was used as a porous substrate to prepare nickel hexacyanoferrate films in its pores to improve the capacity for cesium ion separation. X-ray tomography was used to image the nickel hexacyanoferrate film inside the electrode. Cyclic voltammetry was used to measure the ion exchange capacity and stability. Electrospray ionization-mass spectroscopy (ESI-MS) was used to quantify the Cs^+ loaded and unloaded onto the film to determine its capacity, and the use of graphite as the ESIX film substrate was found to enhance both the capacity and stability of the ion exchange film.

5.1 Introduction

In radioactive waste, the most prevalent radionuclides are monovalent ions. The cesium ion (Cs^+) is of particular concern because it is considered particularly hazardous because of its very high radioactivity and its 30 year half-life (Rayford et al., 1994; Arthur et al., 1973). The separation of Cs^+ from the radioactive fission products is of great importance, as its removal from radioactive liquid waste reduces the radioactivity of the waste and makes the subsequent treatment processes safer. Recovered radioactive cesium can then be repurposed as a radioactive source for gamma irradiation in nuclear research facilities or used in the oil industry for examining the structural integrity of oil pipes (Herbst et al., 2007; Bhaskar et al., 1990; Mohapatra et al., 2009; Mohapatra et al., 2010).

Unfortunately, most of the conventional separation methods, such as precipitation, ion exchange, reverse osmosis, electrodialysis, and adsorption are inefficient for Cs^+. In the case of precipitation, as hydroxide, a low yield is obtained for the separation of Cs^+ from the radioactive fission products waste, as Cs^+ precipitates as a hydroxide and is very soluble in water (Tanihara et al., 1995; Rosa et al., 2001; Mohapatra et al., 2006).

Ion exchange using resins is a common method used in wastewater treatment for the removal of inorganic waste (Rangaraj et al., 2001). Unfortunately, this is not practical for Cs^+ separation due to the need to regenerate the ion exchange resin material after approximately 30 cycles in order to maintain useful levels of Cs^+ removal from the solution. After these 30 cycles, the resin requires regeneration, which consumes a huge amount of costly acid and base materials (Riddle et al., 2007). Even after multiple regeneration cycles, the resins can become unusable or radioactive themselves. The resin would then require proper disposal and treatment as it would then be secondary radioactive waste.

Reverse osmosis is one of the most effective methods for the removal of dissolved matter from waste water, but its main drawback is the high fouling rate of the used membrane during operation. Frequent cleaning results in downtime for the operation, shortens of the membrane life, and increases operating costs (Bartely at al., 2005).

The work of Chao et al. (2008) shows that electrodialysis (ED) can be used for separation of aqueous ions through ion exchange membranes using an electric field as the driving force for ion transport. Electrodialysis reversal (EDR) is a process whose main feature is the reduction of water conductivity, which can help to control the desalination rate as well as the membrane surface fouling. This process increases the initial and operating costs of the EDR system, but it also improvesefficiency.

Adsorption processes are currently of great interest due to their higher potential for the removal of radioactive cesium (Opeyemi et al., 2014; Hussain et al., 2013). A suitable sorbent must have a polar nature and high surface area. These two traits allow for an attractive force between the sorbent surface and the polar substance, in this case Cs^+ (Green et al., 1999; Chanra et al., 1976). One of the promising materials as a sorbent is graphite. It is commercially available, possesses a good mechanical rigidity, is low cost, has a high surface area, and typically has a specific surface area of 45 m^2 g^{-1}. (Shornikova et al., 2009; Luo et al., 2013; Yavuz et al., 2013).

The use of electrically switched ion exchange (ESIX) requires a material with high selectivity for Cs^+, like metal hexacyanoferrates (MHCFs), for example, in order to separate the Cs^+ from a solution containing a mixture of various metal ions (Suna et al., 2012). During the operation of the ESIX process, ion adsorption and desorption can be controlled by modulating the potential on the ESIX film (Lilga et al., 1997).

One method to improve upon typical sorbents is to introduce a film within the sorbent which allows for selectivity under certain circumstances and can also allow for electrical control of the uptake or the release of the adsorbed aqueous ions. MHCFs have previously been grown and used for the selective exchange of alkali cations in solution upon a conductive substrate (Lilga et al., 1997; Rassat et al., 1999). This work forms the basis for electrically switched ion exchange (ESIX), where the adsorption and desorption can be controlled by controlling the redox states of ions interacting with a suitable film through the application of an electrical potential (Lilga et al., 1997). In order for the ESIX to happen, there must be a charge transfer between the film interface and the solution. This transfer is accomplished through the reduction of the ferricyanide film, which in turn requires the uptake of Cs^+ to maintain charge neutrality. Oxidation of the ferricyanide film then requires a release of the same ion for the same reason. This is demonstrated in equation 5.1 (oxidation of the film) and equation 5.2(the reduction of the film).

$$CsKNiFe^{II}(CN)_6 \longrightarrow KNiFe^{III}(CN)_6 + Cs^+ + e^- \qquad (5.1)$$

$$KNiFe^{III}(CN)_6 + Cs^+ + e^- \longrightarrow CsKNiFe^{II}(CN)_6 \qquad (5.2)$$

As a conductive substrate is required for the ESIX to occur, these films are typically deposited on a metal electrode. This process necessitates that the film is a thin layer upon the surface of the electrode. Therefore, by using a conductive, porous electrode, which allows for the permeation of the ESIX film and the contaminated solution throughout the electrode, a much higher capacity ESIX electrode can be developed.

This work represents the development of a graphite electrode as a substrate for the nickel hexacyanoferrate film to be used for the removal of Cs^+ from aqueous solution; this research shows the adsorbed ESIX inside graphite electrode and its performance in the removal of Cs^+ from a contaminated solution.

5.2 Experimental methods

5.2.1 Electrochemical Apparatus

The ESIX system required the use of a standard three-electrode system: a working electrode, a counter electrode, and a reference electrode. The working electrode consisted of the film which was deposited on graphite substrate for ESIX. The counter electrode was a platinum electrode with a surface area of 5 cm^2. The final electrode was the reference electrode which gave the reference level for all of the electrical potential measurements in each experiment, and it was a saturated calomel electrode. The reference and counter electrode were situated less than 2 cm from the working electrode in solution.

The potentiostat/galvanostat system which was employed was a Wave Driver 10 supplied by Pine Research Instrumentation. It was controlled by software also provided by Pine Research Instrumentation (Aftermath 2.0).

Potassium hexacyanoferrate, nickel nitrate, and cesium nitrate ($K_3Fe(CN)_6$, $Ni(NO_3)_2$, $CsNO_3$) were used in the film preparation and were all purchased as reagent-grade chemicals with greater than 99% purity and were used without further purification. Solution preparation and washing was performed using deionized water at a specific electrical resistivity of 18.2 $M\Omega\ cm^{-1}$.

5.2.2 Surface Preparation

The substrate for the working electrode consisted of graphite disks (99.99%). The graphite disk was held in a Teflon holder suspended in the test solution. The portion of the disk exposed to the test solution had a diameter of 0.5 cm and the total volume of the electrode was 0.078 cm^3.

5.2.3 Film Preparation

The graphite electrodes were prepared by first being soaked in a solution of either 0.5 or 0.75 M $K_3Fe(CN)_6$ for 24 hours. This ensured the complete permeation of ferric cyanide into the pores of the graphite electrode. The electrode was then removed from the $K_3Fe(CN)_6$ solution and was washed with deionized water before it was soaked in either a 0.5 or 0.75 M $Ni(NO_3)_2$ solution for another 24 hours to form the nickel hexacyanoferrate material inside the graphite electrode. This process is displayed in figure 5.1. Table (5.1) shows the preparation method of the ESIX inside graphite electrode.

Table 5.1: preparation method

Graphite electrode	1st step (24 hr)	2nd step (24 hr)
A	0.5 M $K_3Fe(CN)_6$	0.5 M $Ni(NO_3)_2$
B	0.75 M $K_3Fe(CN)_6$	0.75 M $Ni(NO_3)_2$

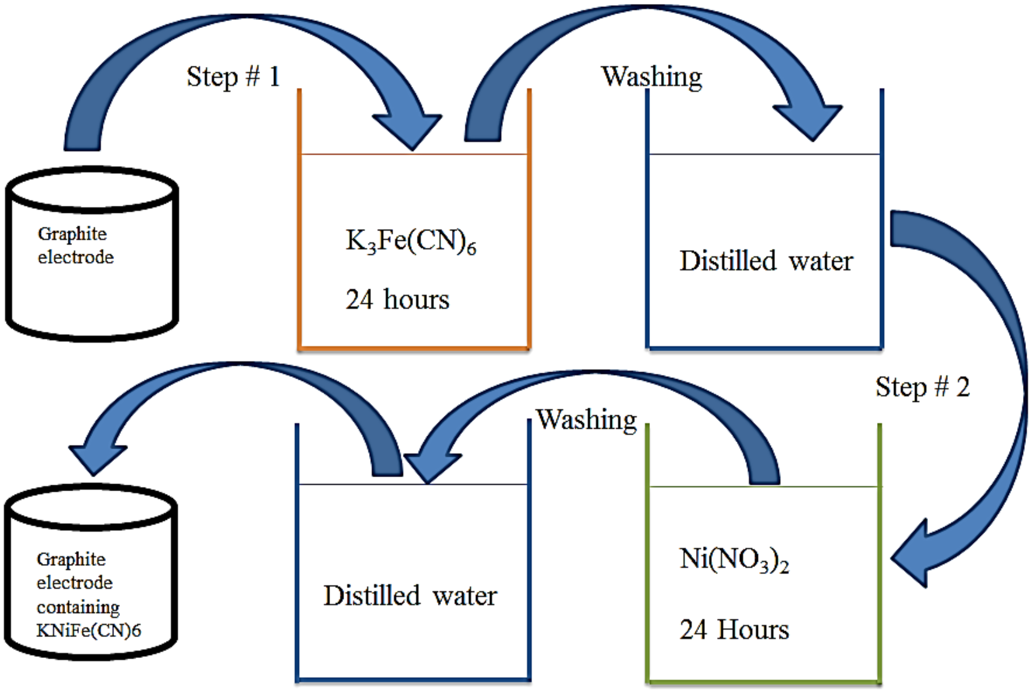

Figure 5.1: Film preparations via nickel hexacyanoferrate adsorption into a graphite electrode

5.2.4 Film characterization

The film was studied in multiple ways to measure its performance capabilities and also to probe the structure of the film itself. The films' capacity, cyclical performance, and morphology were studied using cyclic voltammetry and during these experiments N_2 gas was bubbled throughout the solution in order to reduce the dissolved oxygen. Quantification of Cs^+ was done through electrospray-ionization mass spectroscopy.

5.2.4.1 Film Morphology

X-ray tomography was used to visualize the deposited film inside the graphite electrode. The x-ray tomographer was operated at an electric potential of 100 kV with a current of 100 µA, yielding a power of 10 W. The incident radiation from the instrument was passed through a 0.5mm aluminum filter to reduce artifacts in the images. Software (ImageJ) was used to analyze the relative amount of deposited nickel hexacyanoferrate material inside each electrode.

5.2.4.2 Film Capacity

The film capacity was measured by loading the film in a single, monotonic sweep of the applied potential. A 125mL synthetic wastewater sample was prepared at a concentration of 2.25×10^{-3} M Cs^+. A linear reduction scan was applied to the prepared electrodes under investigation from 0.9 V to -0.2 V at a scan rate 50 mVs^{-1} to uptake the Cs^+. The concentrations were measured using electrospray ionization-mass spectroscopy (ESI-MS), where the concentration was determined by measuring it against a standard curve of prepared samples with known concentrations. All samples were diluted with HPLC-grade methanol in order to be within the detection range of the instruments.

5.2.4.3 Film Performance over Cyclic Loading and Unloading

The prepared film's ability for ESIX was characterized using cyclic voltammetry, which was conducted in a 1 M $CsNO_3$ solution. The cyclic voltammetry consisted of varying the electric potential anodically from 0.2 V to 0.9 V to load the film with Cs^+ and then to scan the voltage from 0.9 V to 0.2 V cathodically for release with scan rate 50 mV/s. The experiments were conducted without heating or stirring.

5.3 Result and Discussion

5.3.1 ESIX characterization (X-Ray tomography)

Visualization of the nickel hexacyanoferrate inside the graphite electrodes was done by x-ray tomography. Figure 5.2 shows the degree to which the hexacyanoferrate film is deposited within the electrodes. The images show that the material is adsorbed inside both of the graphite electrodes (A, B)

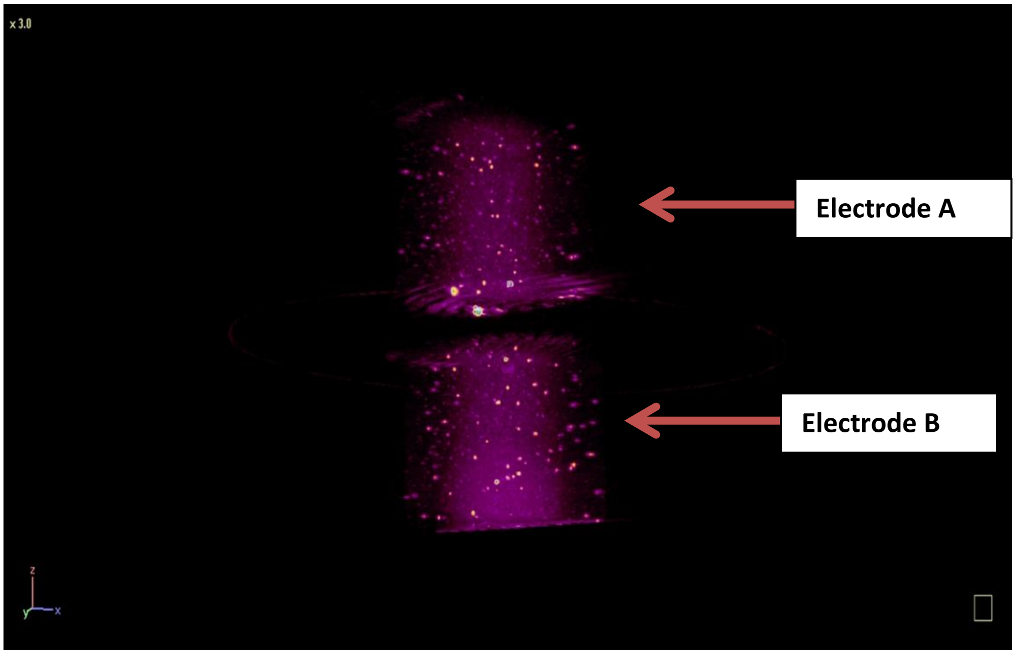

Figure 5.2: X-ray tomography for the two graphite electrodes containing adsorbed nickel hexacyanoferrate

The purple-coloured regions are the adsorbed nickel hexacyanoferrate material inside the graphite electrodes. An image analysis measuring the average intensity over the regions of the electrode confirms that there is a higher concentration of the nickel hexacyanoferrate in Electrode B than there is in Electrode A. The results of this analysis are shown in Table 5.2.

Table 5.2: Results obtained from Image Analysis

Electrode	**Concentrations during film preparation (M)**	**Mean Intensity (a.u)**
A	0.5 M	21.316
B	0.75 M	29.327

5.3.2 Film Capacity

5.3.2.1 Cs^+ adsorption

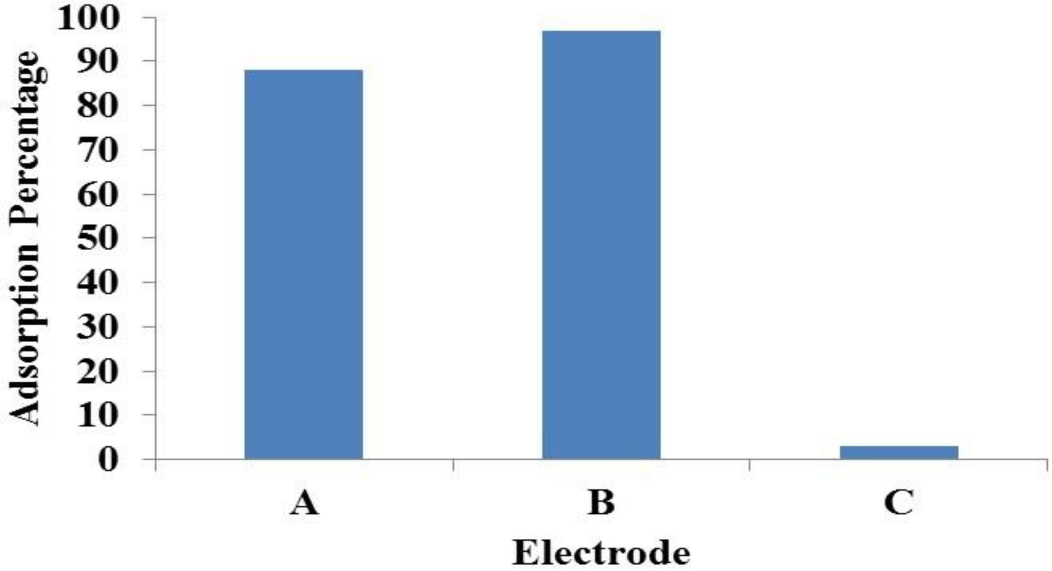

Figure 5.3: Cs^+ adsorption percentages by Electrode A, prepared using 0.5 M $NiFe(CN)_6$, Electrode B, using 0.75 M M $NiFe(CN)_6$, and Electrode C with no film.

Figure 5.3 represents the Cs^+ adsorption percentage from a solution of 2.25×10^{-3} M of Cs^+ by three graphite electrodes. Electrodes A and B are electrodes with adsorbed nickel hexacyanoferrate from initial solutions of concentrations of 0.5 and 0.75 M. Electrode C is a plain graphite electrode with no modification to serve as a control.

The results show that the best result for Cs^+ adsorption was with Electrode B, with a removal percentage 97%. This result is consistent with expectations as higher concentrations of $K_3Fe(CN)_6$ and $Ni(NO_3)_2$ were used in the creation of the film, which would indicate that the film would have more active sites available. However, the film capacity does not scale linearly with concentrations used in the preparation, as can be seen by the 88.7% removal of Cs^+ from Electrode A. There is less than a 8.3 % difference in the amount of Cs^+ removed between the two electrodes, even though Electrode B was created using 50% more of the reagents used to create the film on Electrode A.

The mean value for each electrode result is as follows

5.3.2.2 Cs^+ Desorption

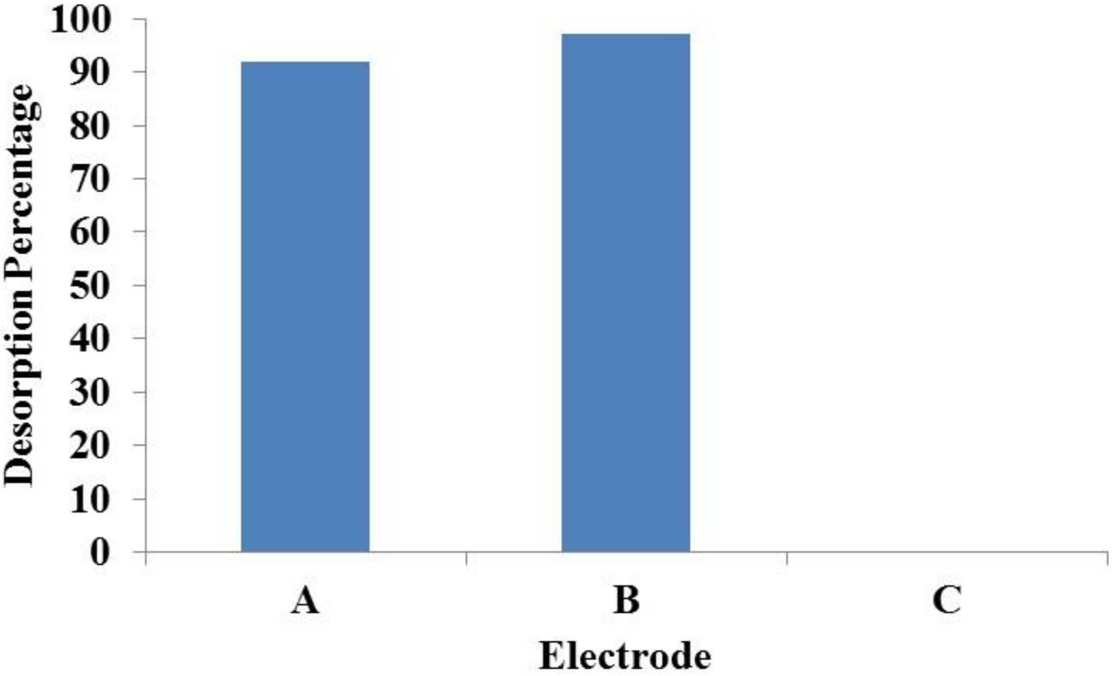

Figure 5.4: Cs^+ desorption percentage by Electrode A, prepared using 0.5 M $NiFe(CN)_6$, Electrode B, using 0.75 M M $NiFe(CN)_6$, and Electrode C with no film

Desorption was carried out in 7.5 x 10^{-3} M K^+ solution, which contained an excess of the number of K^+ ions compared to the number of Cs^+ ions loaded onto the film, to allow for as complete an ion exchange as possible. Figure 5.4 shows the amount of Cs^+ released from the tested ESIX electrodes as a percentage of the amount adsorbed from Section

5.3.2.1. Electrode A releases 92% of the adsorbed Cs^+, while Electrode B released 96%, and Electrode C showed no release. At the start of the cycle Electrode B was able to remove 2.18×10^{-3} M Cs^+ out of a total 2.25×10^{-3} M from the solution. When the cycle was reversed, only 2.09×10^{-3} M Cs^+ was released, leaving a residual 9×10^{-5} M Cs^+ contained within the electrode. This indicates that there is a loss of capacity after a loading and unloading cycle of the film.

5.3.3 Adsorbed material characterization (Cyclic Voltammogram)

Figure 5.5 shows the first cycles from the cyclic voltammetry for Electrodes A and B in a 1 M $CsNO_3$ solution. Electrode A shows a peak current of 2.6 mA at an applied potential of 450 mV, while Electrode B demonstrates a peak current of 4.5 mA, at an applied potential of 550 mV. The difference between the peak currents for the 2 electrodes is related to the concentration of nickel hexacyanoferrate within the film. As Electrode B has higher concentration of nickel hexacyanoferrate than does Electrode A, it is expected to have a higher capacity and thus have higher charge movement into and out of the film, resulting in a higher absolute value for the current.

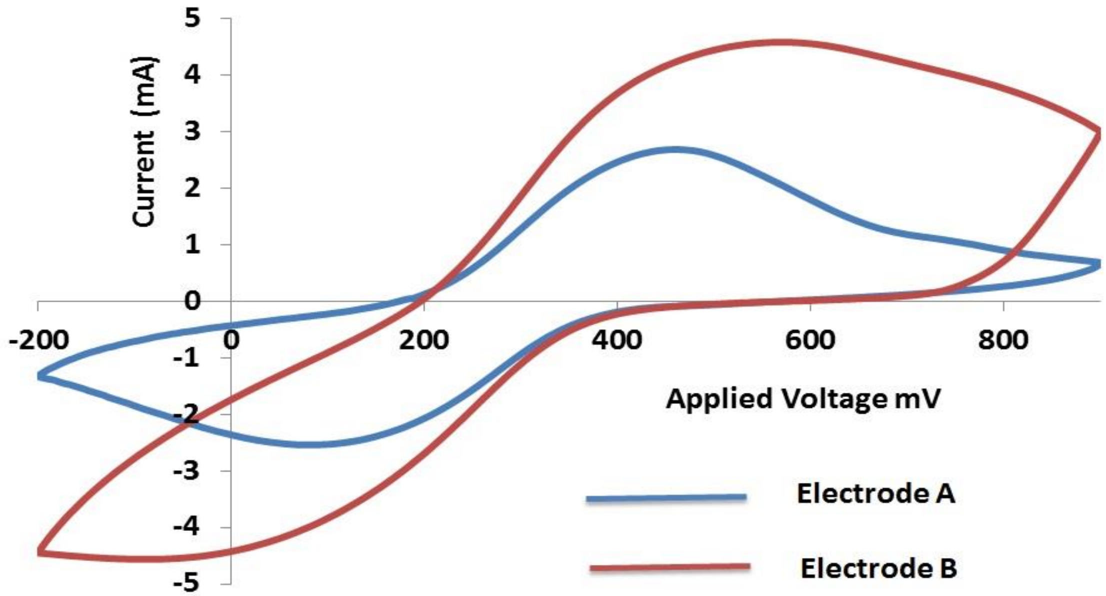

Figure 5.5: Cyclic voltammogram for the first cycle of Electrodes A and B in a 1M $CsNO_3$ solution.

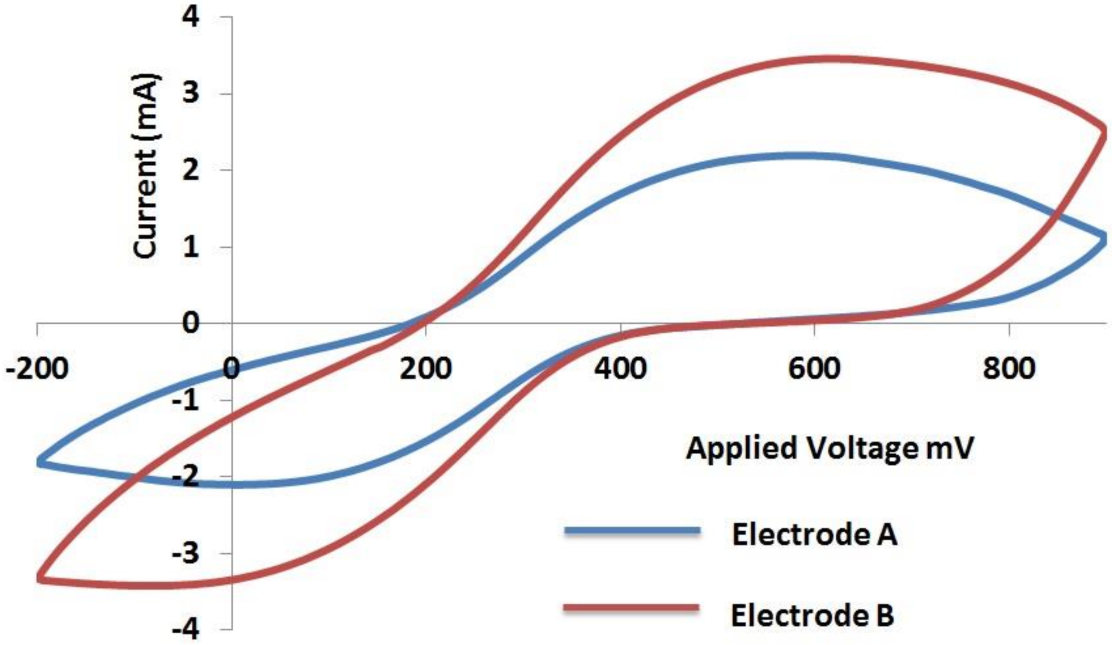

Figure 5.6: Ccyclic voltammogram of cycle number 1000 for electrodes A and B in 1 M $CsNO_3$

Figure 5.6 also shows cycle 1000 for Electrodes A and B in the same solution. In this figure, the peak currents for both electrodes were reduced from the initial cycle. This further confirms that the film capacity reduces over repeated cycling of adsorption and desorption for both electrodes. Even after 1000 cycles, however, Electrode A is still able to adsorb and desorb Cs^+, which is demonstrated by the peak current of 2 mA, but the performance of Electrode B continues to show a significantly higher capacity and performance after 1000 cycles than does Electrode A; its peak current was 3.5 mA, nearly double that of Electrode A.

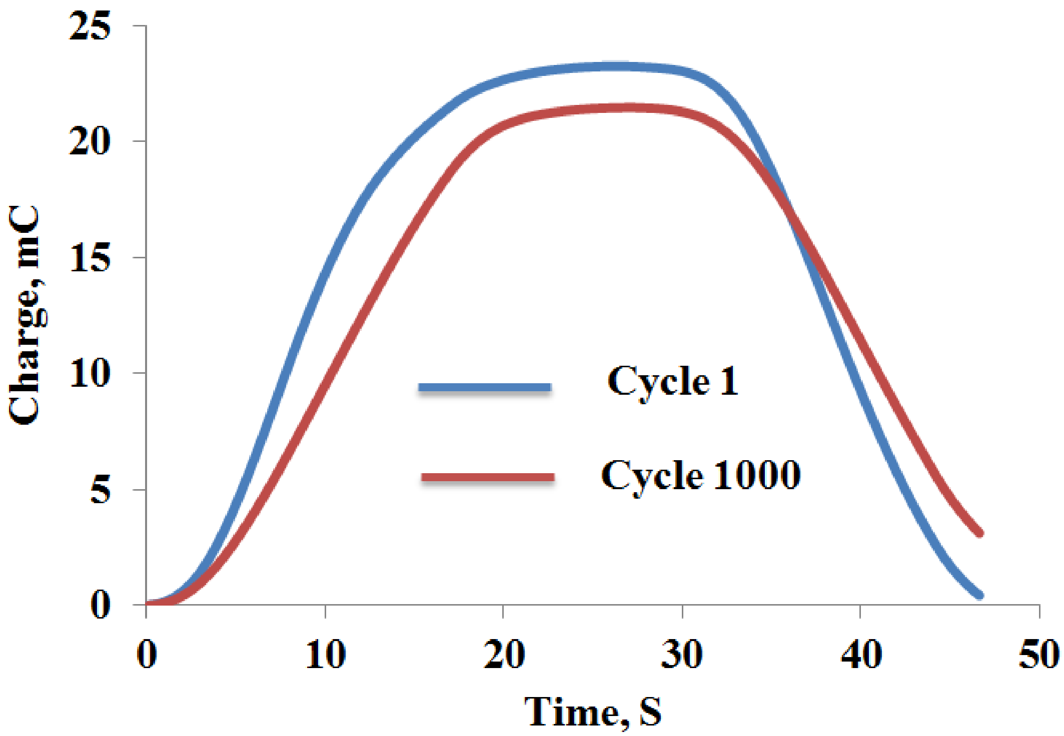

Figure 5.7: Integrating the current passed over cycles (1 and 1000) for electrode A

Figure 5.7 shows the integration of the current over the course of the cycles 1 and 1000 with respect to time. As the integrated current does not return to zero at the end of a cycle, it is determined that there was not the same number of charge carriers being exchanged in the release phase as there was in the loading phase of the ESIX.

The maximum charge capacity of the film was determined by dividing the maximum value of the charge, which is equal 24 mC, by the total volume of the electrode, 0.078 cm^3, totaling 307 mC cm^{-3}. The volume coverage can then be calculated by dividing the maximum charge capacity of the film by Faraday's Constant. The value of the volume coverage equals 3.05 x 10^{-6} mol cm^{-3}.

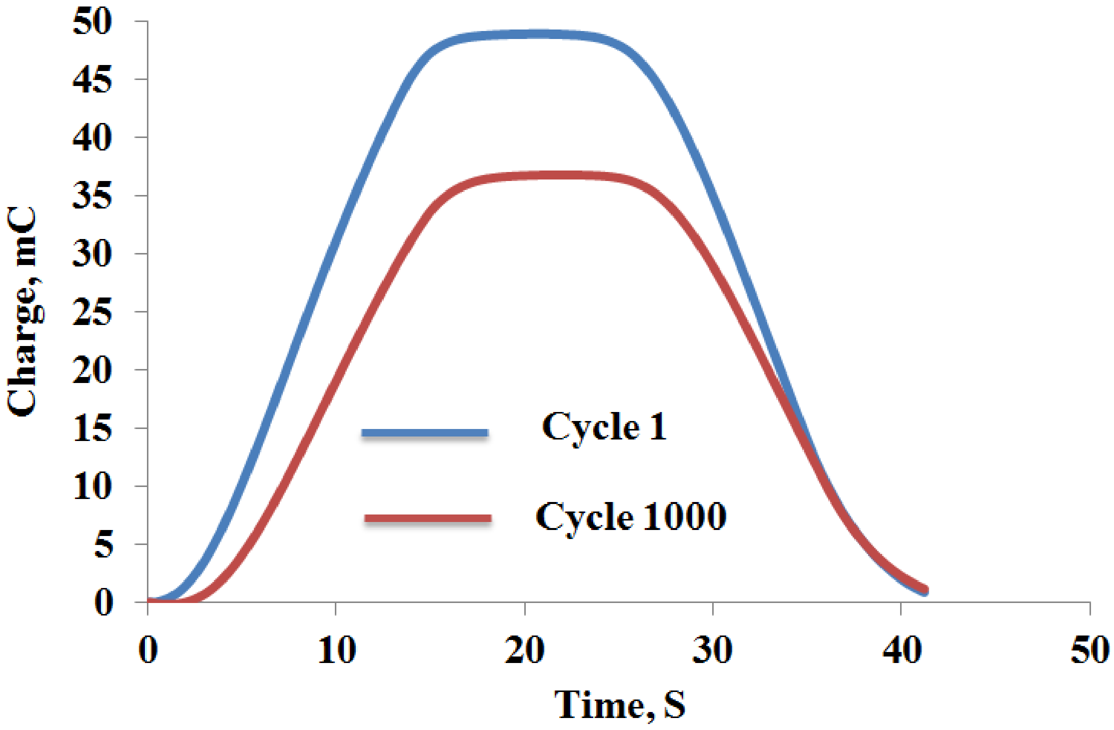

Figure 5.8: Integration of the current passed over cycles (1 and 1000) for electrode (B)

Figure 5.8 shows the maximum charge capacity of the film. Again, the total charge movement does not return to zero after a complete cycle, indicating a loss in the film capacity after each cycle. The maximum charge capacity of the film is equal to 628.2 mC cm^{-3}. The value of the surface coverage was determined to be 6.51 x 10^{-6} mol cm^{-3} after the initial cycle.

From figures 5.7 and 5.8, it is noted that the maximum charge capacity for electrode (B) is almost the double of electrode (A)

5.4 Summary and Discussion

Table 5.3: Characterization of Electrodes A and B

	Electrode A	**Electrode B**
Max. Charge Capacity after cycle 1 (C cm^{-3}) mean value	307 x 10^{-3}	628 x 10^{-3}
Standard deviation	1.6	4.3
Volume Coverage after cycle 1 (mol cm^{-3}) mean value	3.05 x 10^{-6}	6.51 x 10^{-6}
Standard deviation	0.02	0.08
Max. Charge Capacity after 1000 cycles (C cm^{-3}) mean value	269 x 10^{-3}	461 x 10^{-3}
Standard deviation	1.9	4
Volume Coverage after 1000 cycles (mol cm^{-3}) mean value	2.79 x 10^{-6}	4.77 x 10^{-6}
Standard deviation	0.04	1

Table 5.3 shows that Electrode B has a greater charge capacity than Electrode A: Electrode B started at 628.2 x 10^{-3} C cm^{-3} and underwent a loss of 167 x 10^{-3} C cm^{-3} to a capacity of 461 x 10^{-3} C cm^{-3} after 1000 cycles. Even after 1000 cycles Electrode B had a larger capacity than did Electrode A, which had an initial charge capacity of 307 x 10^{-3} C

cm^{-2}. It also suffered a loss in its capacity after repetitive cycling, but that loss was significantly smaller than the loss of Electrode A at only 38 x 10^{-3} mC cm^{-2}.

Reduction in capacity could occur for two possible reasons: (1) some of the film active sites were blocked during the operation, or (2) some parts of the film itself detached from the surface of the graphite, leading to loss of the film integrity and active sites.

It was determined that the second possibility was not likely, as the solutions were tested for the presence of the ferrous and ferric ions after the cyclic voltammetry by electrospray ionization-mass spectroscopy. The results showed the absence of either of these ions, indicating that there was no detectable amount of the nickel hexacyanoferrate material in the solution. It is believed, therefore, that the decrease in capacity is caused by the permanent blockage of some of the active sites on the films.

Though there was the decrease in capacity, this experiment still shows that both electrodes can still perform ESIX after 1000 cycles with adequately enough to remove Cs^+.

5.5 Conclusion

Two graphite electrodes were created for ESIX by adsorbing two different concentrations, 0.5 M and 0.75 M, of $KNiFe(CN)_6$ throughout their interior and were characterized for their ability to be used as ESIX electrodes for the removal of the Cs^+ ion from an aqueous solution. They were characterized by visualizing the ion exchange film morphology through x-ray tomography, and the film capacity as well as cyclic loading and unloading were measured through cyclic voltammetry. The results show that there is significant difference in their performance with regard to cesium ion removal. Electrode B, the electrode with 0.75 M $KNiFe(CN)_6$ deposited, shows a significantly higher capacity for ESIX, as it is able to remove 97% of cesium ions from a contaminated solution containing 2.25 x 10^{-3} mol of Cs^+. Its capacity was also only reduced from 628.2 x 10^{-3} C. cm^{-3} to 461 x 10^{-3} C. cm^{-3} after 1000 cycles, while Electrode A was able to remove 88.7% of Cs^+ with its capacity changing from 307x 10^{-3} C. cm^{-2} to 269 x 10^{-3} C. cm^{-3} after 1000 cycles. This demonstrates that graphite can be used as a suitable electrode for the electronically switched ion exchange of cesium ions from an aqueous solution.

5.6 Acknowledgements

The authors would like to thank the Egyptian Ministry of Defense (EMD) and the Natural Science and Engineering Research Council of Canada (NSERC) (Discovery Grants Program) for supporting this work.

5.7 References

Arthur S., Kubo and David J. Rose. (1973) "Disposal of Nuclear Wastes" Volume 182, PP 4118.

Bartels C. R., Wilf, K., Andes and Iong, J. (2005) "Design considerations for wastewater treatment by reverse osmosis" *Water Science & Technology* Vol 51 PP 473–482.

Bhaskar N. D., and Khla, C. M. (1990) “Adsorption of cesium by polycrystalline graphite-sticking coefficient studies” *Carbon* Vol. 2 pp. 71-78.

Bin, Suna,. Hao, Xiao-Gang. (2012) “Separation of low concentration of cesium ion from wastewater by electrochemically switched ion exchange method: Experimental adsorption kinetics analysis” *Journal of Hazardous Materials* 233-234, PP 177-183.

Chandra D. (1976) “Diffusion of cerium through graphite” *Journal of Nuclear Materials* 62, PP 293-310.

Chao Yu-Mei., and Liang, T.M. (2008) “A feasibility study of industrial wastewater recovery using electrodialysis reversal” *Desalination* 221, PP 433–439.

Green-Pedersen, H., and Korshin, G. V. (1999). “Separation of Cesium from High Ionic Strength Solutions Using a Cobalt Hexacyanoferrate-Modified Graphite Electrode.” *Environmental Science & Technology*, 33, PP 2633–2637.

Herbst R. S. and Law, J. D. (2007) “Development and testing of a cobalt dicarbollide based solvent extraction process for the separation of cesium and strontium from acidic tank waste” *Separation Science and Technology*

Hussain S.N. and Roberts, J. D. (2013) “Oxidation of phenol and the adsorption of breakdown products using a graphite adsorbent with electrochemical regeneration” *Electrochimica* 92, PP 20– 30.

Lilga M.A., Orth, R.J., Sukamto, J.P.H., Haight, S.M., and Schwartz, D.T. (1997) “Metal ion separations using electrically switched ion exchange” *Separation and Purification Technology* 11, PP 147-158.

Lilga, M.A., Orth, R.J., Sukamto, J.P.H., and Rassat, S.D. (2001) “Cesium separation using electrically switched ion exchange” *Separation and Purification Technology* 24, PP 451–466.

Luo, Xiaofeng and Chao, Fang. (2013) “Adsorption behaviors of Cs and I atoms on the graphite surface by the first-principles” *Journal of Nuclear Materials* 441, PP 113–118.

Mohapatra, P.K., Ansari, S.A. and Sarkar, A., 2006 “Evaluation of calix-crown ionophores for selective separation of radio-cesium from acidic nuclear waste solution” *Analytica Chimica Acta* 571, PP 308–314.

Mohapatra, P. K., Lakshmi, D. S., Bhattacharyya, A., and Manchanda, V. K. (2009)“Evaluation of polymer inclusion membranes containing crown ethers for selective cesium separation from nuclear waste solution” *Journal of Hazardous Materials*, 169, PP 472– 490.

Mohapatra, P. K., Bhattacharyya, A., and Manchanda, V. K. (2010) “Selective separation of radio-cesium from acidic solutions using supported liquid membrane containing chlorinated cobalt dicarbollide (CCD) in phenyl trifluoromethyl sulphone (PTMS).” *Journal of Hazardous Materials*, 181, PP 679–85.

Opeyemi, Olanipekun, and Adebola, Oyefusi. (2014) “Adsorption of lead over graphite oxide” *Spectrochimica Acta Part A: Molecular and Biomolecular Spectroscopy* 118, PP 857–860.

Rassat, S.D., Sukamto, J.H., and Lilga, M.A. (1999) “Development of an electrically switched ion exchange process for selective ion separations” *Separation and ectroamai. Chem.*, 210, PP 323-328.

Rayford, G. and Anthony, Robert G. (1994) “Use of Silicotitanates for Removing Cesium and Strontium from Defense Waste” *Ind. Eng. Chem. Res*, 33, PP 2702-2705.

Rengaraj S., Kyeong-Ho Yeon, and Seung-Hyeon, Moon. (2001) “Removal of chromium from water and wastewater by ion exchange resins” *Journal of Hazardous Materials* B87, PP 273–287.

Riddle, C. L. and Baker, J. D. (2007) “Fission Product Extraction (FPEX): Development of a Novel Solvent for the Simultaneous Separation of Strontium and Cesium from Acidic Solutions” Taylor & Francis, PP 449-461

Rosa, J. J. La, W. Burnett, and S. H. Lee. (2001) “Separation of actinides, cesium and strontium from marine samples using extraction chromatography and sorbents” *Journal of Radio Analytical and Nuclear Chemistry*, Vol. 248, No. 3 , PP 765–770.

Shornikova O. N. and Kogan, E. V. (2009) “The Specific Surface Area and Porous Structure of Graphite Materials” *Russian Journal of Physical Chemistry A,* Vol. 83, No. 6, pp. 1022–1025.

Tanihara, K. 1995 “Composite ion exchangers of redox type for cesium separation. Sorption- Deposition-Regeneration cycle with cupric” *J. Radioanal. Nucl. Chem., Letters* 201, PP 509-519 .

Yavuz, Yardım, and Zühre, Şentürk. 2013 “Electrochemical evaluation and adsorptive stripping voltammetric determination of capsaicin or dihydrocapsaic in on a disposable pencil graphite electrode” *Talanta* 112, PP 11–19.

Chapter 6

Nickel hexacyanocobaltate as an electrically switched ion exchange

The contents of this chapter will be submitted to a journal in November 2014 as: Tawfic, A.F., Dickson, S.E., Kim, Y., and Mekky, W., 2014. Nickel hexacyanocobaltate as an electrically switched ion exchange.

Abstract

Certain types of industrial wastewater contain high concentrations of metal ions. Wastewater containing high levels of metals can be treated by conventional methods such as ion exchange, coagulation, and precipitation. In this study, electrically switched ion exchange is studied as a replacement for metal removal from an aqueous solution. This technique employs an electroactive ion exchange film created by electrochemical deposition onto a high surface area electrode. In this ion exchange process, target ions are sequentially loaded and unloaded by controlling electric potential applied to the film. In this research, graphite electrodes were used to prepare nickel hexacyanocobaltate films for electrically switched ion exchange (ESIX) with improved capacities for Cs^+ separation. Cyclic voltammetry was used to measure the ion exchange capacity and stability of the prepared film. The graphite electrodes loaded with the ESIX films were shown to have initial ion exchange capacities of 166.6 x 10^{-3} C cm^{-3} and 133.1 x 10^{-3} C cm^{-3}, depending on the concentrations of the film deposition solutions (0.5 M and 0.75 M of $K_3Co(CN)_6$ and $Ni(NO_3)_2$). Both electrodes showed repetitive capabilities of Cs^+

separation over 1000 cycles with reducing film capacity after each successive cycle of uptake and release.

6.1 Introduction

One of the main concerns for Cs^+ separation from radioactive waste is that it is chemically similar to Na^+. Thus, in the case of environmental release, radioactive Cs^+ easily becomes waterborne and is capable of being widely transported. Upon ingestion, it spreads quickly through the body, causing widespread damage to internal cells and leading to many health hazards and, potentially, to death (Shakir et al., 2007).

The conventional methods for metal ion removal from industrial wastewater generally involve chemical precipitation processes, adsorption, or ion exchange processes (Mayumi et al., 2014; Wi-Ho et al., 2013). Chemical precipitation as with hydroxide has a small yield, as CsOH is very soluble in water, so it requires a lot of chemicals and time to separate Cs^+. Adsorption processes are of great importance due to their high efficiency for the removal of Cs^+ (Opeyemi et al., 2014; Hussain, 2013). Adsorption methods in the separation of Cs^{137} from radioactive liquid waste can make treatment of the waste easier and helps to reduce the radioactivity of the waste. Furthermore, adsorption allows for the recovery of the radioactive Cs^+ which can then be used as a source for gamma irradiation (Bhaskar et al., 1990; Mohapatra et al., 2009; Mohapatra et al., 2010).

High surface area and the polar nature are of important properties of the sorbents, as these characteristics are responsible for the sorbents' ability to form attraction between their surface and the polar substance. This is method is not effective, however, because the desorption process requires a lot of energy, as it is done using heat, and the sorbent itself becomes radioactive after the adsorption of Cs^{137} (Green et al., 1999; Chandra et al., 1976).

In ion exchange, a reversible interchange of ions between the solid ion exchange resin and the contaminated liquid occurs without any significant change in the structure of the resin. Once the resins become fully loaded with metal ions, the resins must be regenerated. This regeneration process can be quite expensive and consumes large quantities of chemicals. Furthermore, the ion exchange processes are typically not selective, and preferential adsorption for benign compounds can occur, thereby reducing the efficiency of the removal of the metal ions of concern (Gulin et al., 2013; Ping et al., 1999; Raffaele et al., 2004; Mainea et al., 2006). Newer methods have been introduced for metal ion separation, such as the use of chelating polymers, chelating sorbents, membranes, and carbon nanostructures, but to date these methods are unable to be regenerated easily, use large amounts of chemicals and heat energy to be recovered, and their capacity to be reused or durability is limited (Browni et al., 2000; Raja et al., 2013; Nagendran et al., 2008; Adeleye et al., 2012; Joet al., 2010; Krystyna et al., 2010).

Electrically switched ion exchange (ESIX) can be seen as an alternative to the previously mentioned methods. In electrically switched ion exchange applications, ion adsorption and desorption can be controlled by regulating the redox states of the ion exchange, only requires low energy to be functional (< 2 V), and is electrically regenerated, so it does not require any additional chemicals, meaning that the secondary waste will be minimal (Suna et al., 2012; Lilga et al., 2001). Conducting ESIX using a material with high selectivity for Cs^+ allows for a greater recovery of the Cs^+ from a solution contains a mixture of various metal ions (Rassat et al., 1999). Because nickel hexacyanocobaltate has a similar chemical structure to nickel hexacyanoferrate, applying the suitable potential to the prepared film Co^{+3} will be reduced the Co^{+2} and, thus, will create a negative charge on the surface of the film, causing the Cs^+ to attach to the film surface.

In this research, graphite electrodes were used to prepare nickel hexacyanocobaltate films by adsorption. The prepared nickel hexacyanocobaltate electrodes were used to remove Cs^+ from contaminated solution.

6.2 Experimental methods

6.2.1 General and electrochemical

A WaveDriver 10 Potentiostat / Galvanostat System (Pine Research Instrumentation) was used to characterize prepared ESIX films. A standard three-electrode system was used in the characterization of electro-active adsorbed material. A saturated calomel electrode (SCE) was employed, and all potential values in this study are measured with respect to the SCE. A platinum counter electrode with a surface area 5 cm^2 was employed in all experiments. The reference and the counter electrode were located less than 2 cm from the working electrode, and the working electrode was the prepared electrode to be studied. It was composed of the hexacyanocobaltate film deposited on the graphite substrate.

Reagent-grade chemicals ($K_3Co(CN)_6$, $Ni(NO_3)_2$, KNO_3 and $CsNO_3$) with > 99% purity were used as purchased without further purification. Deionized water (18.2 MΩ cm^{-1}) was used in all salt solution preparations and for final rinsing of electrochemical cell components.

6.2.2 Surface Preparation

Graphite disks (99.99%) were used as the working electrode, the graphite disk was embedded in a Teflon holder suspended in the test solution. The portion of the disk exposed to test solution had a diameter of 0.5 cm and a volume of 0.078 cm^3.

6.2.3 Film Preparation

Two ESIX films were prepared onto graphite electrodes using chemical concentrations as described in Table 6.1.

Table 6.1: Preparation concentrations of reagents for film adsorption

Graphite electrode	**1st soaking**	**2nd soaking**
A	0.5 M $K_3Co(CN)_6$	0.5 M $Ni(NO_3)_2$
B	0.75 M $K_3Co(CN)_6$	0.75 M $Ni(NO_3)_2$

A graphite electrode was immersed in either 0.5 or 0.75 M $K_3Co(CN)_6$ for 24 hours to ensure complete adsorption of the material throughout the graphite electrode. The saturated electrodes were then removed from the $K_3Co(CN)_6$ solution and washed with deionized water before the second immersion in either 0.5 or 0.75 M $Ni(NO_3)_2$ for another 24 hours to form the nickel hexacyanocobaltate films as a coating for the graphite electrodes. This process is illustrated in figure 6.1.

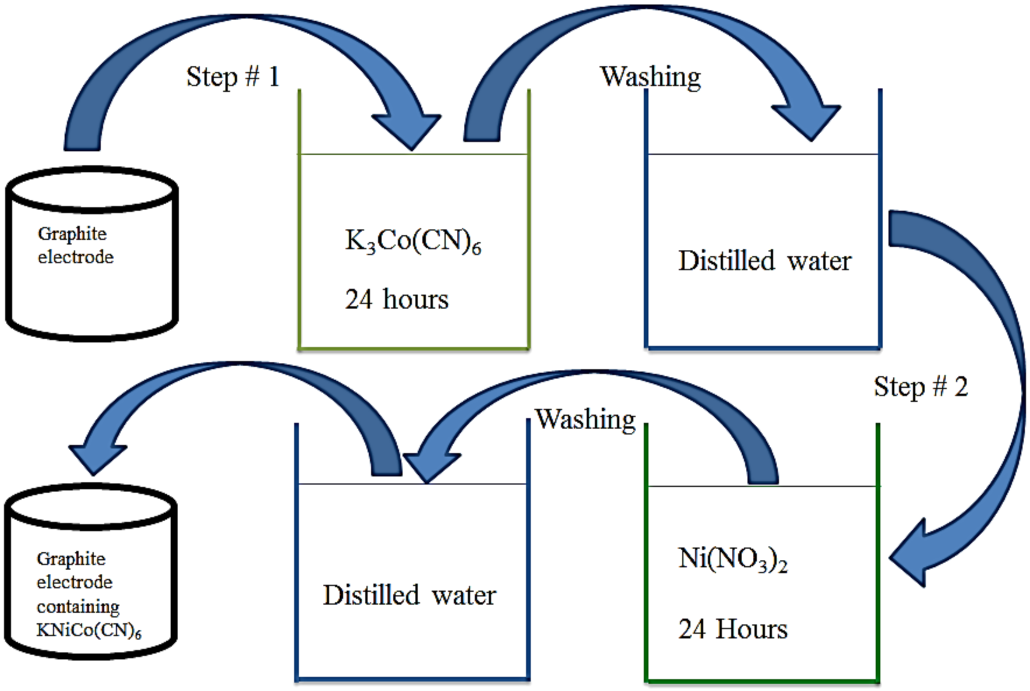

Figure 6.1: Preparation of the nickel hexacyanocobaltate films for the graphite electrodes.

6.2.4 Film Characterization

6.2.4.1 Film Characterization (Cyclic Voltammetry)

The reduction of the cyanocobaltate (III) film requires the uptake of Cs^+ while the oxidation requires a release of the same ion to maintain the electroneutrality of the film. The oxidation of cyanocobaltate (II) film to the cyanocobaltate (III) is demonstrated in equation 6.1, and the reduction of the cyanocobaltate (III) to the cyanocobaltate (II) form is demonstrated in equation 6.2.

$$CsKNiCo^{II}(CN)_6 \longrightarrow KNiCo^{III}(CN)_6 + Cs^+ + e^- \qquad (6.1)$$

$$KNiCo^{III}(CN)_6 + Cs^+ + e^- \longrightarrow CsKNiCo^{II}(CN)_6 \qquad (6.2)$$

The film was characterized using cyclic voltammetry, which was conducted in a 1 M $CsNO_3$ solution. The applied potential started at 0.2 V and was scanned anodically to 1.6 V, then cathodically to -0.3 V, then back to 0.2 V at a scan rate 50 mVs^{-1}. During this process N_2 gas was bubbled throughout the solution in order to reduce the dissolved oxygen and to eliminate any formed oxygen due to water electrolysis as the applied voltage went over 1.23 V vs SCE.

The capacity of the films was measured by removing Cs^+ from a solution with an initial concentration of 2.25×10^{-3} M Cs^+ and measuring the remaining Cs^+ in the solution. A reduction potential was applied to the prepared electrode at -0.2 V for 3 minutes for the removal of the Cs^+ ions, while for desorption, an applied voltage of 1.1 V was applied for 3 minutes in a solution containing 7.5×10^{-3} M K^+. The concentrations were detected using electrospray ionization-mass spectroscopy (ESI-MS). The samples and standard solutions were diluted by a factor of 3 with methanol HPLC-grade to be in the measurement range of the ESI-MS.

6.3 Results and Discussion

6.3.1 Film Characterization (Cyclic Voltammogram)

Figure 6.2 shows the cyclic voltammogram for the first cycles of Cs^+ loading and release for Electrodes A and B in a 1 M $CsNO_3$ solution. The figure shows that the reduction of

Co^{+3} to Co^{+2} occurs at 1.05 V, where the film is adsorbing Cs^{+} from solution. At 0.2 V the Co^{+2} is oxidized to Co^{+3}, where the Cs^{+} is desorbed in solution again. The peak current for Electrode B is higher than that of Electrode A. This is due to the higher concentration of active sites available from the higher concentrations used in the deposition process in Electrode B as compared to Electrode A. Electrode A has a peak height of 3 mA, while the peak's height for Electrode B is at 4 mA, a higher voltage than is typically used as the end point for anodic current. This voltage is applied due to the fact that the standard electrode potential for the reduction of Co^{+3} to Co^{+2} occurs at 1.8 V relative to standard hydrogen electrode (SHE), which is equivalent to 1.55 V vs SCE., so the range of cyclic voltammetry was applied until it reached 1.6 V to ensure that there is no interaction other than the ESIX film with Cs^{+}.

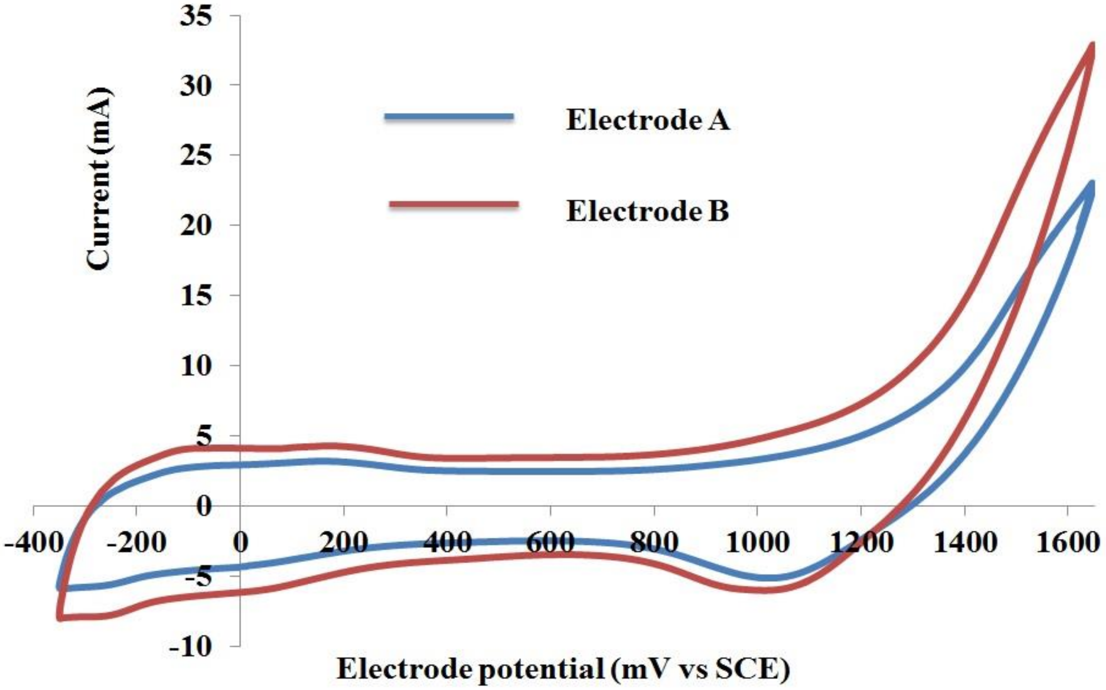

Figure 6.2: Cyclic voltammogram for the first cycle for Electrodes A and B in 1 M $CsNO_3$

Figure 6.3 is a similar voltammogram result for Cycle 1000 of both electrodes in the same 1 M $CsNO_3$ solution. The figure shows a slight decrease in the peak's height for Electrode A, at 2.7 mA, a reduction of 0.3 mA from the initial cycle. The peak current for Electrode B seems to have also been reduced slightly at 3.8 mA, a reduction of 0.2 mA from the initial cycle.

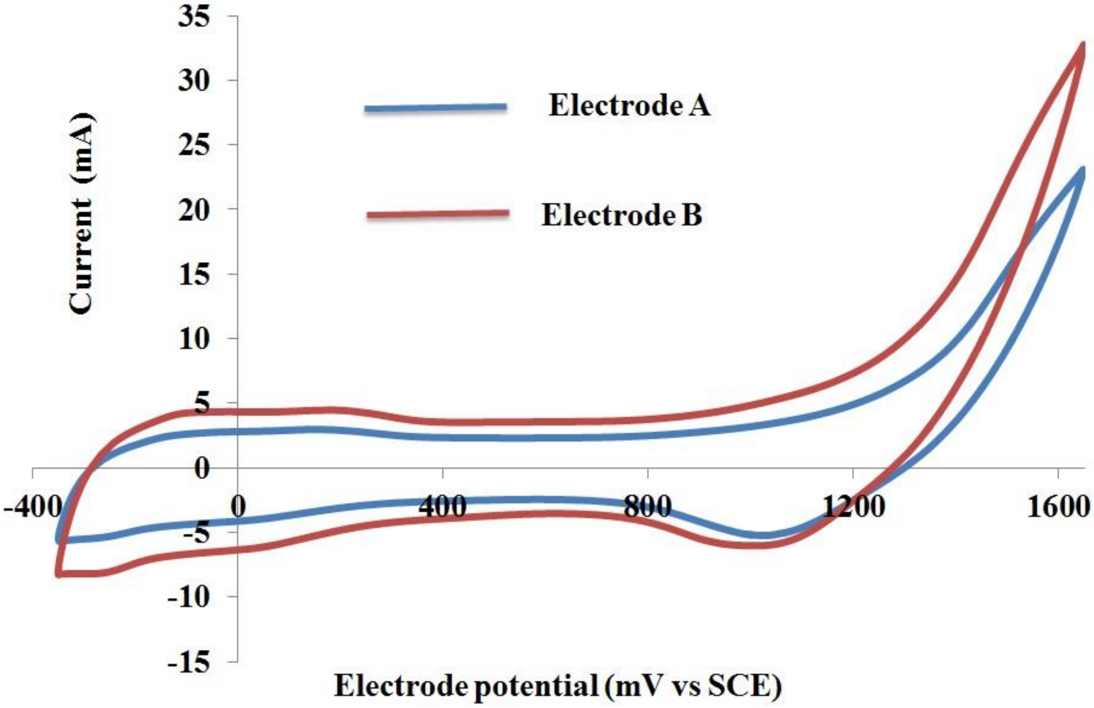

Figure 6.3: Cyclic voltammogram for the cycle 1000 for electrodes (A,B) in 1 M $CsNO_3$

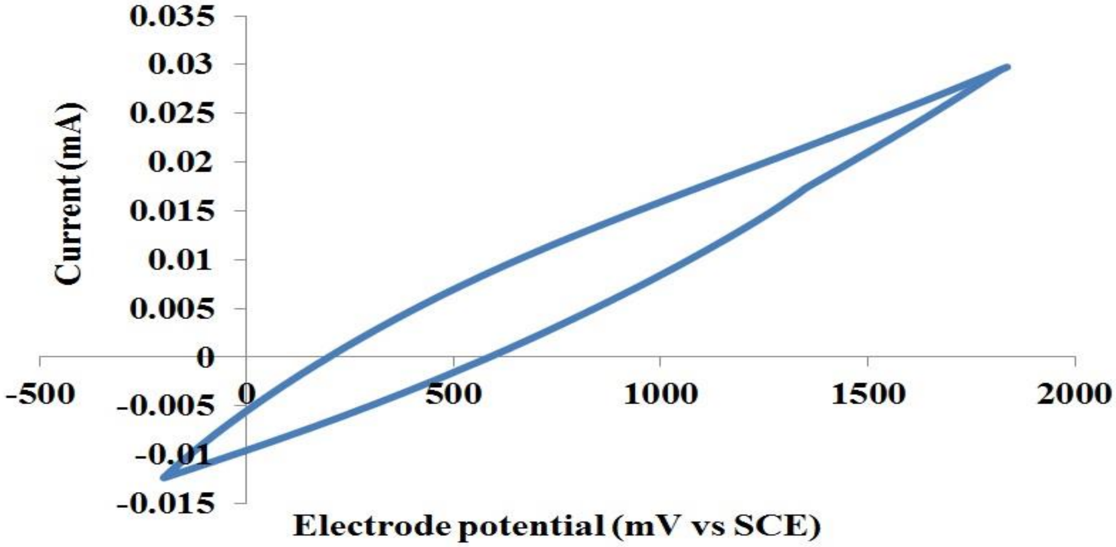

Figure 6.4: Cyclic voltammogram for a graphite electrode in H_2O

Figure 6.4 represents a control experiment to ensure that the peaks observed in figures 6.2 and 6.3 are results of the interaction of nickel hexacyanocobaltate with Cs^+. This figure represents the interaction of a graphite electrode with water after applying a cyclic voltammetry scan starting from -0.2 V to 2 V with scan rate 50 mVs^{-1}. The figure shows no peak for the reduction of oxygen in the water, which shows that the reduction peaks shown in figures 6.2 and 6.3 are caused by the reduction of Co^{+3} to Co^{+2} and, thus, the Cs^+ adsorption.

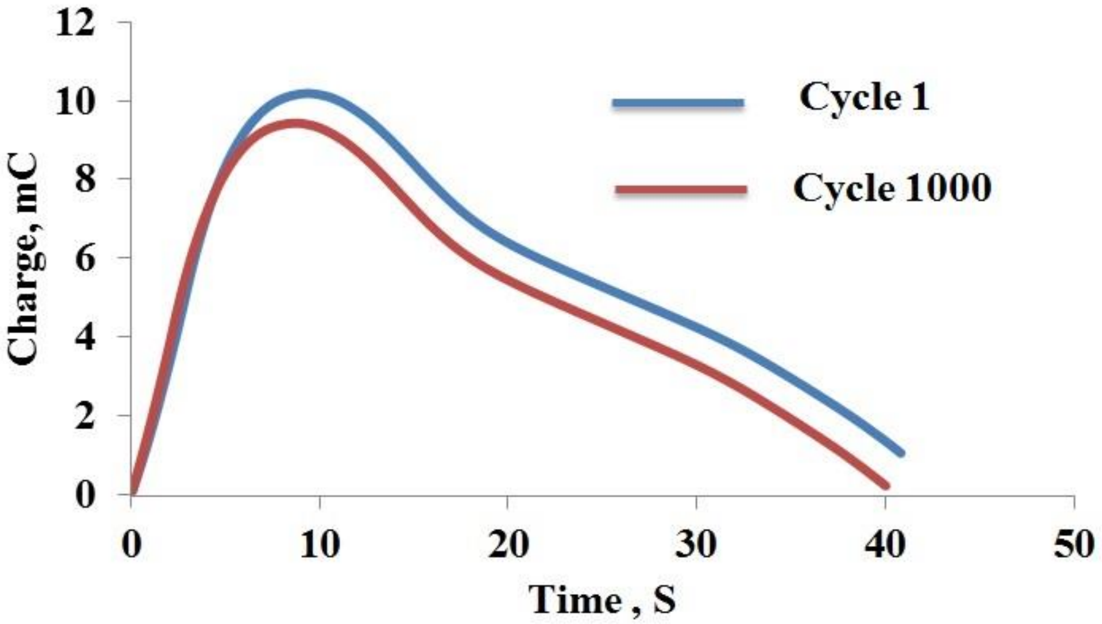

Figure 6.5: The integration of the cycles (1 and 1000) for Electrode A

The maximum charge capacity of Electrode A is shown in figure 6.5 was determined by integrating the current into a single voltammetric sweep. The maximum charge capacity was determined by integrating the sweep (1 and 1000), which gave the results of film equal to 133.1 x 10^{-3} C cm^{-3}. The volume coverage was also determined by 1.38 x 10^{-6} mol cm^{-3}. This value tells us about the number of active sites all over the electrode. Figure 6.5 also shows that the total charge movement does not return to zero after a complete cycle, indicating a loss in the capacity of the film after a cycle, and the total charge deposition on the electrode decreases. This decrease suggests a loss of charge capacity over a single cycle. The residual charge on the film was approximately 133.1 x 10^{-3} C cm^{-3} after the initial cycle and 115 x 10^{-3} C cm^{-3} after cycle 1000.

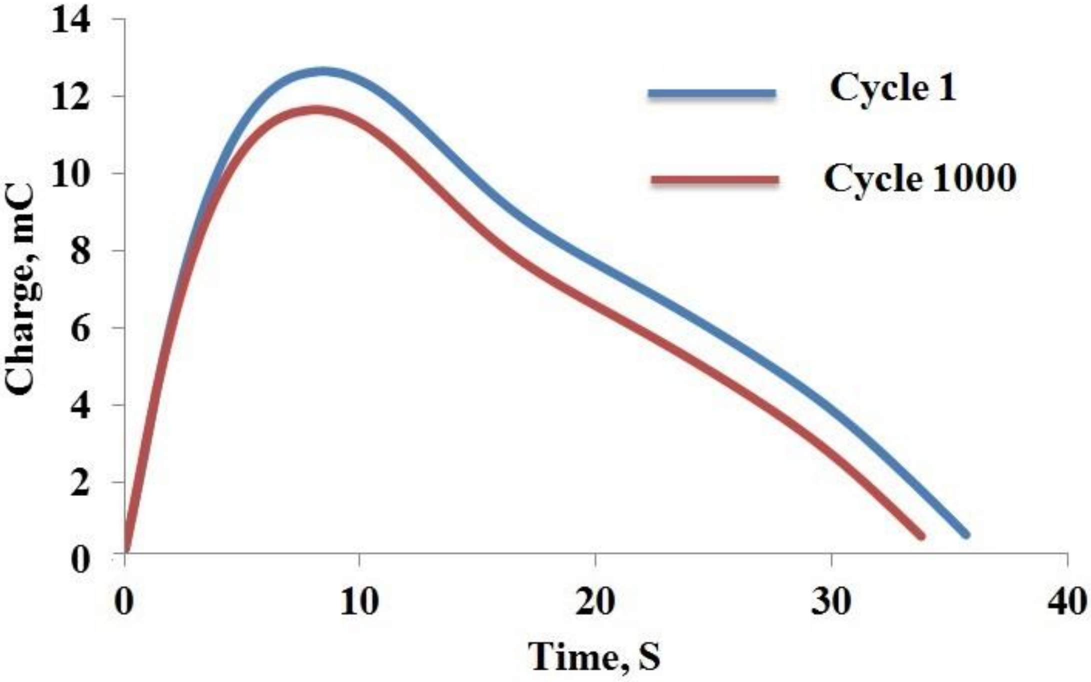

Figure 6.6: The integration of the cycles (1 and 1000) for Electrode B

The integrated current for cycles (1 and 1000) for Electrode B is shown in figure 6.6. The maximum charge capacity of this film was 166.6 x 10^{-3} $C.cm^{-3}$, 20% higher than that of Electrode A. The surface coverage was determined to be 1.72 x 10^{-6} mol cm^{-3}. The total charge movement again does not return to zero after a complete cycle, indicating a loss in the capacity of the film after each cycle. The maximum volumetric charge capacity after the first cycle was 166.6 x 10^{-3} $C.cm^{-3}$, which then drops to 150 x 10^{-3} mC cm^{-3} after the 1000th cycle.

6.3.2 Quantification of Electrode Capacities by ESI-MS

6.3.2.1 Cs^+ Adsorption

Figure 6.7 represents Cs^+ adsorption results from a test solution with an initial concentration of 2.25 x 10^{-3} M Cs^+ using graphite electrodes A and B. The results from the ESI-MS confirm the results from the cyclic voltammogram, namely that Electrode B adsorbs Cs^+ better than Electrode A. Electrode B was able to remove 91% of the initial Cs^+ from the solution, though that was only slightly higher than that of Electrode A at 85% removal. It should be noted that to gain the 6% extra in removal, however, Electrode B required a 50% extra amount of chemicals for electrode preparation than did Electrode A. The control electrode was able to adsorb only a small amount of the Cs^+: 2%. Only 4.5×10^{-5} M out of 2.25×10^{-3} M, this is a very small amount, and it may be due to adsorption of Cs^+ on the outer surface of the electrode, as during the desorption there were zero mol desorbed from that electrode.

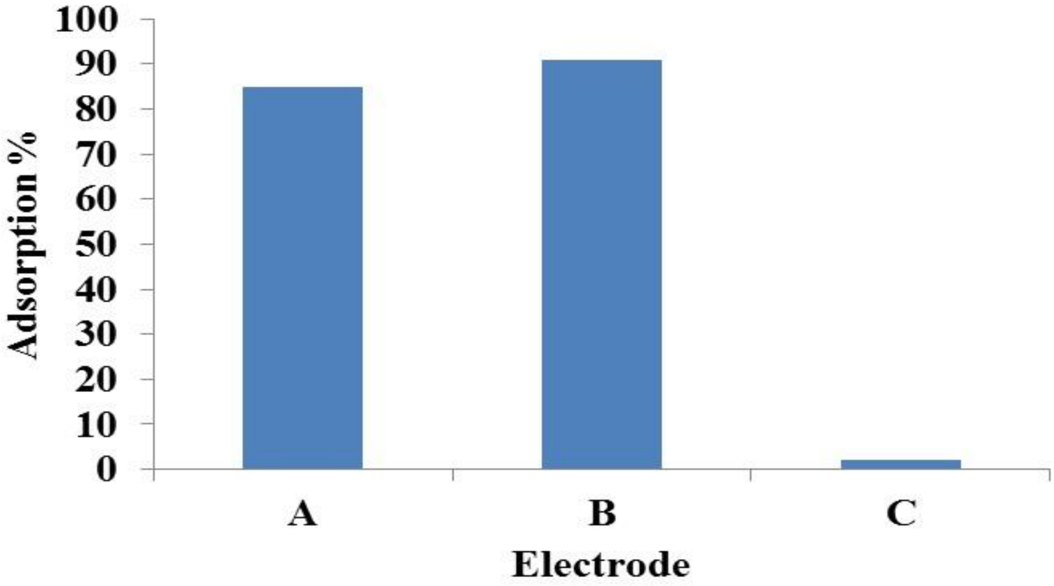

Figure 6.7: Cs^+ adsorption by a control electrode C and Electrodes (A, B) from 2.25×10^{-3} M Cs^+ solution

6.3.2.2 Cs^+ desorption

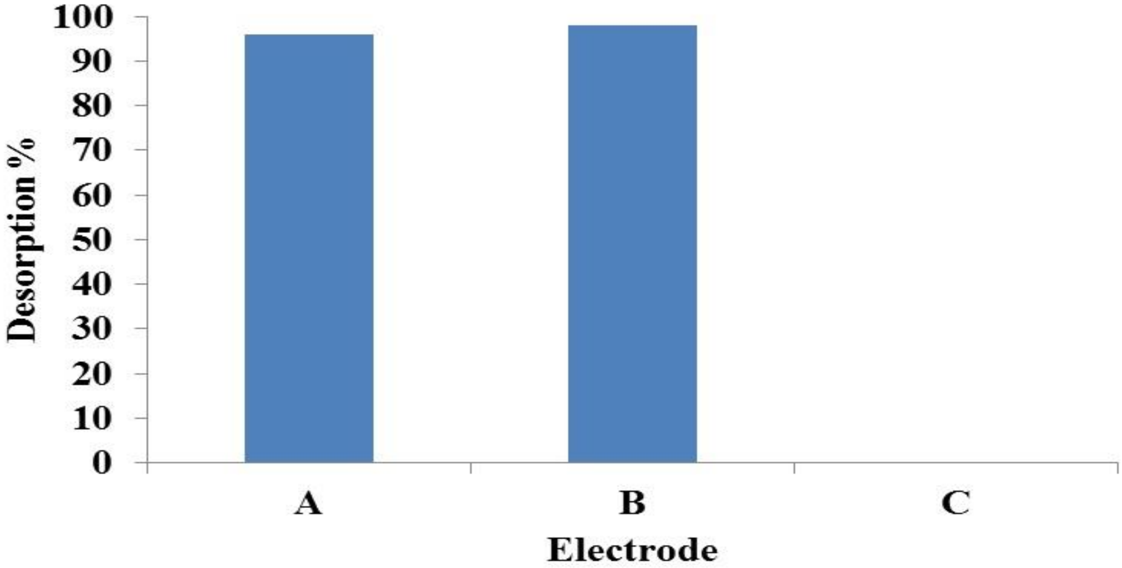

Figure 6.8: Cs^+ desorption by graphite electrodes (A, B, and C)

Figure 6.8 represents Cs^+ desorption as percentage of the amount adsorbed in Section 6.3.2.1 for all of the tested electrodes. Electrode B was able to release 98% of the adsorbed Cs^+, 2.006×10^{-3} M out of 2.05×10^{-3} M, indicating that an amount, 4.4×10^{-5} M, of Cs^+ was trapped inside the electrode. Electrode A was able to release 96% of adsorbed Cs^+, 1.83×10^{-3} M out of 1.91×10^{-3} M.

6.4 Summary and Discussion

Table 6.2: Characterization of Electrodes A and B

	Electrode A	**Electrode B**
Max. Charge Capacity after cycle 1 (C cm^{-3}) mean value	133.1 x 10^{-3}	166.6 x 10^{-3}
Standard deviation	2.66	3
Volume Coverage after cycle 1 (mol cm^{-3}) mean value	1.38 x 10^{-6}	1.72 x 10 $^{-6}$
Standard deviation	0.01	0.06
Max. Charge Capacity after 1000 cycles (C cm^{-3}) mean value	115 x 10^{-3}	150 x 10^{-3}
Standard deviation	2.8	3.1
Volume Coverage after 1000 cycles (mol cm^{-3}) mean value	1.19 x 10 $^{-6}$	1.55 x 10 $^{-6}$
Standard deviation	0.02	0.05

Table 6.2 shows that Electrode B has a greater charge capacity 166.6 x 10^{-3} C cm^{-3} and underwent a loss of capacity from 16.6 x 10^{-3} C cm^{-3} to 150 x 10^{-3} C cm^{-3} after 1000 cycles. Even after 1000 cycles, though, it had a larger capacity than did Electrode A, which had an initial charge capacity of 133.1 x 10^{-3} C cm^{-3}, which was reduced to 18.1 x 10^{-3} mC cm^{-3} after repetitive cycling, though it is notable that this reduction is significantly smaller than that of Electrode B.

The reduction in capacity could occur for two possible reasons: (1) adsorbed Cs^{+} is permanently attached to some of the active sites of the film, causing a blockage of these active sites, or (2) the film itself loses some of its material parts through detachment from the surface of the graphite, leading to the loss of active sites.

The solutions were tested for the presence of the cobalt ions after the cyclic voltammetry by electrospray ionization-mass spectroscopy. The test did not detect any forms of cobalt or nickel, indicating that there was no nickel hexacyanocobaltate material in the solution. It is, therefore, believed that the decrease in capacity is caused by the permanent blockage of some of the films' active sites.

Both electrodes showed some decrease in capacity, but their Cs^+ adsorption was good, and that they can still adequately perform ESIX after 1000 cycles.

6.5 Conclusion

Two graphite electrodes were prepared for separating Cs^+ from contaminated solutions by adsorbing $KNiCo(CN)_6$. The use of graphite electrode as a conductive substrate for the nickel hexacyanocobaltate materials yielded a porous electrode in which successive new sites became active as the contaminated solution penetrated the electrode. These graphite electrodes, therefore, are able to function as ESIX electrodes. These two graphite electrodes were used for Cs^+ separation. The results show that both of them have separation percentages that range from 85% to 91% and that their capacity is reduced during the repeated cycles by 13.5% for Electrode A and by 10% for Electrode B. This result indicates that the deposition of nickel hexacyanocobaltate onto a graphite substrate yields a suitable electrode for ESIX, with layers that become successive available on the interior as those on the exterior become permanently blocked.

6.6 Acknowledgements

The authors would like to thank the Egyptian Ministry of Defense (EMD) and the Natural Science and Engineering Research Council of Canada (NSERC) (Discovery Grants Program) for supporting this work.

6.7 References

Adeleye I. Okewole. (2012) “The separation of nickel(II) from base metal ions using 1-octyl-2-(2′- pyridyl)imidazole as extractant in a highly acidic sulfate medium” *Hydrometallurgy* 121-124, PP 81–89.

Bhaskar, N. D. and C. M. Khla, (1990) “Adsorption of cesium by polycrystalline graphite-sticking coefficient studies” *Carbon* Vol. 2.No. I. PP 71-78..

Browni, P. A. and Gill, V. (2000) “Metal removal from water using peat” Wat. Res. Vol. 34, No. 16, pp. 3907-16.

Chandra D. (1976) “Diffusion of cerium through graphite” *Journal of Nuclear Materials* 62, PP 293-310.

Green-Pedersen, H., and Korshin, G. V. (1999). “Separation of Cesium from High Ionic Strength Solutions Using a Cobalt Hexacyanoferrate-Modified Graphite Electrode.” *Environmental Science & Technology*, 33, PP 2633–2637.

Gulin S.B., and Mirzoyeva, N. Yu, (2013) “Secondary radioactive contamination of the Black Sea after Chernobyl accident: recent levels, pathways and trends” *Journal of Environmental Radioactivity* 124, PP 50-56.

Hussain S.N. and Roberts, J. D. (2013) “Oxidation of phenol and the adsorption of breakdown products using a graphite adsorbent with electrochemical regeneration” *Electrochimica* 92, PP 20– 30.

Jo, Se-Hee, (2010) “Continuous separation of copper ions from a mixture of heavy metal ions using a three-zone carousel process packed with metal ion-imprinted polymer” *Journal of Chromatography* A, 1217, PP 7100–7108.

Lilga M.A., Orth, R.J., Sukamto, J.P.H. and Rassat, S.D. (2001) “Cesium separation using electrically switched ion exchange” *Separation and Purification Technology* 24, PP 451–466.

Mainea M.A. and Sun, N. (2006) “Nutrient and metal removal in a constructed wetland for wastewater treatment from a metallurgic industry” *Ecological Engineering* 26, PP 341–347.

Mayumi, Yoshimura. And Tetsuya, Yokoduka. (2014) “Radioactive contamination of fishes in lake and streams impacted by the Fukushima nuclear power plant accident” *Science of the Total Environment* 482, PP 184–192.

Mohapatra, P. K., Lakshmi, D. S., Bhattacharyya, A., and Manchanda, V. K. (2009) “Evaluation of polymer inclusion membranes containing crown ethers for selective cesium separation from nuclear waste solution.” *Journal of Hazardous Materials*, 169, PP 472– 490.

Mohapatra, P. K., Bhattacharyya, A., and Manchanda, V. K. (2010) “Selective separation of radio-cesium from acidic solutions using supported liquid membrane containing chlorinated cobalt dicarbollide (CCD) in phenyl trifluoromethyl sulphone (PTMS).” *Journal of Hazardous Materials*, 181, PP 679–85.

Nagendran A., (2008) “Toxic metal ion separation by cellulose acetate/sulfonated poly (ether imide) blend membranes: Effect of polymer composition and additive” *Journal of Hazardous Materials* 155, PP 477–485.

Opeyemi, Olanipekun and Adebola, Oyefusi. (2014) “Adsorption of lead over graphite oxide ” Spectrochimica Acta Part A: Molecular and Biomolecular Spectroscopy”118, PP 857–860.

Ping, Zhoui. and Chang Huang, Pu. (1999) “Heavy metal removal from wastewater in fluidized bed reactor” *Wat. Res.* Vol. 33, No. 8, pp. 1918-24.

Pyrzynska. K., (2010) “Carbon nanostructures for separation, pre concentration and speciation of metal ions” *Trends in Analytical Chemistry*, Vol. 29, No. 7 pp 718–727

Raffaele, Molinari and Saverio, Gallo. (2004) “Metal ions removal from wastewater or washing water From contaminated soil by ultrafiltration–complexation” *Water Research* 38, PP 593–600.

Raja, S. (2013) “Batch separation studies for the removal of heavy metal ions using a chelating terpolymer: Synthesis, characterization and isotherm models” *Separation and Purification Technology* 116, PP 366–377.

Rassat, S.D., Sukamto, J.H. and Lilga, M.A. (1999) “Development of an electrically switched ion exchange process for selective ion separations” *Separation and ectroamai. Chem.*, 210, PP 323-328.

Shakir K., Sohsah, M., and Soliman, M. (2007) “Removal of cesium from aqueous solutions and Radioactive waste simulants by coprecipitate flotation” *Separation and Purification Technology* 54, PP 373–381.

Suna Bin, Xiao-Gang Hao (2012) “Separation of low concentration of Cs+ from wastewater by electrochemically switched ion exchange method: Experimental adsorption kinetics analysis” *Journal of Hazardous Materials* 233-234, PP 177–183.

Wi-Ho, Ha, Jaeryong, Yoo, and Seokwon, Yoon (2013) “Radioactive contamination monitoring for theKorean public following Fukushima nuclear accident” *Applied Radiation and Isotopes* 81, PP 371–373.

Chapter 7

Conclusions and Recommendations

7.1 General conclusions

The goal of this thesis was first to enhance the capacity and the ability for ESIX films made of nickel hexacyanoferrate for Cs^+ separation by modifying the applied voltage during the deposition process when using a nickel substrate, and, second, to study the effect of changing the substrate material to graphite to increase the ESIX capacity. The last goal was to introduce a new material for the ESIX process, which is nickel hexacyanocobaltate adsorbed throughout a graphite electrode. The following conclusions were made according to the results of this research:

1- A modified technique was applied for ESIX film deposition on nickel substrate. The results show that a stable and insoluble film being deposited on nickel electrode allows Cs^+ loading and unloading that was controlled by modulating the potential of the film. The results show that this film has a maximum charge capacity 63 times higher than films prepared in previous work, and the same film shows a decrease in capacity of 30% after 1000 cycles.

2- Four ESIX films were prepared by electric deposition on a nickel electrode using different applied potentials. These films were used for Cs^+ separation from an aqueous solution. A comparison was made between them by examining their capacity, their surface morphology, and their performance through cyclic voltammetry. The results show that there is a significant difference in their capacity to load Cs^+, depending on the applied potentials in their loading. The optimal film was prepared by depositing by initial voltage 0.2 V relative to SCE for 30 minutes, followed by a voltage of 1.3 V relative to SCE for another 30 minutes, yielding the film with the highest capacity for Cs^+ loading, even after 1000 cycles. This evidence shows that this film would be a good candidate for electrically switched ion exchange film for the loading of Cs^+ from a contaminated solution.

3- Graphite was introduced as a substrate for ESIX films instead of nickel. Two graphite electrodes carrying nickel hexacyanoferrate as an ESIX film were deposited at two different concentrations, 0.5 M and 0.75 M. They were tested for Cs^+ adsorption from a test solution and were characterized by imaging the ion exchange film morphology through x-ray tomography, and their film capacity as well as repetitive loading and unloading were measured with cyclic voltammetry. The results show a variation in their performance regarding Cs+ adsorption: the electrode that has was made with an initial concentration of 0.75 M $KNiFe(CN)_6$ was able to adsorb 97% of Cs^+ from a 2.25×10^{-3} mol solution of Cs^+. Its capacity was reduced from 628.2×10^{-3} C. cm^{-3} to 461×10^{-3} C. cm^{-3} after 1000 cycles. The electrode with made in a solution of 0.5 M $KNiFe(CN)_6$ was able to adsorb 88.7% of Cs^+ with its capacity changing from 307×10^{-3} C. cm^{-2} to 269×10^{-3} C. cm^{-3} after 1000 cycles. These results confirm that using graphite as a substrate material enhances the ESIX adsorption of CS^+.

4- A new ESIX material, nickel hexacyanocobaltate ($KNiCo(CN)_6$), was introduced. This ESIX material was adsorbed inside two graphite electrodes from solutions at two different concentrations, 0.5 M and 0.75 M. Both of the graphite electrodes were used to remove Cs^+ from solutions. The results show that they were able to achieve a separation percentages ranging from 85% to 91% and that their capacity was reduced during the running of 1000 cycles by 13% and 9%, respectively. This indicates that nickel hexacyanocobaltate deposited onto a graphite substrate yields a suitable electrode for ESIX.

7.2 Recommendations for Future Work

Some recommendations for future work have been identified based on the results shown here:

1- Investigate the reaction between potassium hexacyanoferrate and the Ni^{2+} on the nickel electrode surface during the electric deposition in order to obtain more suitable conditions for film electrodeposition. This will lead to a more uniform and dense ESIX film.

2- Investigate the kinetics of the reaction between nickel hexacyanoferrate and nickel hexacyanocobaltate with the graphite surface. This will help to increase adsorption inside the graphite, which will lead to a higher film capacity and durability.

3- Introduce a new ESIX material for the separation of group two elements, as until now the ESIX process is suitable only for the separation of group one elements.